

UCLA

UCLA Electronic Theses and Dissertations

Title

Combination Therapy Exon Skipping for Duchenne Muscular Dystrophy

Permalink

<https://escholarship.org/uc/item/3655w9xw>

Author

Wang, Derek

Publication Date

2017

Peer reviewed|Thesis/dissertation

UNIVERSITY OF CALIFORNIA

Los Angeles

Combination Therapy Exon Skipping for Duchenne Muscular Dystrophy

A dissertation submitted in partial satisfaction of the
requirements for the degree Doctor of Philosophy
in Microbiology, Immunology & Molecular Genetics

By

Derek Wu Wang

2017

©Copyright by
Derek Wu Wang
2017

Abstract of the Dissertation

Combination Exon Skipping Therapy for Duchenne Muscular Dystrophy

by

Derek Wu Wang

Doctor of Philosophy in Microbiology, Immunology & Molecular Genetics

University of California, Los Angeles, 2017

Professor M. Carrie Miceli, Chair

Duchenne muscular dystrophy is caused by mutations in *DMD*, resulting in loss of dystrophin essential to muscle health. DMD “exon skipping” uses anti-sense oligonucleotides (AON) to force exon exclusion during mRNA processing to restore mRNA reading frame and rescue production of a dystrophin protein with partial functionality. While initial exon skipping drugs in humans show promise, levels of rescued dystrophin protein expression remain suboptimal. Greater benefit is predicted with even modest increases in dystrophin rescue. Using an unbiased screen of FDA approved drugs, we identified dantrolene as a skip-booster when used in combination with AON in human and mouse DMD models. Here, we assess dantrolene booster activity in combination with weekly AON administration in mdx mice over 6 month treatment duration and under conditions that guide pre-clinical evaluation. We find that dantrolene boosts levels of skipped mRNA and rescued

dystrophin, resulting in greater reduction of muscle pathology than AON treatment alone and without apparent toxicity. Dantrolene has already been safely administered to a small DMD cohort. Together these findings provide preclinical support for dantrolene/AON combination therapy to increase the efficacy of exon skipping drugs and highlight the value of unbiased screens, combinatorial approaches, and repurposing of FDA approved drugs for discovery of unsuspected therapeutic application and rapid translation.

The dissertation of Derek Wu Wang is approved.

Donald Barry Kohn

Stanley F. Nelson

April Dawn Pyle

Melissa J. Spencer

M. Carrie Miceli, Committee Chair

University of California, Los Angeles

2017

To my family:

My parents for the years of encouragement,

My sister for her guidance,

And my stepfather for his support.

TABLE OF CONTENTS

Section		Page
Abstract		ii
List of Figures		vii
List of Tables		x
Acknowledgements		xi
Vita		xii
Chapter 1	Duchenne Muscular Dystrophy and Exon Skipping	1
Chapter 2	Repurposing Dantrolene for Long-term Combination Therapy to Potentiate Antisense-Mediated DMD Exon Skipping in the mdx mouse	8
Chapter 3	Growing a Bank of Primary Patient Cells to Model and Test Various Exon Skipping Strategies	57
Chapter 4	Preliminary Studies to Test Engraftment Conditions for a DMD Xenograft Model System for Studying DMD in vivo	73
Chapter 5	Concluding Remarks: Future Perspectives and Directions	88
Appendix	A Single CRISPR-Cas9 Deletion Strategy that Targets the Majority of DMD Patients Restores Dystrophin Function in hiPSC-Derived Muscle Cells	93
References		141

LIST OF FIGURES

Figure 2-1	Overview of long-term dosing experiment.....	40
Figure 2-2	6-month treatment with 10, 50, and 300 mg/kg e23AON with dantrolene did not adversely affect serum biomarkers and histopathology.....	41
Figure 2-3	Dantrolene boosts e23AON to promote RNA exon 23 skipping.....	42
Figure 2-4	Dantrolene boosts 23AON to promote rescue of dystrophin immunofluorescence intensity and percent dystrophin-positive fibers.....	43
Figure 2-5	Dantrolene boosts e23AON to promote rescue of dystrophin protein after chronic treatment.....	44
Figure 2-6	Dantrolene/e23AON combination therapy restores sarcolemmal dystrophin and DGC after chronic treatment.....	45
Figure 2-7	Creatine kinase reduction boosted with dantrolene/e23AON combination therapy.....	46
Figure 2-8	Reduction of centronucleation in the diaphragm and eMHC positive fibers in the quadriceps treatment with e23AON and dantrolene.....	47

Figure 2-S1	Oral Dantrolene synergizes with systemically delivered e23AON to promote exon 23 skipping and restoration dystrophin expression after 3 weeks treatment.....	49
Figure 2-S2	Dantrolene was detected at physiologically relevant levels in the serum of mice fed with dantrolene chow.	50
Figure 2-S3	Results of Friedman’s two-way nonparametric ANOVA on the effect of dantrolene on e23AON treatment for exon 23 skipped / (skipped + unskipped) transcript as measured by ddPCR.....	51
Figure 2-S4	Results of Friedman’s two-way nonparametric ANOVA on the effect of dantrolene on e23AON treatment for dystrophin immunofluorescence quantitation and dystrophin positive fibers.....	52
Figure 2-S5	Results of Friedman’s two-way nonparametric ANOVA on the effect of dantrolene on e23AON treatment for dystrophin protein by western blot.....	53
Figure 2-S6	Combination therapy rescues expression of dystrophin with presence of N-terminal, rod domain, and C-terminal protein sequences.....	54
Figure 2-S7	Results of Friedman’s two-way nonparametric ANOVA on the effect of dantrolene on e23AON treatment for serum CK levels.....	55

Figure 2-S8	Results of Friedman’s two-way nonparametric ANOVA on the effect of dantrolene on e23AON treatment for centronucleation and eMHC positive fibers.....	56
Figure 3-1	Custom CGH array confirms deletion breakpoints in GM05017 used to create iDRM 5017.....	72
Figure 3-2	MyoD Puro Vector (CMV-MyoDER(T)-IRES-Puro.....	73
Figure 4-1	Overview of General Engraftment Experiment.....	84
Figure 4-2	DMD patient–derived iDRM 5017 and iPSC 5017 engraft into mdx TA and express muscle markers.....	85
Figure A-1	CDMD hiPSCs Are Pluripotent and Genetically Stable.	124
Figure A-2	Generation of Stable, Pluripotent CDMD hiPSC Lines with an Exon 45–55 Deletion.....	125
Figure A-3	Reframed CDMD hiPSC-Derived Skeletal Muscle and Cardiomyocytes Restore Dystrophin Expression.....	127
Figure A-4	Reframed hiPSC-Derived Cardiomyocytes and Skeletal Muscle Cells Demonstrate Restored Function In Vitro and In Vivo.....	129
Figure A-S1	gRNA activity and exon 45-55 deletion in 293FT cells	131
Figure A-S2	gRNAs show cutting by Surveyor assay in CDMD hiPSCs.....	132
Figure A-S3	Nucleofection of paired gRNAs results in an exon 45-55 deletion in CDMD hiPSCs.....	133
Figure A-S4	Additional characterization of reframed lines.....	135

LIST OF TABLES

Table 2-1	Friedman’s two-way nonparametric ANOVA and meta-analyses of the effect of dantrolene on e23AON treatment for all quantitative outcomes.....	48
Table 3-1	cDMD Cell Bank (as of 9/20/2017).....	59
Table 3-2	DMD patient cell lines amenable to exon skipping.....	65
Table 4-1	Engraft Conditions Explored for Preliminary Experiments.....	86
Table 4-2	DMD patient–derived iDRM 5017 temporally express muscle markers at the RNA and protein level during the fusion process.....	87
Table A-S1	Expected cleavage product sizes from Surveyor assay	137

ACKNOWLEDGEMENTS

First and foremost, I would like to thank Dr. M. Carrie Miceli and Dr. Stanley Nelson for their guidance, confidence, encouragement and optimism while I have been in the laboratory. Their enthusiasm and commitment to the research conducted in their laboratories have been inspiring. I will value the lessons I have learned from my mentors for the rest of my career.

My committee members, Dr. Donald Kohn, Dr. April Pyle, and Dr. Melissa Spencer, have given me valuable support and guidance at various points through my graduate career. Their input has been fundamental to my growth during my graduate career.

My fellow lab members and collaborating lab members from Dr. Rita Cantor, Dr. Rachelle Crosbie-Watson, Dr. M. Carrie Miceli, Dr. Stan Nelson, Dr. April Pyle, and Dr. Melissa Spencer offered help, wisdom, and insight. Thank you Florian Barthélémy, Diana Becerra, Jillian Crocetti, Janeen Ishii, Genevieve Kendall, Jamie Marshall, Leonel Martinez, Ekaterina Mokhonova, Linda Navarro, Deirdre Scripture-Adams, Oscar Silva, Richard Wang, Jane Wen, and Courtney Young.

VITA

- 2010 B.S., Microbiology, Immunology & Molecular Genetics
University of California, Los Angeles
Los Angeles, California
- 2012 Joined Program in Microbiology, Immunology & Molecular
Genetics
- 2016-2017 University of California, Los Angeles
Dissertation Year Fellowship

PUBLICATIONS AND PRESENTATIONS

Original Research

Young C.S., Hicks M.R., Ermolova N.V., Nakano H., Jan M., Younesi S., Karumbayaram S., Kumagai-Cresse C., **Wang D.**, Zack J.A., Kohn D.B., Nakano A., Nelson S.F., Miceli M.C., Spencer M.J., Pyle A.D. A Single CRISPR-Cas9 Deletion Strategy that Targets the Majority of DMD Patients Restores Dystrophin Function in hiPSC-Derived Muscle Cells. *Cell Stem Cell*. 2016

G.C. Kendall, E.I. Mokhonova, M. Moran, N.E. Sejbuk, **D.W. Wang**, O. Silva, R.T. Wang, Q.L. Lu, R. Damoiseaux, M.J. Spencer, S.F. Nelson, M.C. Miceli. Compound BM.663 enhances antisense-mediated exon skipping in human and mouse models of Duchenne muscular dystrophy. *Sci Transl Med*. 2012 Dec 12;4(164):164ra160.

Abstracts

D.W. Wang, E.I. Mokhonova, G.C. Kendall, L. Martinez, D. Becerra, R.E. Reyes, M.J. Spencer, S.F. Nelson, M.C. Miceli. Long Term Thereapy to Enhance Antisense Mediated Exon Skipping for Duchenne Muscular Dystrophy in the mdx Mouse. 6th Annual Center for Duchenne Muscular Dystrophy at UCLA Retreat, Los Angeles, California, February 24, 2016. Poster and Presentation.

D.W. Wang, E.I. Mokhonova, G.C. Kendall, L. Martinez, D. Becerra, R.E. Reyes, M.J. Spencer, S.F. Nelson, M.C. Miceli. Combination Therapy to Enhance Antisense Mediated Exon Skipping for Duchenne Muscular Dystrophy. 5th Annual Center for Duchenne Muscular Dystrophy at UCLA Retreat, Los Angeles, California, November 21, 2014. Poster.

F. Barthelemy, G. Kendall, **D.W. Wang**, E.I. Mokhonova, S.F. Nelson, M.C. Miceli. Evaluation of RyR Pathway Antagonists to Promote Exon 51 Skipping in DMD Patient Cells. 5th Annual Center for Duchenne Muscular Dystrophy at UCLA Retreat, Los Angeles, California, November 21, 2014. Poster.

H. Xi, T.O. Dial, **D.W. Wang**, E.I. Mokhonova, J. Wen, S.F. Nelson, M.J. Spencer, M.C. Miceli, A.D. Pyle. Deriving skeletal muscle progenitors from human pluripotent stem cells for treatment of Duchenne muscular dystrophy. 5th Annual Center for Duchenne Muscular Dystrophy at UCLA Retreat, Los Angeles, California, November 21, 2014. Poster.

D.W. Wang, E.I. Mokhonova, G.C. Kendall, L. Martinez, D. Becerra, R.E. Reyes, M.J. Spencer, S.F. Nelson, M.C. Miceli. Combination Therapy Enhances Antisense Mediated Exon Skipping for Duchenne Muscular Dystrophy. Annual American Society of Human Genetics Meeting, San Diego, California, October 18-22, 2014. Poster.

D.W. Wang, E.I. Mokhonova, G.C. Kendall, L. Martinez, D. Becerra, M.J. Spencer, S.F. Nelson, M.C. Miceli. Combination Therapy To Enhance Antisense Mediated Exon Skipping for Duchenne Muscular Dystrophy. Annual Center for Duchenne Muscular Dystrophy at UCLA Retreat, Los Angeles, California, November 21, 2013. Poster.

G.C. Kendall, E.I. Mokhonova, M. Moran, N.E. Sejbuk, **D.W. Wang**, O. Silva, R.T. Wang, Q.L. Lu, R. Damoiseaux, M.J. Spencer, S.F. Nelson, M.C. Miceli. (2011) Compound BM.663 enhances antisense-mediated exon skipping in human and mouse models of Duchenne muscular dystrophy. Annual Molecular Biology Institute Retreat, Lake Arrowhead, California, October 14-16, 2011. Poster.

Chapter 1

Introduction

Duchenne Muscular Dystrophy and Exon Skipping

Duchenne Muscular Dystrophy

DMD is a genetic disorder characterized by progressive muscle weakness and wasting. Over the course of a patient's lifetime, muscle is replaced by fibrosis and fat. DMD is an orphan disease, affecting 1 in every 5000 live male births.¹ Roughly 32,000 patients are affected in the US. Two-thirds of cases are inherited from the mother, while the remaining third of cases arise from *de novo* mutations that result in a lack of dystrophin protein expression.

Patients typically present with delayed motor milestones and weakness of proximal muscles by the age of 5.² Before the age of 16, patients become reliant on wheelchairs due to skeletal deformities and muscle weakness. Patients also begin to develop limited use of their arms. As the disease progresses, patients require ventilation to prevent respiratory failure. Patients eventually succumb to cardiomyopathy and respiratory complications in their 30's or 40's. Recent improvements in treatment have extended the lifespan of patients by more than a decade. Most current treatment paradigms are aimed at managing disease pathology. These include steroids to slow muscle degeneration, anticonvulsants to control seizures, and immunosuppressants to reduce inflammation.^{3, 4}

Dystrophin is a key component of the Dystrophin Glycoprotein Complex, which has many components including: sarcospan, the α - and β - sarcoglycans, and the α - and β - dystroglycans.⁵ The Dystrophin glycoprotein complex provides structural stability to the sarcolemmal membrane during muscle contraction by binding the actin cytoskeleton and extracellular matrix. As part of the DGC, dystrophin acts much like a spring, absorbing force, and stabilizing the muscle membrane as it

contracts. Muscles lacking dystrophin and as a result, the DGC, are more susceptible to membrane leakage and tears that are responsible for progressive muscle weakening. ⁶

The gene encoding dystrophin is the largest gene in the human genome, containing 79 exons. ^{7, 8} Dystrophin is a hefty protein, weighing in at 427 kDa. ⁹ It has major functional binding domains including: the actin-binding domain, nNos-binding domain, dystroglycan-binding domain, syntrophin binding domains, and coiled coiled domains. ^{10, 11} The actin-binding domain is found at the N-terminus and functions to bind the actin cytoskeleton of the cell. At the C-terminal region of dystrophin contains the dystroglycan-binding domain, syntrophin binding domains, and coiled coiled domains that are responsible for binding to members of the DGC and the extracellular matrix. The central rod-domain of dystrophin is composed of 24 spectrin-like repeats and contains an nNOS binding region within spectrin repeats 16 and 17. ¹²

Many patients who suffer from DMD have mutations in the dystrophin gene that render an out-of-frame transcript that can be caused by deletions, duplications, and nonsense mutations. ¹³ This can lead to a premature stop codon, forming an incomplete transcript that is targeted for nonsense-mediated decay or an unstable protein product. A majority of DMD mutations occur in area known as a hotspot region. ¹⁴ Hotspot for mutations occurs between exons 3 and 8 as well as exons 45 and 55 due to the gene's propensity to undergo recombination in this region. ¹⁵ Mutations between exons 45 and 55 account for roughly 62% of all DMD mutations.

A subset of patients with mutations in their DMD gene, still express a mutant dystrophin protein, and present with a much milder phenotype and are diagnosed

with Becker's Muscular Dystrophy. ¹⁶ Like DMD patients, Becker's patients present with muscle weakness, calf hypertrophy, and elevated creatine kinase levels. In contrast to DMD patients, Becker's patients remain ambulatory beyond the age of 16; in milder cases, patients have been known to remain ambulatory in their 60s. ^{17, 18} The severity of disease is thought to be highly dependent on the amount and functionality of the mutated dystrophin protein produced by each patient. ¹⁹

Exon Skipping Therapy

One therapeutic approach to treat DMD is exon skipping therapy, which aims to convert DMD patients into BMD-like patients by rendering mutant DMD transcripts back in-frame. Antisense oligonucleotides (AOs) have been developed that are able to bind to exonic splice enhancer sites of targeted exon switching the DMD gene. This is thought to block splicing machinery, and result in the exclusion of the targeted exon and an in-frame transcript.

AOs are synthesized DNA fragments that are manufactured to bind to complementary sequences of target pre-mRNA. An array of chemical backbones have been developed in order to improve the stability of AOs and the efficacy and specificity of binding. The two most studied chemistries of AO are 2'-O-methyl-phosphorothioate AO (2'OMeAO) and phosphorodiamidate morpholino oligomers (PMO). ^{20, 21}

Preclinical studies of exon skipping have been performed in various DMD animal models, including the dystrophin-deficient *mdx* mouse ^{22, 23} and the dystrophic golden retriever model. ^{24, 25} For instance, the *mdx* mouse has a mutation in exon

23, which results in a premature stop codon. Like DMD patients, the *mdx* mouse does not express dystrophin protein. In the mouse, this results in an acute onset of skeletal muscle necrosis at around 3 weeks of age, followed by a period of degeneration and regeneration when stabilized when the mouse reaches adulthood (3-4 months).²⁶ It should be noted that though the muscle pathology of *mdx* is similar to that of young DMD boys, the clinical course is less severe than older patients.

Promising preclinical studies of AOs in *mdx* mice have shown that weekly administration PMO against exon 23 for 6 months to a year is able to induce functional amounts of skipped dystrophin mRNA transcript and protein.^{27, 28} Treated mice were shown to have increased hind limb and forelimb grip strength, decrease serum creatine kinase levels, and improved skeletal muscle histopathology, among other end point measures.

In September of 2016, the FDA granted accelerated approval to Exondys51 (eteplirsen), which is an antisense oligonucleotide that is able to target 14% of DMD patients (the largest single cohort of skippable m patients), through targeted skipping of exon 51.²⁹ Exondys51 is the very first drug approved to treat patients with DMD.

The primary outcome of the clinical trial used to support this approval was the 6-minute walk test (MWT). This test measures the distance that a patient can walk in 6 minutes and has been shown to be a global measure of ambulatory function in DMD.³⁰ Weekly treatment with 30 and 50mg/kg PMO significantly reduced the decline in 6MWT performance typically seen in DMD boys following three years of treatment.³¹ Notably, this significant rescue in function was achieved with

demonstration of statistically significant dystrophin induction, indicating that eteplirsen was successful at inducing exon skipping and suggesting that dystrophin could be a potential biomarker in future studies. The patients in this study saw a significant functional effect and patients expressed an average of 1% dystrophin by WB in skeletal muscle. Given these data, it is expected that even minor improvements in the amount of dystrophin protein expressed can lead to significant improvements in muscle function. Our lab sought to discover small molecule boosters of exon skipping ³².

We performed a small-molecule screen to identify existing drugs that enhance antisense-directed exon skipping. We found that dantrolene, currently used to treat malignant hyperthermia, potentiates antisense oligomer-guided exon skipping to increase exon skipping to restore the mRNA reading frame, the sarcolemmal dystrophin protein, and the dystrophin glycoprotein complex in skeletal muscles of mdx mice when delivered intramuscularly or intravenously. Further, dantrolene synergized with multiple weekly injections of antisense to increase muscle strength and reduce serum creatine kinase in mdx mice. Dantrolene similarly promoted antisense-mediated exon skipping in reprogrammed myotubes from DMD patients. Ryanodine and Rycal S107, which, like dantrolene, targets the ryanodine receptor, also promoted antisense-driven exon skipping, implicating the ryanodine receptor as the critical molecular target.

This study highlighted the discovery and efficacy as dantrolene as a booster of exon skipping in both human and mouse models of DMD. Of note, the treatments performed in this study were relatively short (<3 weeks) and dosed in a manner that is not amenable to human treatment (IP injections.) This study also does not

elucidate the long term safety profile of combination therapy with antisense oligonucleotide and dantrolene. In the following Chapter, I outline the experiments performed to assess dantrolene's exon skip boosting activity in the mdx DMD mouse model in the context of long-term 6 month chronic treatment with weekly IV e23AON at high (300mg/kg), medium (50 mg/kg) or low (10mg/kg) dose in combination with dantrolene dosed orally. These conditions are more relevant to potential combination therapy in Duchenne patients currently prescribed ExonDys51 or exposed to other skipping drugs currently in the pipeline.

Chapter 2

Repurposing Dantrolene for Long-term Combination
Therapy to Potentiate Antisense-Mediated DMD Exon
Skipping in the mdx mouse

This chapter represents a manuscript that was submitted to *Molecular Therapy* by Derek Wang in the laboratories of Dr. M. Carrie Miceli and Dr. Stanley Nelson titled, "Repurposing Dantrolene for Long-term Combination Therapy to Potentiate Antisense-Mediated DMD Exon Skipping in the mdx mouse." My contributions include: 1) planning and leading the implementation of mouse experiments, 2) performing the RNA skipping quantification experiments, pathophysiology experiments, and serum biomarker experiment, 3) interpreting the data collected, and 4) writing the manuscript. This chapter represents the bulk of my thesis project.

Introduction

Duchenne muscular dystrophy (DMD) is the most common lethal genetic disease of childhood, with an incidence that ranges from 10.7 to 27.8 per 100,000 population³³. DMD is mainly caused by frame-shifting multi-exon deletions in the *DMD* gene resulting in loss of expression of the encoded protein, dystrophin, which is critical to muscle cell health³⁴. Dystrophin stabilizes the muscle membrane in the context of contraction by linking the cytoskeleton to the extracellular matrix through N-terminal association with F-actin and C-terminal association with the Dystrophin associated Glycoprotein Complex (DGC). The DGC spans the membrane and binds laminin $\alpha 2$ within the basal lamina and requires dystrophin for its sarcolemmal localization, stability and function. Additionally, dystrophin and the DGC contribute to muscle cell signaling and stem cell self-renewal³⁵.

Loss of dystrophin and DGC expression results in muscle membrane damage, altered signaling and defective muscle regeneration. Membrane damage drives increased intracellular Ca^{2+} levels, calpain activation, protein degradation and cell death³⁶. Proper nitric oxide synthase (NOS) localization at the DGC is lost in the absence of dystrophin, resulting in hyper-nitrosylation of the ryanodine receptor 1 (RyR1)³⁷, which also contributes to Ca^{2+} dysregulation. Inflammation and replacement of muscle with fat and fibrosis, further interferes with muscle regeneration and function. Over time, this leads to progressive loss of body-wide skeletal muscle and cardiac function. Boys with DMD become dependent on a wheelchair- at approximately age 10-12 years and succumb to respiratory and/or cardiac failure between the ages of 18 and 30 years³⁴.

Becker muscular dystrophy (BMD), a milder form of dystrophy, is also caused by mutations in *DMD*^{38, 39}. However, in most instances, *DMD* mutations in those with BMD preserve the mRNA reading frame and lead to the production of an internally deleted dystrophin with partial functionality. BMD patients can range in severity from loss of ambulation by 16 years old to asymptomatic, depending largely on the stability and functionality of the mutant dystrophin. Of note, several in-frame Becker mutations cluster within a hotspot between exons 45 and 55 and encode internally deleted dystrophin proteins with partially functionality and generally progress with a milder disease course relative to Duchenne. These findings provide the basis for therapies aimed at reframing mRNA to rescue Becker-like proteins with partial functionality⁴⁰.

One therapeutic strategy, termed exon skipping, forces targeted exon exclusion during pre-mRNA splicing to restore *DMD* reading frame through systemic administration of anti-sense oligo-nucleotides (AON)⁴¹⁻⁴³. Reframing by exon skipping rescues the expression of a BMD-like internally deleted dystrophin. AON-guided *DMD* exon skipping has proven effective in increasing Becker-like dystrophin, and improving skeletal muscle function in both mouse and dog *DMD* models⁴⁴⁻⁴⁹.

Exondys51, a morpholino AON designed to restore *DMD* reading frame by excluding exon 51, was recently granted accelerated approval in the USA and is relevant to 13% of *DMD* patients^{43, 50, 51}. In a small but multi-year study, 12 boys who were amenable to reframing by skipping exon 51 were administered Exondys51 weekly by intravenous infusion³¹. All patients received 30mg/kg except for one who received 60mg/kg. After 3 years, those treated with Exondys51 walked 151 meters further than predicted by a longitudinal natural history of *DMD* boys from a cohort well-matched for genotype, age and functional parameters at study initiation³¹. By year 4, only 20% of Exondys51 treated subjects had lost ambulation, whereas 80% of the matched historical control lost ambulation over the same time frame⁵².

Skeletal muscle biopsies from subjects administered Exondys51 demonstrated a statistically significant induction of dystrophin relative to pre-treatment control biopsies and, ultimately, accelerated approval was granted based on this biomarker. Levels of induced dystrophin ranged from 0-2.47%, distributed

across an average of 16% of myofibers, within the range known to impart some functional benefit in the *mdx* DMD mouse model, and in a BMD patient⁵³⁻⁵⁷. Higher levels of dystrophin are predicted to impart even greater function^{27, 55, 56, 58-60}.

We previously identified dantrolene as a booster of antisense-mediated exon skipping through an unbiased small molecule screen of the BioMol Library and validated its efficacy in short-term *mdx* mouse and human DMD culture models³². The *mdx* mouse has a premature termination within exon 23 of *DMD* leading to a muscular dystrophy similar to human DMD. Intravenous administration of e23AON promotes exon 23 skipping, and rescue of an internally deleted dystrophin protein that is capable of significant functionality and rescue of the DMD-like phenotype^{23, 61}. We have reported that dantrolene (10mg/kg), administered twice daily intraperitoneally, boosted low dose AON-directed exon 23 skipping (e23AON), dystrophin protein expression and strength in the *mdx* mice over the course of short-term experiments (1-3 weeks). Further, DMD patient-derived reprogrammed myotubes bearing an exon 45-50 deletion treated with dantrolene/e51AON combination induced greater levels of in frame skipped DMD exon51 mRNA than either drug alone, establishing relevance to human DMD treatment⁶².

Here we assess dantrolene's exon skip boosting activity in the *mdx* DMD mouse model in the context of long-term 6 month chronic treatment with weekly IV e23AON at high (300mg/kg), medium (50 mg/kg) or low (10mg/kg) dose in combination with dantrolene dosed orally. These conditions are more relevant to potential combination therapy in Duchenne patients currently prescribed ExonDys51 or exposed to other skipping drugs currently in the pipeline. We demonstrate that

dantrolene boosts e23AON-directed *DMD* mRNA exon skipping, dystrophin protein expression and rescue of dystrophic pathology in *mdx* mice in the context of long-term chronic treatment without toxicity. These findings provide data in support of the feasibility and efficacy of repurposing dantrolene as a skip-boosting drug for use in combination with exon skipping AON. Because dantrolene and Exondys51 are both FDA approved drugs with good safety profiles in Duchenne, combination therapy could be rapidly tested in human.

Results

Orally Administered Dantrolene Enhances Antisense-Mediated Exon Skipping and Dystrophin Protein Rescue in *mdx* mice.

Previous studies using twice daily intra-peritoneal (IP) injections identified dantrolene as a booster of DMD exon skipping in short term treatment using non-clinical grade dantrolene (Sigma). Dantrolene is already clinically available in tablet form for oral administration under the trade name, Dantrium. Because oral dosing is much more practical both for long term mouse studies and translation to human DMD, we performed a series of 3 week pilot studies to determine if orally administered dantrium incorporated into chow *ad libitum* boosted dystrophin induction of systemically administered e23AON. We found that orally administered dantrolene administered in combination with 50mg/kg e23AON E23AON boosted dystrophin immunofluorescence intensity per cross sectional area relative to e23AON treatment alone (**Supplementary Figure 1**). Therefore, we relied on oral dantrium incorporated into chow to assess dosing, efficacy and safety during the course of chronic combination treatment.

6-month combination therapy promotes increased exon skipping and dystrophin expression in skeletal muscle

We next assessed the efficacy of long-term administration of combination therapy of e23AON and dantrolene in *mdx* mice. We designed a blinded, placebo-controlled, multi-dose six month study, in which *mdx* mice were fed a diet containing 30-70mg/kg/day dantrolene *ad libitum* in combination with weekly retro-orbital injections of e23AON at either 0, 10, 50, or 300mg/kg (**Figure 1**). Experiments were blinded and performed within recently published guidelines⁶³. At the beginning of the study, 6-8 week old mice underwent stratified randomization based on age and weight. Mice were acclimated to the facility for one week. Then, using a staggered start method, cohorts of 9 mice (from random treatment groups) were initiated into the experiment because our workflow is limited to harvest of muscles of 9 mice per day. Mice were weighed weekly and dantrolene chow dose adjusted to maintain consistent dosing throughout the study. Serum levels of dantrolene were assessed at the end of the treatment period demonstrated levels of 0.27 +/- 0.18 ug/ml were achieved (**Supplementary Figure 2a,b,c**).

During the 6-month treatment, the mice did not show any change in body weight or feeding habits. Because of the potential for liver and kidney damage upon chronic treatment we assessed serum levels of γ -glutamyl transferase (GGT), creatinine, bilirubin and blood urea nitrogen (BUN) one week prior to sacrificing animals. We found no significant changes in these measures that were reflective of

kidney or liver toxicity (**Figure 2**). Dantrolene treatment led to a 18% decrease in serum BUN levels in all treated groups (**Figure 2**), though this decrease is not anticipated to be biologically significant. Hematoxylin and eosin staining did not reveal any differences in pathology of the heart, liver, and kidney associated with e23AON and dantrolene dosing (not shown).

After 6 months of combination therapy, levels of DMD exon skipping were determined in quadriceps and diaphragm using ddPCR (figure 3A). The data were not normally distributed but trended toward enhanced exon skipping with dantrolene/E23AON combination therapy relative to dantrolene alone. Further, dantrolene skip boosting activity was determined across multiple E23AON concentrations. Therefore, we determine that a Friedman's two way nonparametric ANOVA by ranks is ~~most~~ the most appropriate statistical tool. For this analysis, quantitative ddPCR readout for exon skipping in each mouse was ranked. Once ranked, the findings for each muscle, considered separately, were first fitted for E23AON, followed by dantrolene, and the possibility of their interaction. Based on this analysis, we find that E23AON has a highly significant positive treatment effect when considered across all E23AON concentrations combined in both quadriceps and diaphragm ($p < 0.0001$ for each, **Supplemental Figure 3**). Further, dantrolene/E23AON combination treatment significantly boosts mRNA exon skipping relative to E23AON treatment alone, when all E23AON concentrations tested are considered together ($p = 0.012$ for quadriceps, $p = 0.0008$ for diaphragm, **Figure 3b and Supplemental Figure 3**). Meta-analysis of the p values, utilizing the chi-squared distribution with 4 degrees of freedom, from quadriceps and diaphragm

combined demonstrate even higher confidence in dantrolene/E23AON treatment effect on exon skipping ($p=0.00012$), **Figure 3b**).

We next assessed dystrophin protein expression in mice treated with combination therapy both by quantitating the intensity of dystrophin immunofluorescence staining (**Figure 4a**) and the percentage of dystrophin positive fibers (**Figure 4b**) within transverse muscle sections. We used the same statistical model (Friedman's nonparametric two-way ANOVA by ranks) to demonstrate that dystrophin protein levels were also boosted when dantrolene was used in combination with e23AON with a high degree of confidence, when all E23AON concentrations are considered together for dystrophin immunofluorescence intensity in the quadriceps ($p=0.0032$) and for dystrophin positive fibers in the quadriceps ($p=0.0069$) and diaphragms ($p=0.0035$) (**Figure 4a,b,c,d and Supplemental Figure 4**). Using this analysis, statistical significance was not achieved for dystrophin immunofluorescence intensity in the diaphragm ($p=0.086$). However, meta-analysis of the p values, from quadriceps and diaphragm combined demonstrate greater confidence in dantrolene/E23AON treatment effect on dystrophin immunofluorescence ($p=0.0025$) and dystrophin positive fibers ($p=0.00028$, **Figure 4c**). The size of the effect is considerable. For example 300 mg/kg the dantrolene boost led to a doubling of dystrophin fluorescence from 13.9% to 27.5% and percent positive fibers from 12.6% to 23.1% of levels observed in control C57Bl6 mice in the quadriceps (**Figure 4a, 4b**).

Accordingly, combination therapy boosted dystrophin protein expression induced by e23AON, as measured by Western blot analysis of total protein in the

quadriceps (**Figure 5a,b**), with a high degree of certainty, determined using our statistical model ($p=0.0054$, **Figure 5c and Supplemental Figure 5**). Increases were on the order of 1% - 1.7% absolute levels of wildtype dystrophin.

To determine whether dantrolene helps promote sarcollemmal DGC protein stability ~~expression~~ in the context of e23AON treatment, we assessed dantrolene's effect on other members of the DGC. Long-term dantrolene combined with e23AON treatment rescued the sarcollemmal localization of both α -sarcoglycan and β -dystroglycan, indicators of DGC rescue. Figure 6 shows images from 50mg/kg e23AON treatment group (**Figure 6**); although similar results were seen at 10 and 300mg/kg e23AON (Data not shown). Immunostaining of skeletal muscle demonstrated the presence of intact N-terminal, rod domain, and C-terminal dystrophin protein sequences (**Supplementary Figure 6**). Serial sections of the quadriceps and diaphragm indicate that dystrophin-positive fibers colocalized with fibers expressing DGC proteins. Together, these findings demonstrate that dantrolene boosts e23AON activity during long-term treatment to facilitate restoration of dystrophin protein with sufficient functionality to enable DGC rescue and localization to the sarcolemma.

Dantrolene/e23AON combination therapy reverses pathology to a greater extent than e23AON alone.

Serum creatine kinase (CK) levels are an indicator of muscle fiber integrity, as muscle CK leaks into the serum upon membrane damage. After 6 months of treatment serum CK levels in *mdx* mice were reduced in response to e23AON, as expected. These levels were further reduced significantly with daily oral dantrolene

supplementation across all E23AON treatments combined as determined by our statistical model ($p < 0.0001$, **Figure 7a,b and Supplemental Figure 7**). In keeping with a previous report, *mdx* treatment with dantrolene alone, lowers CK to some extent^{64, 65}, but not to the same degree as treatment with dantrolene and e23AON combined. However, the high degree of rescue induced by each dantrolene and PMO alone preclude distinguishing between a synergistic versus additive effect.

To determine the effect of combination therapy on *mdx* muscle histopathology, we quantitated: 1) ongoing regeneration of myofibers by assessing embryonic myosin heavy chain (eMHC) expression; 2) degeneration/regeneration by assessing myofiber centronucleation⁶⁶⁻⁷¹. In the *mdx* model, muscle injury leads to increases in regeneration/degeneration, thus eMHC and centronucleation are each anticipated to decrease with dystrophin rescue. eMHC and centronucleation were both decreased in response to e23AON treatment alone (Supplementary Figure 8). Dantrolene further facilitates the decrease in centronucleation in the diaphragm to a high degree of certainty when examined across all E23AON treatments combined as determined by our statistical model ($p = 0.017$, **Figure 8a,d and Supplemental Figure 8**). Using this analysis, statistical significance was not achieved for centronucleation in the quadriceps ($p = 0.066$) Dantrolene also further facilitates the decrease in eMHC positive fibers in the quadriceps ($p = 0.021$) and diaphragm ($p = 0.025$) to a high degree of certainty using the same statistical tool (**Figure 8b,c,d and Supplemental Figure 8**). Meta-analysis of the p values, from quadriceps and diaphragm combined demonstrate even higher confidence in dantrolene/E23AON treatment effect on centronucleated fibers ($p = 0.0087$) and eMHC positive fibers ($p = 0.0045$, **Figure 4c**). These findings highlight that

dantrolene boost can impact *mdx* pathophysiology predicted to impact muscle function and highlights the potential of combination therapy to facilitate therapeutic outcome without detectable toxicity.

Meta-analyses performed on the results of a multivariate Friedman's two-way nonparametric ANOVA show that dantrolene significantly boosts the AON effect on all quantitative outcomes

To better evaluate the significance of dantrolene boost across both muscles, results from the multivariate analyses and meta-analyses across all outcomes are shown side by side in **Table 1**. Together, our meta-analyses demonstrate that dantrolene boosts the e23AON effect on all quantitative outcomes measured across both muscles with high significance (p-value 0.00012-0.0087).

Discussion

Here we provide preclinical mouse data in support of ~~using~~ repurposing dantrolene to boost AON-guided *DMD* exon skipping. Dantrolene is already FDA approved for both malignant hyperthermia and spasticity⁷² and has been used broadly in the pediatric population⁷³. When used in combination with e23AON, dantrolene increased e23 skipped mRNA, dystrophin protein expression, and rescue of pathophysiology after 6 months of chronic dosing in the *mdx* DMD mouse model,. We used a dosing scheme more compatible with human DMD treatment than our previous studies, attempting to more closely approximate a regimen of chronic oral dosing of dantrium.

While no published study exactly recapitulates our dosing scheme, two published studies report a higher degree of dystrophin rescue in mdx mice after long-term treatment with similar doses of morpholino. The reason for this is unclear. Possible explanations for differences observed between studies include: timing of dosing, length of study, quantitation or injection the input morpholino, or sensitivity of the methods used to measure dystrophin. Of note, the dystrophin output reported in the two published studies vary by two fold, implying that either dosing or variation in laboratory protocol can impact reported rescued dystrophin levels. Regardless, because we observed a significant dantrolene boost effect across all concentrations of PMO tested, such differences should not impact the conclusions reach regarding dantrolene efficacy as a skip booster. It should be noted that the relative fold change with dantrolene treatment reported in Table 1 is averaged across all e23AON concentrations tested. At higher doses of e23AON, dantrolene provides a greater therapeutic effect to the outcome measures assessed.

Mouse to human equivalence formulas would predict that a 30mg/kg/week Exondys51 dosing in boys weighing 20kg would be equivalent to 240 mg/kg weekly dosing in mice. However, AON exon skipping drug appears not to scale typically from mouse to dog using standard equivalence formulas based on surface area⁷⁴ and therefore, is unlikely to scale typically in humans. In our experiments the 300mg/kg e23AON dose in e23 skipping in mdx, induces 7% dystrophin distributed across 13% of the quadriceps fibers. By comparison, ExonDys51 induces significantly less dystrophin in DMD boys, on average 0.93% (range 0-2.47%), distributed across 16% of fibers (range 1.4-33.5%) relative to normal human muscle³¹. We suggest that the 50mg/kg morpholino e23AON dose in mdx is the

most equivalent to current human ExonDys51 dosing of 30mg/kg; at 50mg/kg e23AON we observed on average 5% dystrophin distributed across 7.1% of quadriceps fibers. Here, we demonstrate a boost of exon skipping activity at each 10, 50 and 300mg/kg/week e23AON dosing, when administered chronically with oral dantrolene. This broad range spans both the calculated and apparent equivalence estimates for Exondys51.

The pivotal Exondys51 trial used to support accelerated approval relied on 30-50 mg/kg weekly dosing in humans and was suggestive of some functional benefit. Along with accelerated approval, the FDA suggested that exploring higher and/or more frequent Exondys51 dosing to increase dystrophin rescue and clinical efficacy further. However, increasing the number of doses is unlikely to be practical and it is unclear if higher dosing is feasible from either a production or toxicity perspective. AON modifications that promise better delivery and that use skip boosting agents represent alternative approaches to increasing dystrophin levels. In addition to our identifying dantrolene boost activity, others have reported skip boosting using CELF2a inhibitors, 6-thioguanine, NOL8 protein, and carbohydrate-based infusions⁷⁵⁻⁷⁸. However, dantrolene is an already FDA approved drug with previous exposure in boys with DMD and a good safety profile. Given that dantrolene is effective across all concentrations of e23AON tested, it is reasonable to predict that it may boost Exondys51 activity at the approved dose.

We have previously published that dantrolene boosts AON exon 51 skipping in human patient fibroblast-derived myotube cultures³². Ongoing work in our laboratory indicates that dantrolene boosts human *DMD* exon skipping in combination with AON directed against additional *DMD* exons relevant to drugs

currently in the pipeline. (Barthélémy and Miceli, unpublished findings). Our published findings showing that dantrolene can boost skipping in combination with either AON or 2-o-methyl AON chemistries may indicate that dantrolene boost is agnostic to AON chemistry.

Dantrolene is an FDA approved drug indicated for chronic use for spasticity (1.5-6.5mg/kg⁷²) and acutely for malignant hyperthermia (4-8mg/kg⁷²) and widely studied in multiple animal models and humans⁷⁹⁻⁸³. It targets the RyR1, responsible for Ca²⁺ release from the sarcoplasmic reticulum and regulating levels of cytosolic and SR luminal Ca²⁺ levels essential for EC (excitation-contraction) coupling. In DMD, RyR is dysregulated, contributing to increased intracellular calcium and DMD pathology³⁷. As a potential means of controlling calcium-handling-defects in DMD, Bertorini et al administered 8 mg/kg/day dantrolene to 7 DMD boys over a two year period⁷³. In those studies, Dantrolene was well tolerated in 6/7 patients; 1/7 experienced increased, but mild muscle weakness that was reversed upon lowering the dose to 6mg/kg/day. A trend toward reducing manual muscle testing deterioration was observed in some patients and a statistically significant reduction in CK levels was reported. Though the data were insufficient to establish functional benefit, this study demonstrates long-term treatment with dantrolene can be tolerated in children with DMD.

We demonstrated reduced CK levels in mdx mice treated with dantrolene alone, but observed no effect on any other measures of mdx histopathology or exon skipping in the absence of e23AON, consistent with published data^{64, 65}. In one published study in mdx mice, 6 week dantrolene treatment reduced both CK levels and some, but not all, measures of strength, despite no observed effect on

histopathology.⁶⁴ Therefore, any planned AON/dantrolene combination therapy should include strength assessment and dose adjusting to minimize potential acute weakness induced by dantrolene.

In the current study, we measured dantrolene serum levels to be an average of 0.26 ug/mL +/-0.18, at the low end of the known therapeutic range used for other indications in humans (0.37 to 1.24 ug/mL)^{79, 84, 85}. Together with findings that other RyR calcium modulators, like RyCal S107, can also boost exon skipping, it is likely dantrolene boost activity results from RyR calcium modulation⁸⁶⁻⁸⁸. Calcium regulation of alternative splicing has been described in other models⁸⁹⁻⁹¹.

In our studies dantrolene boosts dystrophin levels by as much as 1-1.7 percent of wild type levels and allow expression in an additional 4-10 % of the fibers at the most relevant AON doses, an increase predicted to increase muscle function. Our findings provide pre-clinical support and guidance for combination AON/dantrolene therapy for enhancement of Exondys51 or other skipping drugs in the research pipeline. Because Exondys51 and dantrolene are already FDA approved, our findings can be rapidly translated from mouse to human trial, highlighting the value of screening FDA approved drugs for combination therapies that promise greater efficacy.

Methods

Long-term Treatment Blinding

The present randomized, blinded, placebo-controlled study was performed on 180 *mdx* mice. Factorial randomization was used and mice were stratified into treatment groups based on animal age and weight and randomly assigned to each

treatment group. 24 or 18 *mdx* mice aged 4-6 weeks were used in each group. Procedures involving all *mdx* mice were approved by the Institutional Animal Care and Use Committee (IACUC) of the University of California, Los Angeles (UCLA). Individuals dosing the mice and performing data-generating assays were blinded. Once all the data was collected, the blind was lifted for the individual performing statistics

Mice and Tissue Preparation

Procedures involving all *mdx* mice were approved by the Institutional Animal Care and Use Committee (IACUC) of the University of California, Los Angeles (UCLA). For three weeks and 6 months experiments with systemic injections of e23AON, the quadriceps were harvested and the right muscle was frozen in optimal cutting temperature compound (OCT) for sectioning and analysis by immunohistochemistry, whereas the left muscle was cut in half and snap-frozen for analysis by Western blot and ddPCR. For the diaphragm, one half of the muscle was designated for immunohistochemistry and one-fourth for Western blot and RT-PCR. Mice and chow were weighed weekly.

AON and dantrolene administration to *mdx* mice

e23AON morpholino⁹² (5'-GGCCAAACCTCGGCTTACCTGAAAT-3'; provided by Sarepta Therapeutics) was injected intravenously (retro-orbitally) in 100uL of saline. For three week experiments, Revonto (dantrolene sodium NDC 27505-001-65; DSM Pharmaceuticals, Inc.) was resuspended in water and administered by oral gavage in a 100uL bolus twice-daily. For 6 month experiments, control and

experimental feed was formulated into 58YP chow at 0, 1121 & 1328 parts per million (ppm) Dantrium from capsules (NDC 0115-4433-1 GlobalRPH) (Lot 10007332) and irradiated (Newco Distributors, Inc.) Mice were given *ad libitum* access to chow. The amount of chow consumed was weighed weekly to calculate daily dose of dantrolene per mouse.

RNA isolation, qPCR, and ddPCR

Total RNA was isolated from frozen skeletal muscle with the Qiagen RNeasy Fibrous Tissue Kit and reverse transcribed to complementary DNA (cDNA) using the iScript cDNA Synthesis Kit (Bio-Rad). The final concentration of digested total DNA was adjusted to fall within the linear range for the Poisson calculation for the expected number of droplets in the digital PCR. Each sample was partitioned into 15,000 droplets on a DG8 cartridge (Bio-Rad) and each droplet was amplified by PCR using the following protocol: initial denaturation step at 95 °C for 10 min, 40 cycles of 94°C for 30s and 60°C for 60s, followed by 98°C for 10 minutes. Primer-probe sets to assess specific full-length or skipped *Dmd* exon 23 mRNAs have been previously described³². For amplification of exons from 22-24; the percentage of exon skipping was expressed as the total exon 23 skipped transcript as a percentage of total (skipped +unskipped) *Dmd* transcript. Samples were loaded onto the QX200 droplet reader and ddPCR data were analyzed with QuantaSoft analysis software⁹³. The target concentration in each sample was expressed as copies per nanogram.

Measurement of serum creatine kinase, γ -glutamyl transpeptidase, creatinine, total bilirubin, and blood urea nitrogen

Blood was collected by retro-orbital bleeding of the mice. After clotting, samples were spun at 6,000 rpm at 4°C. Serum was collected, snap frozen in liquid nitrogen, and stored at -80°C. Creatine kinase analysis was performed with the Genzyme Creatine Kinase kit (BioPacific Diagnostic Inc.) γ -glutamyl transpeptidase, creatinine, total bilirubin, and blood urea nitrogen measurements were performed by the UCLA Division of Laboratory Animal Medicine (DLAM) Pathology & Laboratory Medicine Services.

Measurement of dantrolene serum levels

Blood was collected by retro-orbital bleeding of the mice. After clotting, samples were spun at 6,000 rpm at 4°C. Serum was collected, snap frozen in liquid nitrogen, and stored at -80°C. Dantrolene serum analysis was performed with the Dantrolene ELISA Kit (Neogen Corp.; Product #106319; Lot 140923) Samples were run in duplicate. Diluted dantrolene solution was used to generate a standard curve.

Western blot protocol

Total protein was isolated from flash-frozen quadriceps and diaphragms from the treated *MDX* and control C57 mice. Tissues were homogenized in Mito buffer [0.2 mM EDTA, 0.25 mM sucrose, 10 mM tris-HCl (pH 7.4)] with protease/phosphatase inhibitor cocktail (Pierce) and deoxyribonuclease/ribonuclease and subjected to low-speed (3000g) centrifugation for 10 min at 4°C. The supernatant was centrifuged at 100,000g (high-speed centrifugation) for 1 hour for isolation of membrane fraction. Isolated membranes and pellet after low-speed centrifugation were combined and resuspended in 300 ml

of extraction buffer [50 mM tris-HCl (pH 7.4), 7 M urea, 2 M thiourea, 4% CHAPS, 2% SDS, 50 mM β-mercaptoethanol]. Protein concentration was determined by 2-D Quant Kit (GE Healthcare Life Sciences).

Forty micrograms of total protein were run on a 6% polyacrylamide gel and transferred onto a nitrocellulose membrane for 2 hours at 4°C. The membrane was blocked for 1 hour in 5% milk and then incubated with MANDYS8 (Sigma) (anti-dystrophin), 1:400 in TBS-T, hVin-1 (Sigma), 1:5000 in TBST (antivinculin), a skeletal muscle membrane protein not associated with the DGC that was used as a loading control.

For analysis, dystrophin protein levels were normalized to the loading and then pooled across treatment groups to determine the average dystrophin rescue. Serial dilutions of C57 sample into untreated *MDX* sample were run simultaneously. All western data included were run through quality control, as defined by linearity of dilution of C57 controls. The average densitometry value for 100% of dystrophin in C57 was calculated as mean of densitometry values of C57 serial dilutions multiplied by dilution factor. Densitometry analysis was performed with ImageLab 5.1 gel documentation system (Bio-Rad).

Histology and Immunofluorescence

Immunohistochemistry (IHC) was performed on unfixed 10-mm tissue sections using MouseOnMouse kit (Vector Labs). IHC assessment used the following primary antibodies: MANDYS8 (dystrophin rod domain), Ab15277 (dystrophin C terminus; Abcam), and Manex1A (dystrophin N terminus; Developmental Studies Hybridoma Bank). □-Sarcoglycan was detected with NCL-□□ -SARC (Novocastra), □-

dystroglycan with NCL- DG (Novocastra), eMHC (DSHB; BF-G6-c), and DNA with 4',6-diamidino-2-phenylindole (DAPI). Secondary labeling was performed with fluorescein isothiocyanate (FITC) anti-mouse or FITC anti-rabbit (Vector Labs). Sections were mounted in Vectashield Mounting Medium (Vector Labs). Fluorescent images were acquired and analyzed using Ariol SL-50 (Applied Imaging Corp., San Jose, CA). The Ariol scanner is based on an Olympus BX61 microscope with motorized stage and autofocus capabilities, equipped with a black and white video camera (Jai CVM2CL). Scanning and analyses were performed through the Translational Pathology Core Laboratory, Department of Pathology and Laboratory Medicine, David Geffen School of Medicine at UCLA. For quantifying dystrophin immunofluorescence, the minimum threshold was placed above background level for all sections. Analytical readouts included: area of IFL signal (area of signal above the signal threshold) and total area of the section. The total area of positive pixels above the minimum threshold per muscle section was counted using AxioVision Rel.4.6.3.0 acquisition software. Each sample's dystrophin immunofluorescent levels are expressed as a percentage of area of positive pixels in C57 (100%). For quantifying dystrophin positive fibers, the minimum threshold was placed above background level for all sections. For each sample, fibers were counted across the entire section. Dystrophin positive fibers were defined as fibers that had sarcolemmal dystrophin expression above background and surrounding >75-80% of each fiber. For both measurements, all of our readings were well below the maximal intensity threshold (pixel saturation was avoided). DGC localized on revertant fibers were controlled for in IHC by inclusion of placebo-treated mdx controls for all experiments. For quantifying centronucleation and

eMHC positive fibers, diaphragms and quads from the 3-6 mice per treatment group, which had total dystrophin levels by western blot near the median were selected. The average percentage of fibers with centrally located nuclei in the diaphragm per group was determined by counting entire muscle cross sections. For quantifying eMHC positive fibers, quadriceps/diaphragms from 6 mice per group which had total dystrophin levels by western blot near the median were selected. The total number of eMHC positive fibers were counted and compared to the total number of muscle fibers per section. For pathology, a standard protocol was used for hematoxylin and eosin (H&E) staining. All mouse liver, heart, and kidney were reviewed blindly by a certified pathologist.

Statistical Analysis

We observed that the data from our study were not normally distributed. Therefore, we performed a Friedman's Two-way Nonparametric ANOVA by ranks using SAS software (version 9.4, SAS Institute Inc., Cary, NC), where we ran a statistical analyses on the ranks of the observations for each of the 7 traits (or assays). We ran the data taken from the quadriceps, diaphragm or serum separately. The model fit E23AON first followed by dantrolene and the possibility of their interaction. In every case, E23AON was highly significantly ($p < 0.0001$) with the trait except for centronucleated fibers in the quadriceps, which was still significant ($p < 0.04$) (data not shown). Table 1 presents the p-values for dantrolene for each of the outcome measures. For this portion of the analyses, a conservative significance was set at 0.01 to allow for testing multiple traits and the possibility of their non-independence. A meta analyses was performed on the p-

values from the quadriceps and diaphragm utilizing the chi-squared distribution with 4 degrees of freedom.

Acknowledgements

We thank J. Wen and L. Martinez for providing technical support. We thank F. Barthélémy for critical reading and provide expert input throughout the project. Scanning, quantitative analysis of muscle cross-sections, and staining & histological analysis of organs were performed at the UCLA Translational Pathology Core Laboratory. Funding: This work was primarily funded from grants from the NIH (1T32AR65972A1) and the California Institute of Regenerative Medicine (TRX-05426). Support for the research was also provided by the UCLA Muscular Dystrophy Core Center (NIH grant 5P30AR057230) within the Center for Duchenne Muscular Dystrophy at UCLA. Author contributions: D.W.W. led the implementation of mouse experiments and performed the RNA skipping quantification experiments, pathophysiology experiments, and serum biomarker experiments. E.I.M. performed muscle sectioning and quantitative immunohistochemistry and Western blotting for dystrophin. Y.B.N. performed pathological assessment. D.W.W. contributed as first author. EKM, G.C.K., and D.B. provided technical support. D.W.W., M.C.M., and S.F.N. wrote the manuscript with input from the other authors. M.C.M. and S.F.N. conceived the project, designed the experiments, supervised the entire study, and contributed equally. M.J.S. helped supervise, and implement the mouse dosing together with M.C.M. and S.F.N. R.C. helped to create the statistical model and meta-analysis used in the study. M.C.M. and S.F.N. contributed equally as senior authors. Competing interests: S.F.N., M.C.M. are inventors on a pending patent on

identification of small molecules that enhance exon skipping filed by UCLA.

Competing interests: S.F.N., M.C.M., and M.M. are inventors on a pending patent on identification of small molecules that enhance exon skipping filed by UCLA.

Figure Legends

Figure 2-1. Overview of long-term dosing experiment.

(a) Treatment groups for 6-8 week old mdx mice subjected to 6 months combination therapy. (b) Protocol outline for long-term dosing experiment.

Figure 2-2. 6-month treatment with 10, 50, and 300 mg/kg e23AON with dantrolene did not adversely effect serum biomarkers and histopathology.

(a) The levels of the following serum enzymes were analyzed: γ -glutamyltransferase (GGT) (U/L), creatinine (mg/dL), total bilirubin (mg/dL), blood urea nitrogen (BUN) (mg/mL). A significant reduction in BUN levels were observed with addition of dantrolene in mice receiving 0, 10, 50, and 300 mg/kg e23AON when compared to their e23AON only counterparts. (* $P \leq 0.05$ compared to e23AON only control, # $P \leq 0.01$ compared to e23AON only control, † $P \leq 0.001$ compared to e23AON only control. Two-tailed t-test)

Figure 2-3. Dantrolene boosts e23AON to promote RNA exon 23 skipping.

(a) Effect of dantrolene on e23AON induction of *Dmd* exon 23 skipping as determined by the ratio of skipped/(skipped+unskipped) DMD mRNA-for the quadriceps and diaphragm. mRNA from each muscle in each treatment group was

quantified independently. Each point represents a single mouse; ‡ Dantrolene was dosed at 30-70mg/kg/day. (b) P-values from the multivariate assessment of the effect of dantrolene on e23AON treatment for exon 23 skipped / (skipped + unskipped) transcript as measured by ddPCR. P-values were determined by performing a Friedman's Two-way Nonparametric ANOVA by ranks using SAS software. A conservative significance was set at 0.01 to allow for testing multiple traits and the possibility of their non-independence. A meta analyses was performed on the p-values from the quadriceps and diaphragm utilizing the chi-squared distribution with 4 degrees of freedom.-

Figure 2-4. Dantrolene boosts 23AON to promote rescue of dystrophin immunofluorescence intensity and percent dystrophin-positive fibers.

(a) Effect of dantrolene on e23AON-induced skipped dystrophin protein as measured by quantitative immunofluorescence of individual quadriceps and diaphragms stained with an anti-dystrophin antibody (MANDYS8) that recognizes the rod domain of dystrophin. One cross-section per muscle per animal was evaluated for total dystrophin signal above a minimum background threshold and normalized to total cross sectional area as described in the methods. Data are presented a percent of C57 control levels of dystrophin. (b) Effect of dantrolene on e23AON-induced expression of dystrophin protein in mdx mice treated for 6 months. in as measured by % dystrophin-positive fibers in individual quadriceps and diaphragms. One cross-section per muscle per animal was evaluated for dystrophin expression. ‡ Dantrolene was dosed at 30-70mg/kg/day. (c) P-values from the multivariate assessment of the effect of dantrolene on e23AON treatment

for dystrophin immunofluorescence quantitation and dystrophin positive fibers. P-values were determined by performing a Friedman's Two-way Nonparametric ANOVA by ranks using SAS software. A conservative significance was set at 0.01 to allow for testing multiple traits and the possibility of their non-independence. A meta analyses was performed on the p-values from the quadriceps and diaphragm utilizing the chi-squared distribution with 4 degrees of freedom. For dystrophin immunofluorescence quantitation. (d) Effect of dantrolene on e23AON sarcolemmal dystrophin expression as illustrated by representative images from quadriceps and diaphragms of mdx mice after treatment with e23AON +/- dantrolene. Scale bar, 50µm.

Figure 2-5. Dantrolene boosts e23AON to promote rescue of dystrophin protein after chronic treatment.

(a) Western blot demonstrating the effect of dantrolene on e23AON-induced expression of total dystrophin protein in mdx mice treated for 6 months. Protein from each muscle of mice in all treatments group was isolated and quantified independently. † Dantrolene was dosed at 30-70mg/kg/day. (b) Representative Western blots for dystrophin protein expression from quadriceps are shown. C57Bl/6 protein was loaded at 25%, 12.5%, and 6.25% dilutions (diluted in protein samples from mdx mice to serve as a standard.) (c) P-values from the multivariate assessment of the effect of dantrolene on e23AON treatment for dystrophin protein by western blot. P-values were determined by performing a Friedman's Two-way Nonparametric ANOVA by ranks using SAS software. A conservative significance was set at 0.01 to allow for testing multiple traits and the possibility of their non-

independence. A meta analyses was performed on the p-values from the quadriceps and diaphragm utilizing the chi-squared distribution with 4 degrees of freedom.

Figure 2-6. Dantrolene/e23AON combination therapy restores sarcolemmal dystrophin and DGC after chronic treatment.

Effect of dantrolene/e23AON combination therapy on rescue of DGC components as illustrated by representative immunofluorescence images of serial cross-sections from treated mdx quadriceps. Dystrophin was detected with an antibody specific to the rod domain (MANDYS8). Additional DGC components, α -sarcoglycan and β -dystroglycan, were detected with NCL- α -SARC and NCL- β -DG antibodies, respectively. ‡ Dantrolene was dosed at 30-70mg/kg/day.

Figure 2-7. Creatine kinase reduction boosted with dantrolene/e23AON combination therapy.

(a) A reduction in creatine kinase levels with addition of dantrolene in mice receiving 0, 10, and 50 mg/kg e23AON/dantrolene combination (b) P-values from the multivariate assessment of the effect t of dantrolene on e23AON treatment for serum CK levels. P-values were determined by performing a Friedman's Two-way Nonparametric ANOVA by ranks using SAS software. A conservative significance was set at 0.01 to allow for testing multiple traits and the possibility of their non-independence.

Figure 2-8. Reduction of centronucleation in the diaphragm and eMHC positive fibers in the quadriceps treatment with e23AON and dantrolene.

(a) Cross-sections of diaphragm muscles were stained with H&E, highlighting centronucleated fibers, and the percentage of fibers with centrally located nuclei was counted (b,c) Cross-sections of diaphragm and quadriceps muscles were stained with anti-eMHC, highlighting regenerating fibers. (* $P \leq 0.05$ compared to e23AON only control. *** $P \leq 0.001$ compared to e23AON only control. Two-tailed t-test; † Dantrolene was dosed at 30-70mg/kg/day. (d) P-values from the multivariate assessment of the effect of dantrolene on e23AON treatment for centronucleation and eMHC positive fibers. P-values were determined by performing a Friedman's Two-way Nonparametric ANOVA by ranks using SAS software. A conservative significance was set at 0.01 to allow for testing multiple traits and the possibility of their non-independence. A meta analyses was performed on the p-values from the quadriceps and diaphragm utilizing the chi-squared distribution with 4 degrees of freedom.

Table 2-1. Friedman's two-way nonparametric ANOVA and meta-analyses of the effect of dantrolene on e23AON treatment for all quantitative outcomes

Relative fold change and p-values of the effect of dantrolene on e23AON treatment for all quantitative outcomes measured in the study. P-values were determined by performing a Friedman's Two-way Nonparametric ANOVA by ranks using SAS software. A conservative significance was set at 0.01 to allow for testing multiple traits and the possibility of their non-independence. A meta analyses was

performed on the p-values from the quadriceps and diaphragm utilizing the chi-squared distribution with 4 degrees of freedom.

Supplementary Figure 2-1. Oral Dantrolene synergizes with systemically delivered e23AON to promote exon 23 skipping and restoration dystrophin expression after 3 weeks treatment.

Effect of Dantrolene on e23AON-induced skipped dystrophin protein as measured by quantitative immunofluorescence of individual quadriceps and diaphragms. Mice were dosed systemically with once weekly e23AON at 0, 10, 50, and 300 mg/kg. One cross-section per muscle per animal was evaluated for dystrophin expression, and data are presented as a percent of C57 control levels of dystrophin. Error bars represent one standard deviation from the mean. n = 4 – 5. ‡ Dantrolene was dosed at 30-70mg/kg/day. (*P≤0.05 compared to e23AON only control by two-tailed t-test.)

Supplementary Figure 2-2. Dantrolene was detected at physiologically relevant levels in the serum of mice fed with dantrolene chow.

(a) Serum was isolated from all mice after 26 weeks of treatment. Dantrolene was detected by ELISA. Each sample run in duplicate. Variability shown is between mice, not samples n = 60. (b) A standard curve was included on each plate to ensure linearity and all experimentally determined points were within the limits of the dantrolene standard curve.

Supplementary Figure 2-3. Results of Friedman's two-way nonparametric ANOVA on the effect of dantrolene on e23AON treatment for exon 23 skipped / (skipped + unskipped) transcript as measured by ddPCR.

For this analysis, quantitative ddPCR readout of skipped/(skipped+unskipped) for exon skipping in each mouse was ranked. Once ranked, the findings for each muscle, considered separately, were first fitted for PMO, followed by dantrolene, and the possibility of their interaction.

Supplementary Figure 2-4. Results of Friedman's two-way nonparametric ANOVA on the effect of dantrolene on e23AON treatment for dystrophin immunofluorescence quantitation and dystrophin positive fibers.

For this analysis, quantitative dystrophin immunofluorescence quantitation and dystrophin positive fibers.readout in each mouse was ranked. Once ranked, the findings for each muscle, considered separately, were first fitted for PMO, followed by dantrolene, and the possibility of their interaction.

Supplementary Figure 2-5. Results of Friedman's two-way nonparametric ANOVA on the effect of dantrolene on e23AON treatment for dystrophin protein by western blot.

For this analysis, quantitative readout of dystrophin protein by western blot.in each mouse was ranked. Once ranked, the findings for each muscle, considered separately, were first fitted for PMO, followed by dantrolene, and the possibility of their interaction.

Supplementary Figure 2-6. Combination therapy rescues expression of dystrophin with presence of N-terminal, rod domain, and C-terminal protein sequences.

Dystrophin was detected with antibodies specific to the N-terminal domain (Manex1A), rod domain (MANDYS8), and C-terminal domain (Ab15277) , respectively. “-” defined as 0mg/kg daily dose dantrolene. “+” defined as 30-70mg/kg daily dose dantrolene.

Supplementary Figure 2-7. Results of Friedman’s two-way nonparametric ANOVA on the effect of dantrolene on e23AON treatment for serum CK levels.

For this analysis, quantitative readout of serum CK levels in each mouse was ranked. Once ranked, the findings for each muscle, considered separately, were first fitted for PMO, followed by dantrolene, and the possibility of their interaction.

Supplementary Figure 2-8. Results of Friedman’s two-way nonparametric ANOVA on the effect of dantrolene on e23AON treatment for centronucleation and eMHC positive fibers.

For this analysis, quantitative readout for centronucleation and eMHC positive fibers in each mouse was ranked. Once ranked, the findings for each muscle, considered separately, were first fitted for PMO, followed by dantrolene, and the possibility of their interaction.

Figures

Figure 2-1. Overview of long-term dosing experiment.

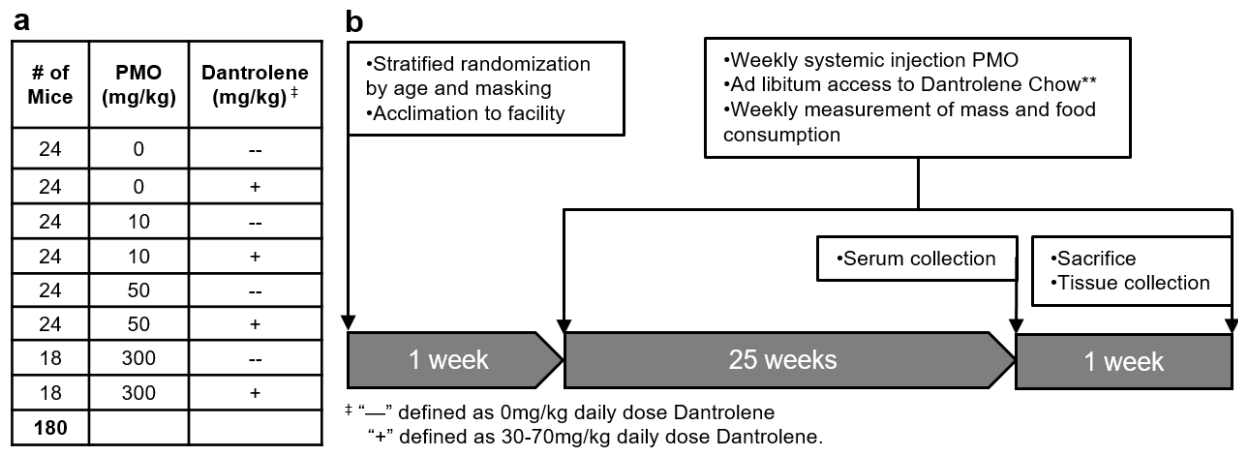


Figure 1 Overview of long-term dosing experiment. (a) Treatment groups for 6-8 week old *mdx* mice subjected to 6 months combination therapy. **(b)** Protocol outline for long-term dosing experiment.

Figure 2-2. 6-month treatment with 10, 50, and 300 mg/kg e23AON with dantrolene did not adversely affect serum biomarkers and histopathology.

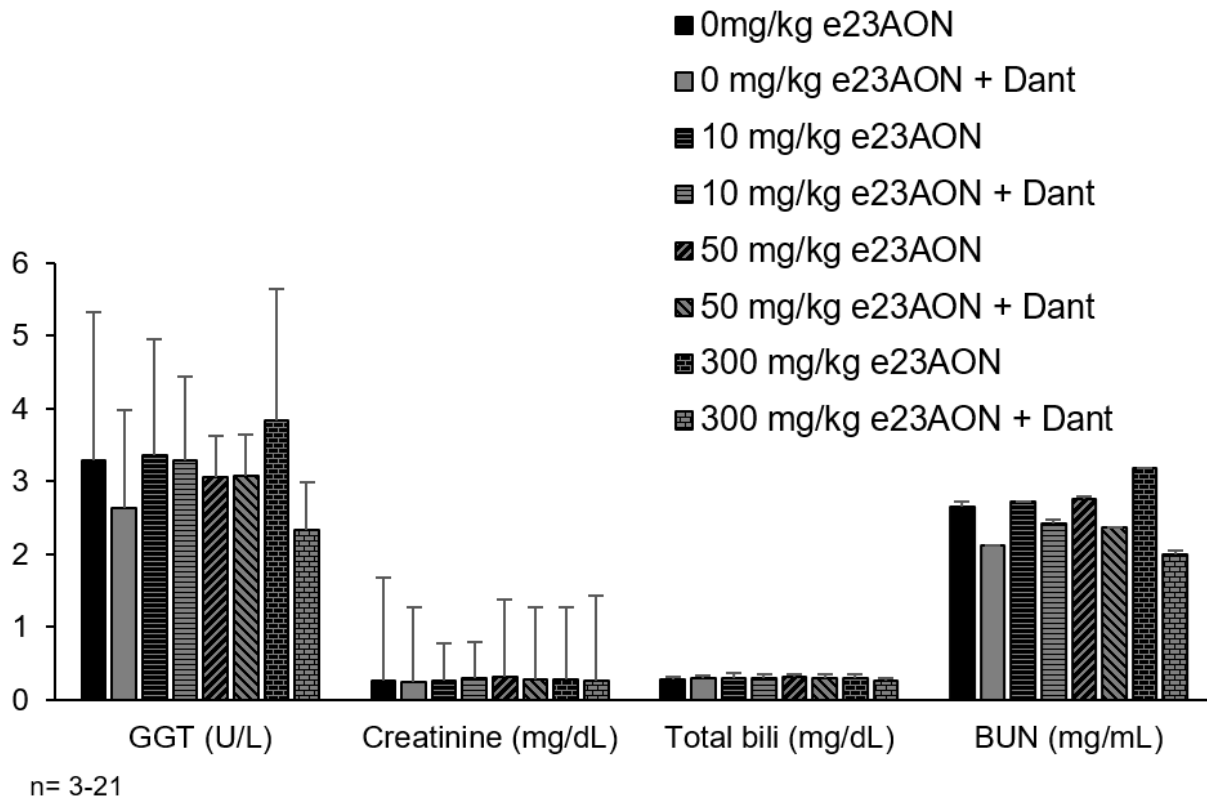
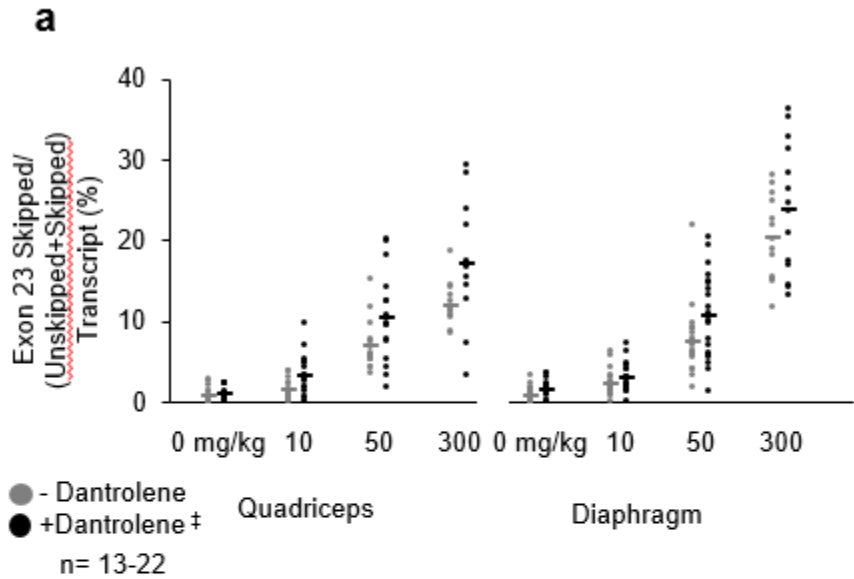


Figure 2-3. Dantrolene boosts e23AON to promote RNA exon 23 skipping.



b

Outcome Measure	Relative Fold Change with <u>Dantrolene Treatment</u>	Friedman's Two-way ANOVA by ranks		Meta analysis
		Quadriceps (p-value)	Diaphragm (p-value)	
Exon 23 skipped / (skipped + unskipped) transcript (%)	1.37	0.012	0.0008	0.00012

Figure 2-4. Dantrolene boosts 23AON to promote rescue of dystrophin immunofluorescence intensity and percent dystrophin-positive fibers.

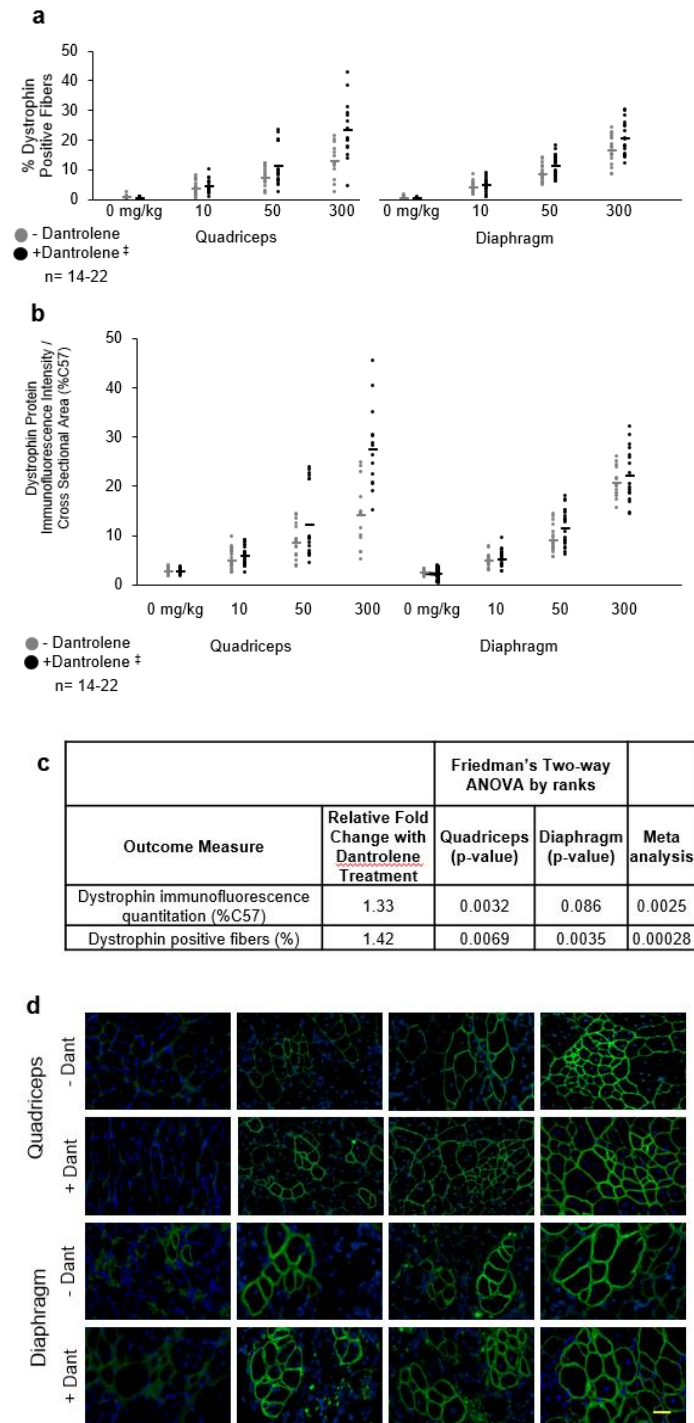
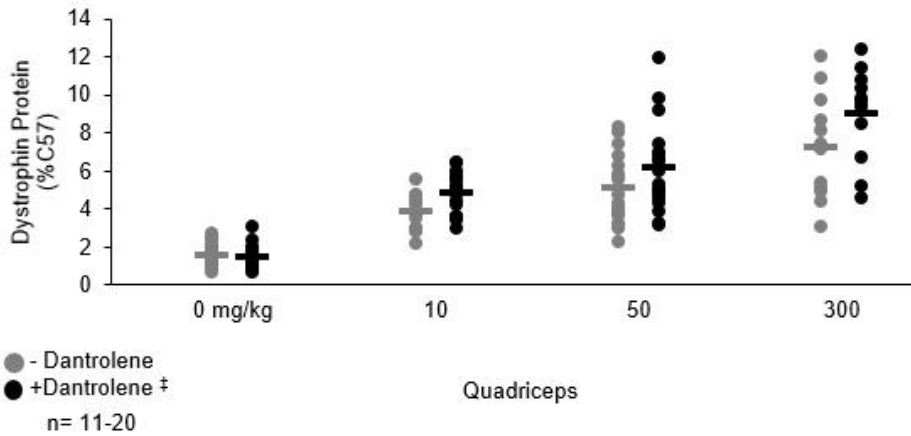
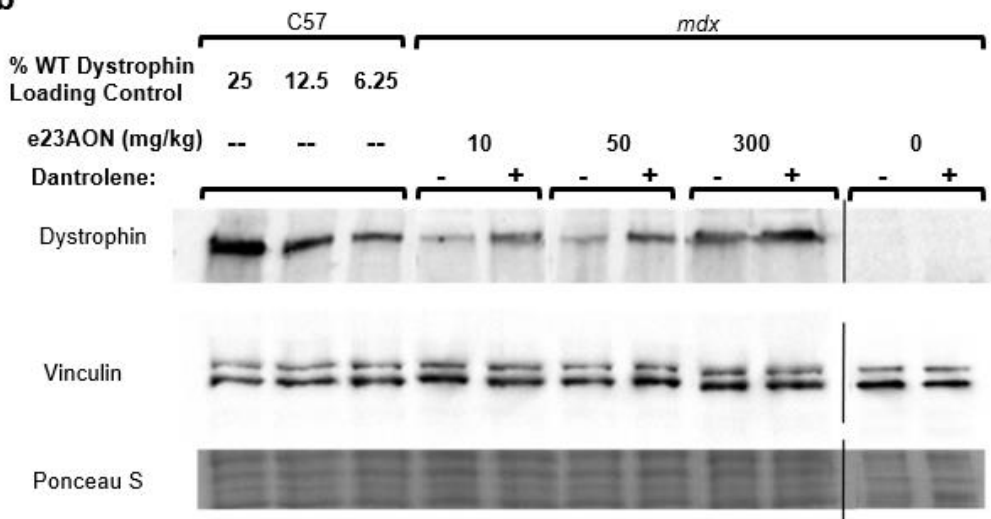


Figure 2-5. Dantrolene boosts e23AON to promote rescue of dystrophin protein after chronic treatment.

a



b



c

		Friedman's Two-way ANOVA by ranks
Outcome Measure	Relative Fold Change with <u>Dantrolene Treatment</u>	Quadriceps (p-value)
Dystrophin protein by Western blot (%C57)	1.23	0.0054

Figure 2-6. Dantrolene/e23AON combination therapy restores sarcolemmal dystrophin and DGC after chronic treatment.

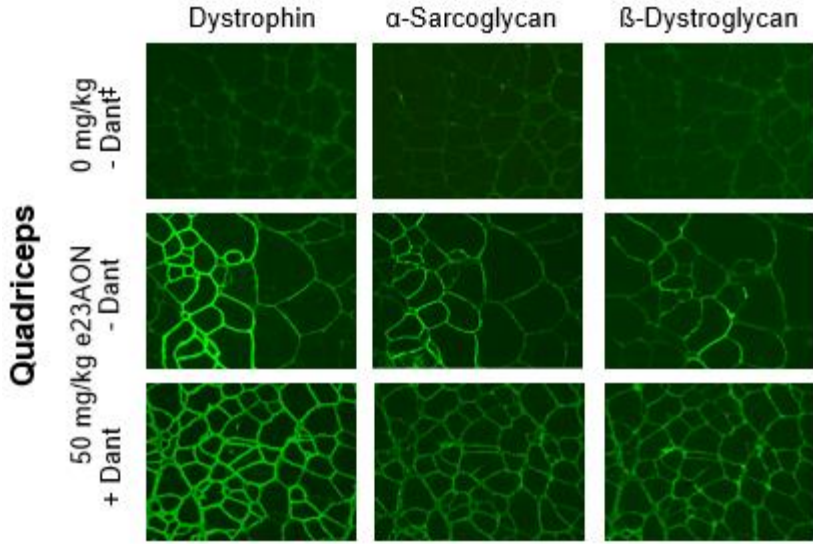
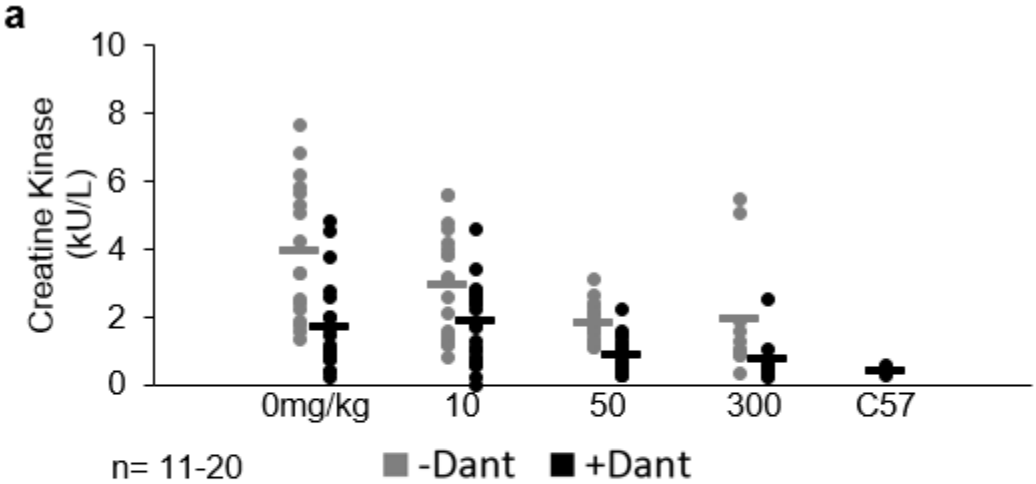


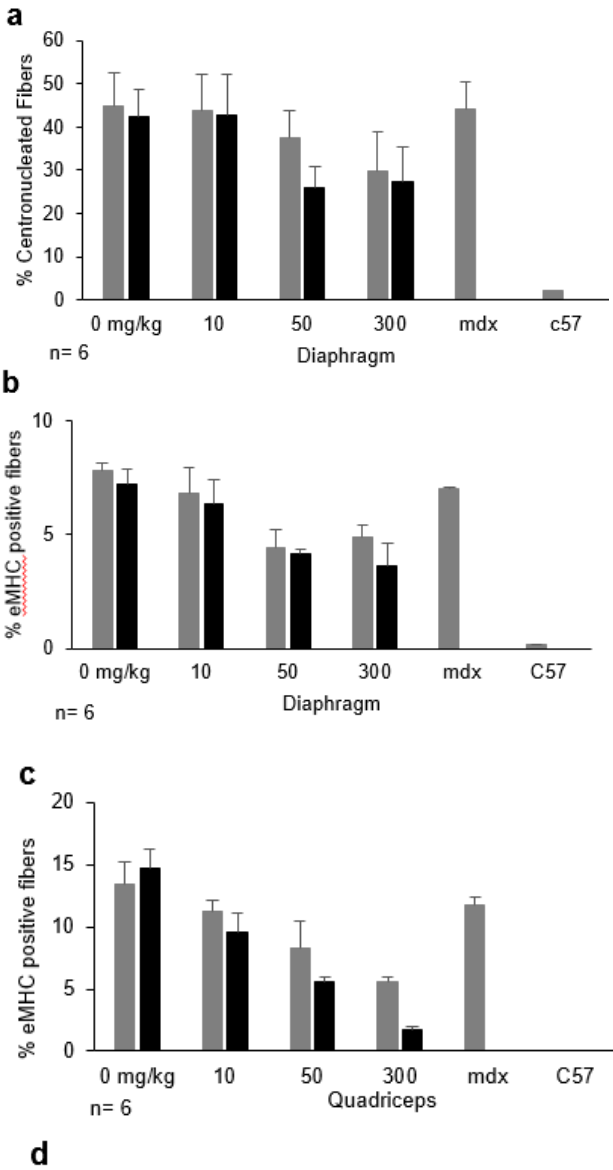
Figure 2-7. Creatine kinase reduction boosted with dantrolene/e23AON combination therapy.



b

		Friedman's Two-way ANOVA by ranks
Outcome Measure	Relative Fold Change with <u>Dantrolene Treatment</u>	Serum (p-value)
Serum CK	0.49	<0.0001

Figure 2-8. Reduction of centronucleation in the diaphragm and eMHC positive fibers in the quadriceps treatment with e23AON and dantrolene.

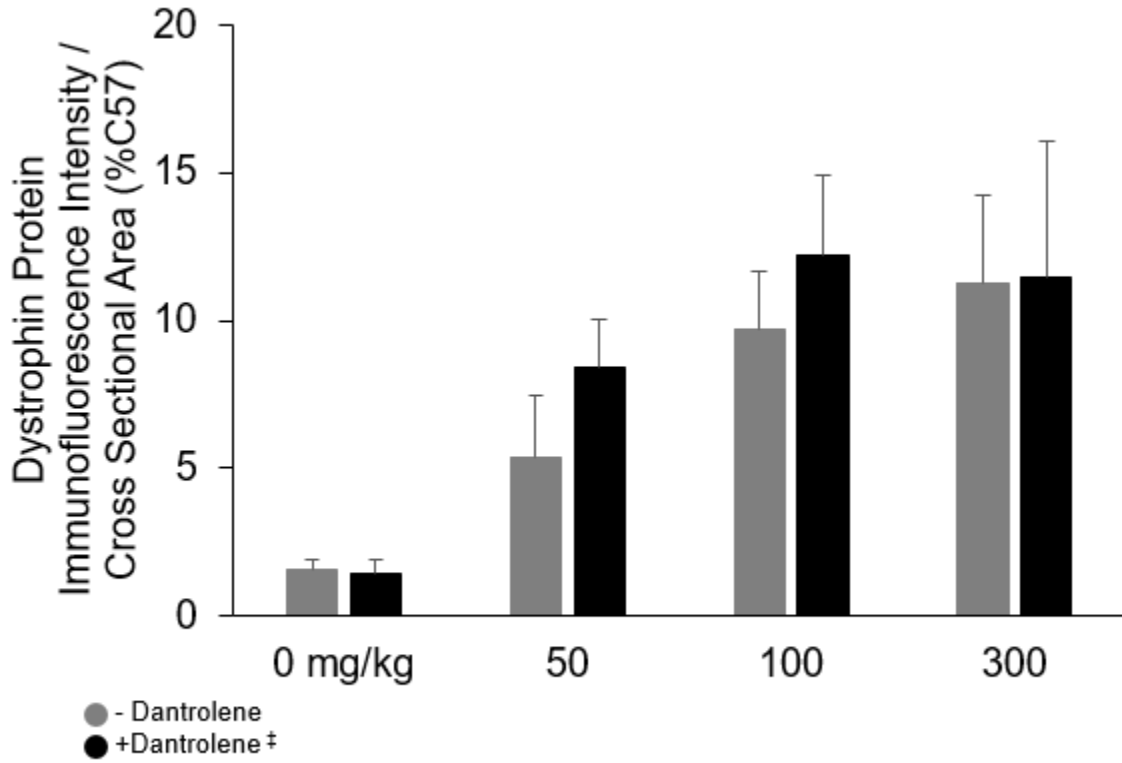


Outcome Measure	Relative Fold Change with Dantrolene Treatment	Friedman's Two-way ANOVA by ranks		Meta analysis
		Quadriceps (p-value)	Diaphragm (p-value)	
Centronucleated fibers (%)	0.97	0.066	0.017	0.0087
eMHC positive fibers (%)	0.83	0.021	0.025	0.0045

Table 2-1. Friedman’s two-way nonparametric ANOVA and meta-analyses of the effect of dantrolene on e23AON treatment for all quantitative outcomes

Outcome Measure	n	Relative Fold Change with <u>Dantrolene Treatment</u>	Quadriceps (p-value)	Diaphragm (p-value)	Serum (p-value)	Meta analysis
Exon 23 skipped / (skipped + unskipped) transcript (%)	124	1.37	0.012	0.0008	--	0.00012
Dystrophin immunofluorescence quantitation (%C57)	152	1.33	0.0032	0.086	--	0.0025
Dystrophin positive fibers (%)	154	1.42	0.0069	0.0035	--	0.00028
Dystrophin protein by Western blot (%C57)	131	1.23	0.0054	--	--	--
<u>Centronucleated</u> fibers (%)	47	0.97	0.066	0.017	--	0.0087
<u>eMHC</u> positive fibers (%)	47	0.83	0.021	0.025	--	0.0045
Serum CK	132	0.49	--	--	<0.0001	--

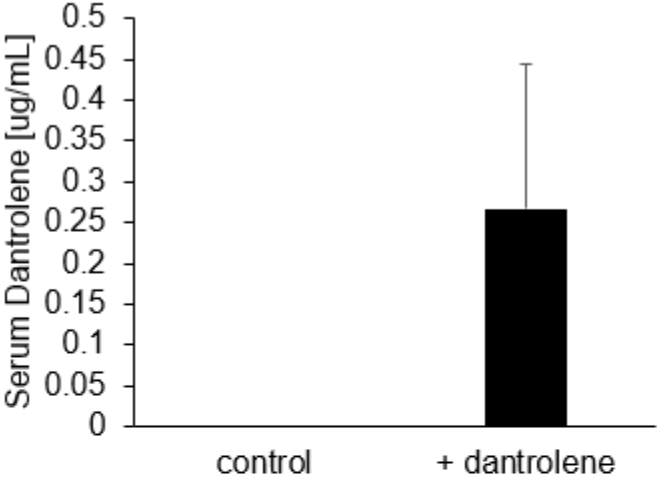
Supplementary Figure 2-1. Oral Dantrolene synergizes with systemically delivered e23AON to promote exon 23 skipping and restoration dystrophin expression after 3 weeks treatment.



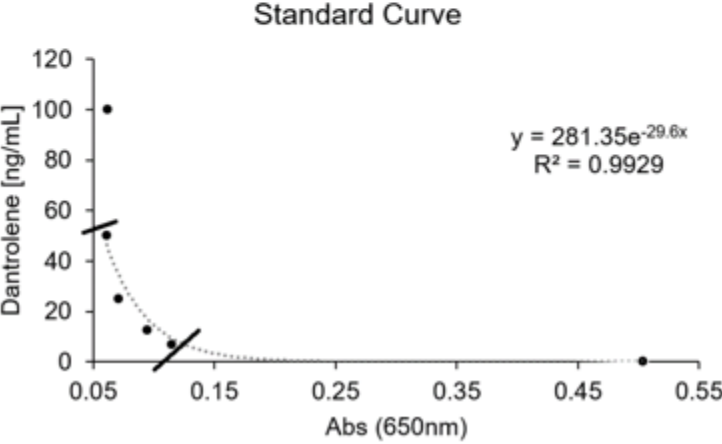
Supplemental Figure 1.

Supplementary Figure 2-2. Dantrolene was detected at physiologically relevant levels in the serum of mice fed with dantrolene chow.

a



b



Supplementary Figure 2-3. Results of Friedman's two-way nonparametric ANOVA on the effect of dantrolene on e23AON treatment for exon 23 skipped / (skipped + unskipped) transcript as measured by ddPCR.

Friedman's Two-way Nonparametric ANOVA

The ANOVA Procedure

Dependent Variable: RPCR_Q Rank for Variable PCR_Q

Source	DF	Sum of Squares	Mean Square	F Value	Pr > F
Model	7	125825.9029	17975.1290	57.16	<.0001
Error	117	36794.5971	314.4837		
Corrected Total	124	162620.5000			

R-Square	Coeff Var	Root MSE	RPCR_Q Mean
0.773739	28.14871	17.73369	63.00000

Source	DF	Anova SS	Mean Square	F Value	Pr > F
PMO	3	121276.2635	40425.4212	128.55	<.0001
Dantrolene	1	2051.5705	2051.5705	6.52	0.0119
PMO*Dantrolene	3	2498.0689	832.6896	2.65	0.0522

Dependent Variable: RPCRD Rank for Variable PCR_D

Source	DF	Sum of Squares	Mean Square	F Value	Pr > F
Model	7	203225.7682	29032.2526	71.56	<.0001
Error	138	55990.2318	405.7263		
Corrected Total	145	259216.0000			

R-Square	Coeff Var	Root MSE	RPCRD Mean
0.784002	27.40496	20.14265	73.50000

Source	DF	Anova SS	Mean Square	F Value	Pr > F
PMO	3	198329.0385	66109.6795	162.94	<.0001
Dantrolene	1	4756.2345	4756.2345	11.72	0.0008
PMO*Dantrolene	3	140.4953	46.8318	0.12	0.9509

Supplementary Figure 2-4. Results of Friedman’s two-way nonparametric ANOVA on the effect of dantrolene on e23AON treatment for dystrophin immunofluorescence quantitation and dystrophin positive fibers.

Friedman's Two-way Nonparametric ANOVA

The ANOVA Procedure

Dependent Variable: RC57_Q Rank for Variable C57_Q

Source	DF	Sum of Squares	Mean Square	F Value	Pr > F
Model	7	229837.8073	32833.9725	69.48	<.0001
Error	145	68523.1927	472.5737		
Corrected Total	152	298361.0000			

R-Square	Coeff Var	Root MSE	RC57_Q Mean
0.770335	28.23216	21.73876	77.00000

Source	DF	Anova SS	Mean Square	F Value	Pr > F
PMO	3	222163.5627	74054.5209	156.70	<.0001
Dantrolene	1	4256.7113	4256.7113	9.01	0.0032
PMO*Dantrolene	3	3417.5333	1139.1778	2.41	0.0693

Dependent Variable: RC57D Rank for Variable C57D

Source	DF	Sum of Squares	Mean Square	F Value	Pr > F
Model	7	300546.6800	42935.2400	188.79	<.0001
Error	151	34341.8200	227.4293		
Corrected Total	158	334888.5000			

R-Square	Coeff Var	Root MSE	RC57D Mean
0.897453	18.85095	15.08076	80.00000

Source	DF	Anova SS	Mean Square	F Value	Pr > F
PMO	3	299112.7209	99704.2403	438.40	<.0001
Dantrolene	1	677.9429	677.9429	2.98	0.0863
PMO*Dantrolene	3	756.0161	252.0054	1.11	0.3478

Dependent Variable: RPostiveQ Rank for Variable PostiveQ

Source	DF	Sum of Squares	Mean Square	F Value	Pr > F
Model	7	246586.4318	35226.6331	81.65	<.0001
Error	147	63418.5682	431.4188		
Corrected Total	154	310005.0000			

R-Square	Coeff Var	Root MSE	RPostiveQ Mean
0.795427	26.62901	20.77062	78.00000

Source	DF	Anova SS	Mean Square	F Value	Pr > F
PMO	3	239888.7374	79962.9125	185.35	<.0001
Dantrolene	1	3234.0959	3234.0959	7.50	0.0069
PMO*Dantrolene	3	3463.5985	1154.5328	2.68	0.0494

Dependent Variable: RPostiveD Rank for Variable PostiveD

Source	DF	Sum of Squares	Mean Square	F Value	Pr > F
Model	7	316449.4676	45207.0668	185.92	<.0001
Error	154	37446.5324	243.1593		
Corrected Total	161	353896.0000			

R-Square	Coeff Var	Root MSE	RPostiveD Mean
0.894188	19.13321	15.59357	81.50000

Source	DF	Anova SS	Mean Square	F Value	Pr > F
PMO	3	312734.6671	104244.8890	428.71	<.0001
Dantrolene	1	2141.8141	2141.8141	8.81	0.0035
PMO*Dantrolene	3	1572.9864	524.3288	2.16	0.0955

Supplementary Figure 2-5. Results of Friedman's two-way nonparametric ANOVA on the effect of dantrolene on e23AON treatment for dystrophin protein by western blot.

Friedman's Two-way Nonparametric ANOVA

The ANOVA Procedure

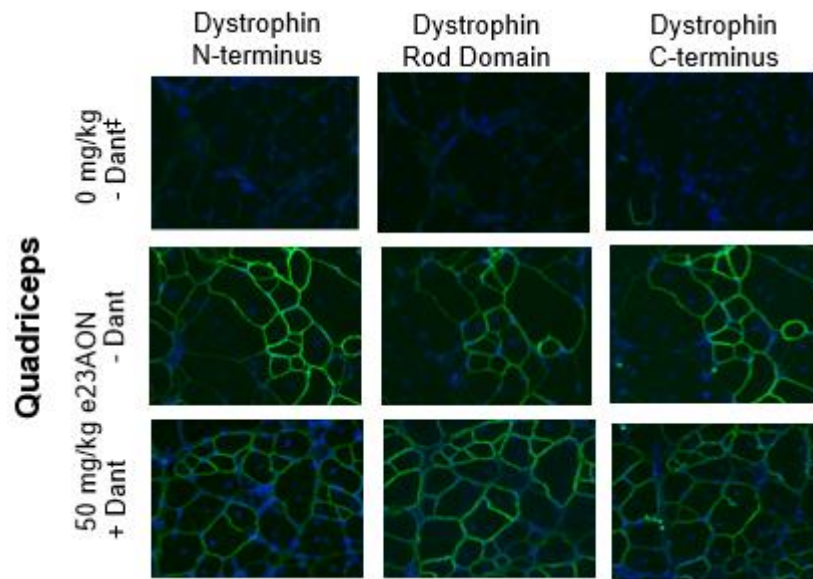
Dependent Variable: RWB_Q Rank for Variable WB_Q

Source	DF	Sum of Squares	Mean Square	F Value	Pr > F
Model	7	135014.2588	19287.7513	42.27	<.0001
Error	124	56582.7412	456.3124		
Corrected Total	131	191597.0000			

R-Square	Coeff Var	Root MSE	RWB_Q Mean
0.704678	32.12251	21.36147	66.50000

Source	DF	Anova SS	Mean Square	F Value	Pr > F
PMO	3	130985.5562	43661.8521	95.68	<.0001
Dantrolene	1	3662.6436	3662.6436	8.03	0.0054
PMO*Dantrolene	3	366.0590	122.0197	0.27	0.8488

Supplementary Figure 2-6. Combination therapy rescues expression of dystrophin with presence of N-terminal, rod domain, and C-terminal protein sequences.



Supplementary Figure 2-7. Results of Friedman’s two-way nonparametric ANOVA on the effect of dantrolene on e23AON treatment for serum CK levels.

Friedman's Two-way Nonparametric ANOVA

The ANOVA Procedure

Dependent Variable: RCK_Serum Rank for Variable CK_Serum

Source	DF	Sum of Squares	Mean Square	F Value	Pr > F
Model	7	76303.8689	10900.5527	11.38	<.0001
Error	125	119736.6311	957.8930		
Corrected Total	132	196040.5000			

R-Square	Coeff Var	Root MSE	RCK_Serum Mean
0.389225	46.19380	30.94985	67.00000

Source	DF	Anova SS	Mean Square	F Value	Pr > F
PMO	3	30801.59067	10267.19689	10.72	<.0001
Dantrolene	1	39072.39425	39072.39425	40.79	<.0001
PMO*Dantrolene	3	6429.88396	2143.29465	2.24	0.0872

Supplementary Figure 2-8. Results of Friedman's two-way nonparametric ANOVA on the effect of dantrolene on e23AON treatment for centronucleation and eMHC positive fibers.

Friedman's Two-way Nonparametric ANOVA

The ANOVA Procedure

Dependent Variable: RCentroQ Rank for Variable CentroQ

Source	DF	Sum of Squares	Mean Square	F Value	Pr > F
Model	7	1501.416667	214.488995	2.02	0.0769
Error	40	4256.083333	106.402083		
Corrected Total	47	5757.500000			

R-Square	Coeff Var	Root MSE	RCentroQ Mean
0.260776	42.10261	10.31514	24.50000

Source	DF	Anova SS	Mean Square	F Value	Pr > F
PMO	3	993.1666667	331.0555556	3.11	0.0369
Dantrolene	1	379.6875000	379.6875000	3.57	0.0662
PMO*Dantrolene	3	128.5625000	42.8541667	0.40	0.7518

Dependent Variable: RCentroD Rank for Variable CentroD

Source	DF	Sum of Squares	Mean Square	F Value	Pr > F
Model	7	4773.000000	681.857143	7.82	<.0001
Error	40	3489.000000	87.225000		
Corrected Total	47	8262.000000			

R-Square	Coeff Var	Root MSE	RCentroD Mean
0.577705	38.12013	9.339433	24.50000

Source	DF	Anova SS	Mean Square	F Value	Pr > F
PMO	3	3973.500000	1324.500000	15.18	<.0001
Dantrolene	1	546.750000	546.750000	6.27	0.0165
PMO*Dantrolene	3	252.750000	84.250000	0.97	0.4183

Dependent Variable: ReMHCQ Rank for Variable eMHCQ

Source	DF	Sum of Squares	Mean Square	F Value	Pr > F
Model	7	6486.250000	926.607143	13.62	<.0001
Error	40	2722.250000	68.056250		
Corrected Total	47	9208.500000			

R-Square	Coeff Var	Root MSE	ReMHCQ Mean
0.704376	33.67192	8.249621	24.50000

Source	DF	Anova SS	Mean Square	F Value	Pr > F
PMO	3	5587.375000	1862.458333	27.37	<.0001
Dantrolene	1	391.020833	391.020833	5.75	0.0213
PMO*Dantrolene	3	507.854167	169.284722	2.49	0.0743

Dependent Variable: ReMHC D Rank for Variable eMHC D

Source	DF	Sum of Squares	Mean Square	F Value	Pr > F
Model	7	6192.946429	884.706633	17.67	<.0001
Error	38	1902.553571	50.067199		
Corrected Total	45	8095.500000			

R-Square	Coeff Var	Root MSE	ReMHC D Mean
0.764986	30.10986	7.075818	23.50000

Source	DF	Anova SS	Mean Square	F Value	Pr > F
PMO	3	5742.540559	1914.180186	38.23	<.0001
Dantrolene	1	272.695652	272.695652	5.45	0.0250
PMO*Dantrolene	3	177.710217	59.236739	1.18	0.3290

Chapter 3

Growing a Bank of Primary Patient Cells to Model and
Test Various Exon Skipping Strategies

This chapter outlines the contributions I made to the cell bank at the Center for Duchenne Muscular Dystrophy. This bank was built to give DMD and other muscular dystrophy researchers a resource for studying primary patient samples. This bank enables the pursuit and development of personalized therapies, such as exon skipping. Part of my thesis work entails growing a bank of primary patient cells by processing skin biopsies from DMD patients. I helped solidify the protocols used to isolate fibroblasts from skin biopsies and helped determine the best methods of expansion and differentiation.

The CDMD currently has over 100 cell lines banked (**Table 3-1**). 40 of these cell lines are amenable to exon skipping (**Table 3-2**) within the hotspot mutation region in the dystrophin gene between exons 44 and 55. Of these 40 cell lines: 9 are amenable to exon 51 skipping, 4 are amenable to exon 53 skipping, 8 are amenable to exon 45 skipping, and 8 are amenable to exon 44 skipping. A majority of DMD mutations occur in area known as a hotspot region.¹⁴ Hotspot for mutations occurs between exons 3 and 8 as well as exons 45 and 55 due to the gene's propensity to undergo recombination in this region.¹⁵ Mutations between exons 45 and 55 account for roughly 62% of all DMD mutations. These cell lines will enable researchers to perform clinically relevant experiments, as antisense oligonucleotides targeting exon 51, 53, 45, and 44 are either on the market or in the clinical pipeline. These cell lines are available to the research community for a wide range of applications especially in muscular dystrophy

For each sample, we record the DMD mutation and whether or not the patient can be treated with exon skipping therapy.

We also perform a run select samples through a custom comparative genomic hybridization (CGH) array (**Figure 3-1**) with 14,022 probes tiling the DMD gene to confirm patient mutations. Probe number one maps to genomic position chrX:31047266 and probe 14,022 maps to genomic position chrX:33267570. Some of these samples have been included in a genetic modifier study, transduced to become induced directly reprogrammed myotubes and cultured into induced-pluripotent stem cell lineage.

For DMD, many *in vitro* assays performed with patient cells are performed on myotubes that have been directly reprogrammed from patient fibroblasts. In order to achieve regulated myogenesis of patient-derived fibroblasts to myotubes by addition of 4OH-Tamoxifen, our cells have been transduced by a lentiviral vector, Lv-CMV-MyoD-ER(T)⁶² (gift from J. Chamberlain). The vector contains a MyoD gene with a mutated estrogen receptor. The addition of 4OH-Tamoxifen to these cell cultures allows it to bind to the mutated estrogen receptor which is inserted between the MyoD1 gene. This causes the estrogen receptor to dimerize, allowing functional MyoD to translocate to the nucleus and halt the cell cycle, pushing the fibroblasts towards muscle cell differentiation. This viral vector is human-tropic and is missing packaging proteins, rendering it non-replicative.

Our lab also created a sister construct, Lv-CMV-MyoD-ER(T)-IRES-Puro (**Figure 3-2**), that contains a puromycin selectable marker with its own internal ribosomal entry site. This marker allows us to select for only the patients fibroblasts that have been efficiently transfected with the vector. This marker has proven critical for improving the quality of myotubes differentiated in the laboratory as well as the selection of transfected iPSC described in Chapter 4.

As one of our goals is to create a bank of DMD patient-derived fibroblasts that others can use, we have also transduced our cells with a lentiviral vector containing hTERT⁹⁴ (gift from Woody Wright). The vector, RRL-sin-hTERT, is a self-inactivating lentiviral vector containing the human telomerase reverse transcriptase gene to immortalize our cells. This viral vector is human-trophic and is missing packaging proteins, rendering it non-replicative.

To date, the cell bank has had application in screening for drugs, testing of therapies (exon skipping and CRISPR/Cas9), and identifying modifiers of disease. In collaboration with Dr. Stanley Nelson, Dr. April Pyle's laboratory, and the Broad stem cell core at UCLA, some of these samples have been included in a genetic modifier study, transduced to become induced directly reprogrammed myotubes and cultured into induced pluripotent stem cell lineage and characterized. The immediate goal is to generate 10 additional patient-derived pluripotent stem cell lines that will span the diversity of the DMD disease. This will allow for cross-validation between patient-specific mutation models and allow for greater confidence that the results are not influenced by patient-specific genetic modifiers.

The cell bank has been and will continue to be an important resource to investigators on and off campus who are interested in human models of neuromuscular disease.

MATERIALS AND METHODS

Derivation of Fibroblast from Human Skin Biopsy

Skin punches were placed in 10mL sterile DMEM (HIGH GLUCOSE, --Phenol red, --L-glutamine) + 1x Pen/strep and stored on ice during transport. Tissues were processed within an hour of the skin punch, following aseptic precautions throughout the process. 2% AOF collagenase was prepared fresh every time and resuspended in HBSS (+calcium, +MgCl₂, no serum). 6 well plates were coated with 0.1 % gelatin and left overnight at 37c. Transportation medium was aspirated from the tissue and tissue was rinsed twice with HBSS (+ca, +MG, NO SERUM). 3 ml of HBSS was added to the tissue and transferred with tissue into a 6cm Corning dish. HBSS was aspirated gently and 300ul of 2% AOF collagenase was added. Tissue was chopped into 1mm pieces with sterile individual use scalpels. 3.7ml collagenase was added to the well and incubated with chopped tissue for 90min at 37°C. Sample was gently shaken every 20min. 5ml of MSCBM was added to the collagenase and pipetted into a 15mL tube. Another 5ml of MSBCM was added to 6cm dish for final rinse and added to the same 15ml tube. Sample was centrifuged at 300g for 5min. The supernatant was aspirated and the pellet was rinsed with 5ml of MSCBM. Sample was centrifuged at 300g 5min. Supernatant was aspirated. Resuspend Cell pellet was resuspended in 3ml media and added to gelatin coated well. After 2-3 weeks cells were transferred into a t75 flask. After 3-4 days (or until sub-confluent) cells were transferred into a t175. Cells were frozen at 1.10^6 cells/vial in 10% DMSO-FBS.

CGH Array

A custom oligonucleotide array was designed with 14,022 probes tiling the DMD gene with a resolution of approximately 1 probe every 160bp (Agilent). Probe number one maps to genomic position chrX:31047266 and probe 14,022 maps to genomic position chrX:33267570. Genomic DNA from iDRM5017 was labeled with Cy3, and non-mutated human genomic DNA was labeled with Cy5 using a random priming kit (Agilent) and labeled DNA was co-hybridized to the custom designed array. Arrays were scanned with the DNA Microarray Scanner with SureScan High-Resolution Technology (Agilent) and data were extracted with Feature Extraction Software version 10.5.1.1. The values were extracted from the software and analyzed in R. Probes 4409 to 5615 demonstrated lower Cy3 signal and are consistent with a deletion from chrX: 31928123 in intron 44 to chrX: 31725186 in intron 50, which includes exons 45-50 of DMD. Base pair positions are reported relative to build HG18 and the log ratio of the Cy3/Cy5 (iDRM5017/normal) intensity is plotted for all probes.

hTERT Transduction

- Day 1 (09/27/10): Plate GM05114 p. 15 in a 6-well plate at 150,000 cells per well.
Day 2 (09/28/10): Transduce with 0.1 μ g LV-hTERT and 0.1 μ g LV-GFP.
Day 3 (09/29/10): Image 24 hr timepoint on microscope.
Day 4 (09/30/10): Image 48 hr timepoint on microscope.
Day 5 (10/01/10): Image 72 hr timepoint on microscope. Check for GFP positivity by FACS.

Plate Layout:



Day 2 Protocol: (09/27/2010)

- 1) Perform the following dilutions to achieve 0.1 μ g of virus per well (approx. a MOI of 30) in 1 mL of media:
 - a. 1 WELL= Mock treatment (Negative Control)
Per well:
Fibroblast Growth Media= 996 μ L
Protamine Sulfate= 4 μ L
 - b. 2 WELLS= LV-GFP (Positive Control)- virus concentration at 0.58 μ g/mL
Each well has its own 1.5mL tube; Per well:
Per well:
RL-cPPT-GFP virus= 172.4 μ L
Fibroblast Growth Media= 823.6 μ L
Protamine Sulfate= 4 μ L
 - c. 3 WELLS= LV-hTERT- virus concentration at 1.00 μ g/mL
Each well has its own 1.5mL tube; Per well:
LV-hTERT= 100 μ L
Fibroblast Growth Media= 896 μ L
Protamine Sulfate= 4 μ L
- 2) Aspirate off medium from 6-well plate. Transfer 1mL of each viral supernatant dilution to each well. Incubate at 5% CO₂ and 37C overnight.

MyoD Transduction

Day 1 (4/30/12): Plate GM05112 Well 4 p 16. and GM02339 Well 6 p 21. each in a 6-well plate at 100,000 cells per well.

Day 2 (5/1/12): Transduce with 0.1ug LV-MyoD.

Day 3 (5/2/12): Wash 2x with fibroblast growth media. Repeat Day 2.

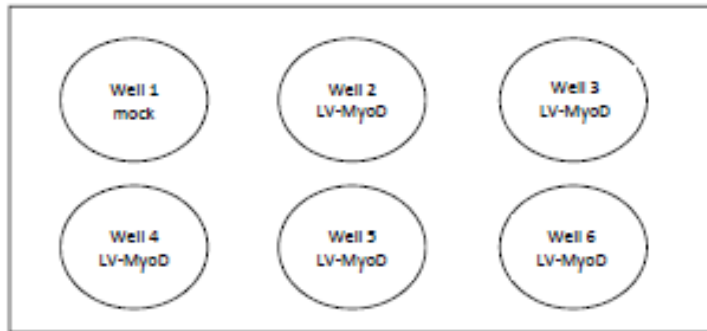
Day 4 (5/3/12): Wash 2x with fibroblast growth media and add 2mL per well.

:When cells are recovered, harvest and transfer to another flask to continue growing.

Check transduction efficiency by IHC for induction of MyoD after Tamoxifen exposure.

Test for fusion and terminal muscle markers by differentiating for 8 days using fusion protocol and stain for MHC

Plate Layout:



Day 2 & 3 Protocol: (09/30/2010, (10/01/2010)

1) Perform the following dilutions to achieve 0.1ug of virus per well (approx. a MOI of 50) in 1 mL of media:

a. 1 WELL= Mock treatment (Negative Control)

Per well:

Fibroblast Growth Media= 996uL

Protamine Sulfate= 4uL

b. 5 WELLS= LV-MyoD- virus concentration at .8 ug/mL

Each well has its own 1.5mL tube; Per well:

Per well:

LV-MyoD virus = 125uL x5 625 uL

Fibroblast Growth Media= 871uL 4.355 mL

Protamine Sulfate= 4uL 20uL

2) Aspirate off medium from 6-well plate. Transfer 1mL of each viral supernatant dilution to each well.

Spin at 1250rpm for 90 minutes. Paraffin wrap the edges of the plate.

Incubate at 5% CO₂ and 37C overnight.

Note: Protamine sulfate at 1mg/mL (1000x stock) in sterile PBS. Keep at 4C, stable 6 months.

TABLES AND FIGURES

Table 3-1. cDMD Cell Bank (as of 9/20/2017)

Cell Line Name	Source	Date of BIOPSY	Sex	Age	DMD Mutation	Skip to Render in Frame
CDMD 1001	UCLA	9/9/2010	F	40Y R+	WT	n/a
CDMD 1002	UCLA	9/9/2010	M	40Y R+	WT	n/a
CDMD 1003	UCLA	10/26/2010	M	9YR	Δ E46-51	E45
CDMD 1004	UCLA, Perry Shieh	2/2/2011	M	60Y R+	WT	n/a
CDMD 1006 (alias: DMD 1005)	Children's National Hospital, Washington DC	5/19/2011 received: (5/20/2011)	M	10Y R	Δ E46-47	E45
CDMD 1008	UCLA	11/3/2011	M	13Y R	E50 DUP	E50single OR E50_51
CDMD 1012	UCLA	11/11/2011	M	12Y R	Δ E8-11	E12
CDMD 1013	Dr. Kathryn Wagner from Kennedy Krieger Institute.		M	20Y R	Δ E51	E50 or E52
CDMD 1015	UCLA	11/23/2011	M	8YR	Δ E45	E44 or 46
CDMD 1021	UCLA	12/7/2011	M	16Y R	E2 DUP	E2single
CDMD 1022	UCLA Neuromuscular Clinic	12/14/2011	F	40Y R+	Carrier Mother with E12-22 DUP	--
CDMD 1023	UCLA Neuromu	12/15/2011	M	9YR	Δ E3-23	BMD

	scular Clinic					
CDMD 1023 muscle biopsy	UCLA Neuromu scular Clinic	12/23/2 011	M	9YR	Δ E3-23	BMD
CDMD 1024	UCLA Neuromu scular Clinic	12/16/2 011	M	10Y R	E6-7 DUP	--
CDMD 1025	UCLA Neuromu scular Clinic	12/17/2 011	F	40Y R+	Carrier Mother with E6-7 DUP	--
CDMD 1026	UCLA Neuromu scular Clinic	12/18/2 011	M	8YR	Δ E51-54	E55
CDMD 1027	UCLA Neuromu scular Clinic	12/19/2 011	M	20Y R	pending	BMD or DMD
CDMD 1028	UCLA Neuromu scular Clinic	12/20/2 011	F	40Y R+	c.4100_delA (1 bp DEL)	--
CDMD 1029	UCLA Neuromu scular Clinic	12/21/2 011	M	10Y R	c.4100_delA (1 bp DEL)	--
CDMD 1037	UCLA		M	20Y R	c.1961_delT>A, p.LEU654* (point mut. @E16)	--
CDMD 1039	UCLA	4/26/20 12	M	2YR	c.7327_7328del_AC (2bp DEL @ E51)	--
CDMD 1044	UCLA	6/4/201 2	M	5YR	Δ E45-50	E51
CDMD 1045	UC Davis Neuromu scular Clinic (Evan de Bie, Eric Henricson).	1/7/201 3	M	11Y R	Δ E45-50	E51
CDMD 1056	UCLA Neuromu	2/20/20 13	M	13Y R	Δ E49-50	E51

	scular Clinic					
CDMD1 062	Cincinnati Children's Hospital (Dr. Brenda Wong)	3/19/20 13	M	22Y R	--	--
CDMD1 063	UC Davis Neuromu scular Clinic	3/18/20 13	M	11Y R	Δ E45-50	E51
CDMD1 064	UCLA	4/4/201 3	M	16Y R	Δ E45	E44 or 46
CDMD1 065	UCLA	6/19/20 13	M	7YR	E2 DUP	
CDMD1 066	UCLA	6/19/20 13	F	40Y R+	E2 DUP	
CDMD1 067	UCLA	7/3/201 3	M	5YR	E2-E12 DUP	
CDMD1 075	UCLA	7/15/20 13	M		Δ E10-42	
CDMD1 076	UCLA	7/24/20 13	M	19Y R	pending	--
CDMD1 077	UCLA	8/30/20 13	M	44Y R	WT	--
CDMD1 078	UCLA	3/18/20 13	M	8mo	WT	--
CDMD1 079	UCLA	3/18/20 13	F		WT	--
CDMD1 080	UCLA	3/18/20 13	M		WT	--
CDMD1 081	Dallas/UM N	5/23/20 13	F	29Y R	WT	--
CDMD1 082	Dallas/UM N	5/23/20 13	M	40Y R+	WT	--
CDMD1 083	Dallas/UM N	5/23/20 13	F	40Y R+	WT	--
FSHD2 muscle biopsy	UCLA	1/20/20 12	--	--	WT	--
CDMD1 084	UCLA	10/23/2 013	M	14	Δ E46-47	E45
CDMD1 085	UCLA	10/23/2 013	M	8	Δ E45-50 (**see description)	E51

CDMD1086		11/1/2013	M			$\Delta E45$	E44 or 46
CDMD1087		1/27/2014	M	60		--	--
cDMD1088	UCLA	5/21/2014	M	14Y R		$\Delta E49-50$	E51
cDMD1090	UCLA	5/21/2014	M	8YR		$\Delta E45-52$	E53
cDMD1089	UCLA	5/21/2014	M	11Y R		$\Delta E45$	E44 or 46
cDMD1091	UCLA	recieved: 7/18/2014	M	6		IVS32 +1 G>T	32
cDMD1092	UCLA	recieved: 7/18/2014	M	9		IVS32 +1 G>T	32
cDMD1093	Stanford	recieved: 7/18/2014	M			$\Delta E8-41$	E6+ E7
cDMD1094	CHOC	8/12/2014				--	
cDMD1095	UCLA	6/24/2015	M	13		Dup E45-52	
cDMD1096	UCLA	10/1/2014	M	6		c.6283C>T	
cDMD1097	UCLA	10/15/2014	M	13		c.6472-6473 del	
cDMD1098	UCLA	10/15/2014	M	15		$\Delta E46-48$	E45
cDMD1099	UCLA	10/15/2014	M	8		$\Delta E46-48$	E45
cDMD1100	UCLA	10/15/2014	M	10		$\Delta E45-48$	
cDMD1101	UCLA	10/15/2014	M	11		$\Delta E18-50$	
cDMD1102	UCLA	12/10/2014	F	63		None	
cDMD1108		6/1/2015	M	9		dup E8-12	

cDMD 1109	ucla	6/3/2015	F	5	unknown mutation cf notes	
cDMD 1110	ucla	6/24/2015	M	9	E 50 del	E51
cDMD 1111	ucla	6/25/2015	M	29	none	
cDMD 1118	ucla	7/8/2015	M	11	E44 dup	
cDMD 1134	NIH	not in UCLA, 10/27/15	M	13	pseudoexon 62 inclusion	
cDMD 1145	UCLA	12/17/2015	F	12		
cDMD 1146	UCLA	12/29/2015	M	3	Mutation is deletion of all of exon 49-53 and the 5' part of exon 54	
cDMD 1166	UCLA	5/25/2016	M	8yo	4 base pair deletion at nucleotide locations 6936 to 6939 causing a frameshift mutation in of exon 48	E48
cDMD 1168 A muscle bx	UCLA	06/09/2016	M	4yo		
cDMD 1168 B skin bx	UCLA	06/09/2016	M	4yo		
cDMD 1175	UCLA	08/17/16	M	11yo		
cDMD 1184	UCLA	09/28/2016	M	14yo	del 3-7	E8
cDMD 7001	UCLA	muscle bx on 03/08/17	M	10yo	del 49-52	53
1229	cincinnati		M			
1230	UCLA	muscle bx on 03/23/17	M	7yo	nonsense mutation in exon 70	
cDMD 7002	UCLA	muscle bx on 03/17/17	M	13yo	del46-47	45
cDMD 7003	UCLA	muscle bx on	M	7yo	del 46-55	45

		04/17/17				
cDMD 7004/1239	UCLA	muscle bx on 05/1/17	M	11y o	del 48-52	53
1282	UCLA	muscle bx on 08/08/17	M	39y o	UDN patient	
cDMD 7005/1288	UCLA	muscle bx on 08/11/17	M	11y o	del 46-48	45
cDMD 7006/1298	UCLA	muscle bx on 08/17/17	M	9yo	del 44	45
cDMD 7007/1299	UCLA	muscle bx on 09/01/17	M	14y o	del 45-52	
cDMD 7008/1371	UCLA	muscle bx on 09/21/17	M	10y o		
cDMD 8001	UCLA	06/21/2016	M	55y o	healthy control	
cDMD 8002	UCLA	09/30/2016	M	46y o	healthy control	
cDMD 8003	UCLA	10/28/2016	F	52y o	carrier c.4100_delA (1 bp DEL)	30
cDMD 8004	UCLA	12/13/16	F	43y o	carrier	
cDMD 8006	UCLA	12/21/16	F	33y o	healthy control	
cDMD 8010	UCLA	02/28/17	M	26y o	Becker DMD exon 51-52 deletion	
cDMD 8011	UCLA	04/17/17	M	14y o	Becker DMD exon 3-7 deletion	8
cDMD 8012	UCLA	08/08/17	M		del exon 51	50
cDMD 8013	UCLA	09/18/17	M	17y o	pseudoexon inclusion in intron 37 that causes a stop codon	
cDMD 8014	UCLA	09/18/17	F	41y o		

Exon Amenable to Skipping	# Cell Lines
51	9
53	4
45	8
44	8
others	11

Table 3-2. DMD patient cell lines amenable to exon skipping

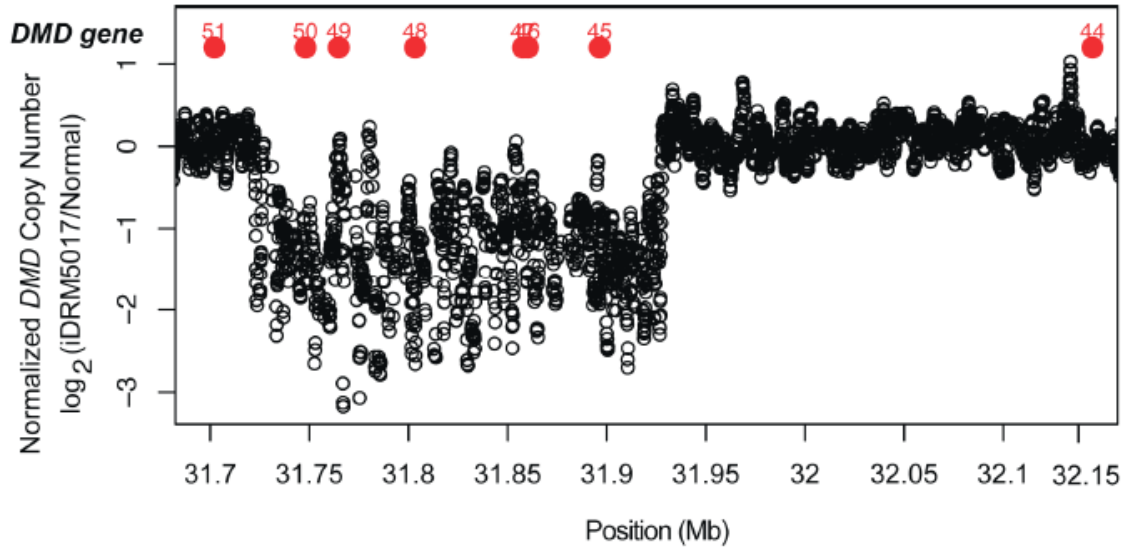


Figure 3-1. Custom CGH array confirms deletion breakpoints in GM05017

used to create iDRM 5017. A custom oligonucleotide array was designed with 14,022 probes tiling the DMD gene with a resolution of approximately 1 probe every 160bp (Agilent). Probe number one maps to genomic position chrX:31047266 and probe 14,022 maps to genomic position chrX:33267570. Genomic DNA from iDRM5017 was labeled with Cy3, and non-mutated human genomic DNA was labeled with Cy5 using a random priming kit (Agilent) and labeled DNA was co-hybridized to the custom designed array. Arrays were scanned with the DNA Microarray Scanner with SureScan High-Resolution Technology (Agilent) and data were extracted with Feature Extraction Software version 10.5.1.1. The values were extracted from the software and analyzed in R. Probes 4409 to 5615 demonstrated lower Cy3 signal and are consistent with a deletion from chrX: 31928123 in intron 44 to chrX: 31725186 in intron 50, which includes exons 45-50 of DMD. Base pair

positions are reported relative to build HG18 and the log ratio of the Cy3/Cy5 (iDRM5017/normal) intensity is plotted for all probes.

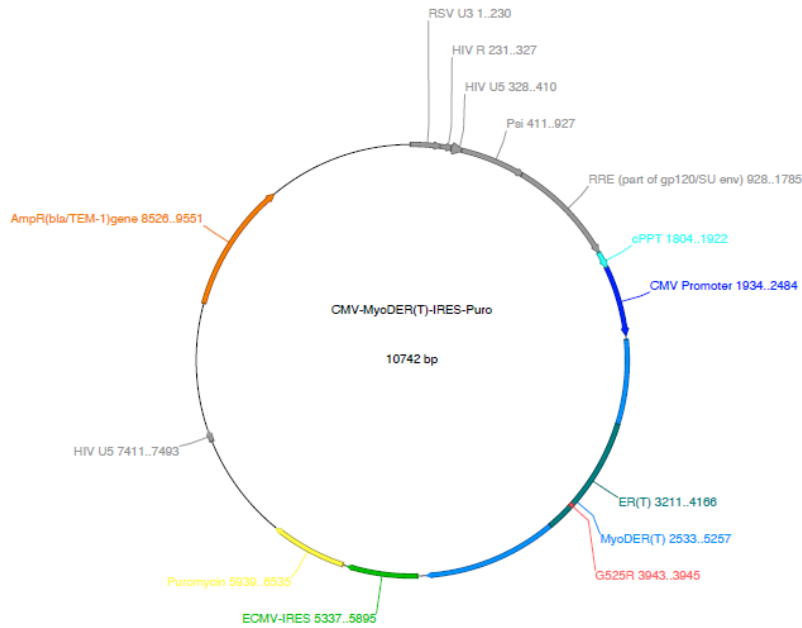


Figure 3-2. MyoD Puro Vector (CMV-MyoDER(T)-IRES-Puro)

A vector construct containing a tamoxifen-inducible MyoD transgene, driven by the CMV promoter. This vector also contains a puromycin selectable marker with its own internal ribosomal entry site. This marker allows us to select for only the patients fibroblasts that have been efficiently transfected with the vector.

Chapter 4

Preliminary Studies to Test Engraftment Conditions for a
DMD Xenograft Model System for Studying DMD *in vivo*

Introduction

The mdx mouse is a well-characterized *in vivo* model system for studying DMD. Thus far, we have conducted studies in human patient-derived fibroblasts, whereby we have developed methods of differentiating them into myoblasts and myotubes. We have used these cell lines to test the effectiveness and specificity (to particular exons of dystrophin) of small molecule drugs in improving functional dystrophin production and overall cell phenotype, with or without the presence of specific antisense oligonucleotides that alter dystrophin exon splicing.

We sought to develop a model that would enable DMD researchers to study DMD patient cell lines in the context of a complete muscle niche. In collaboration with April Pyle and Melissa Spencer's lab, we performed a set of experiments to determine the best method for engrafting DMD patient cells into the mouse muscle and differentiating these cells into muscle lineage. In very early experiments, FK506 was used to suppress the immune system, but engraftment was not successful.

We then decided to move into immunocompromised mice to allow for better engraftment. The goal was to develop a set of engraftment conditions that could ultimately be used on immunocompromised/mdx mice.

As a general overview, on Day 0 we prepare the muscle niche for injection **(Figure 4-1)**. We also begin IP injections of tamoxifen in mice that will be receiving iDRM patient cells. iDRMs are patient-derived fibroblasts that are from either wild type or DMD patients. iDRMs contain a tamoxifen-inducible MyoD expression vector. Expression of MyoD in the presence of tamoxifen forces these cells to differentiate into muscle lineage. On Day 1, we inject the patient cells

intramuscular into the TA. On day 8, allowing sufficient time to engraft/differentiate, we deliver a systemic injection of PMO in mice that were engrafted with dystrophic cells in order to assess rescued dystrophin in the event of exon skipping. On day 14, we harvest the skeletal muscle for assessment of mRNA and protein biomarkers.

For these experiments, there were 5 key experimental conditions we chose to optimize: Mouse genetic background, muscle niche pre-treatment, cell type, cell number, and length of experiment (**Table 4-1**).

Our human xenograft studies required the use of immunocompromised mice, in order to avoid xenograft rejection. *Mdx/nude* mice were our ideal mouse background but were not readily available at the time. Due to mutation induced disruption of the FOXP1 gene, nude mice have a deteriorated or absent thymus, resulting in a lack of mature T lymphocytes but the presence of NK cells. We sought to establish engraftment conditions, while our *mdx/nude* mouse colony was being established. The two most established immunodeficient backgrounds we considered were SCID/Beige and Rag-2/ γ -chain^{-/-} mice. SCID/Beige are congenic mice that possess both autosomal recessive mutations SCID (*Prkdcscid*) and beige (*Lystbg*). The SCID mutation results in severe combined immunodeficiency affecting both the B and T lymphocytes. The beige mutation results in defective natural killer (NK) cells. The Rag-2/ γ -chain^{-/-} mouse are a cross between common gamma knockout and Rag2 (recombinase activating gene) deficient mice. The common gamma knockout mouse lacks functional receptors for IL-2, IL-4, IL-7, IL-9, and IL-15. This results in compromised lymphocyte development. These mice lack NK cells and produce very small numbers of T and B cells. Crossing the Rag2-deficient

background onto the common gamma knockout mouse results in a mouse that lacks NK, T, and B cells.

We also sought to determine which pre-treatment condition was necessary to prepare the muscle niche for engraftment (**Figure 4-1**). Cardiotoxin has been previously used in engraftment experiments in *mdx* mice to induce muscle damage and open a niche where injected cells could localize and integrate into the muscle milieu.⁹⁵⁻⁹⁷ We also sought to determine whether pre-treatment with irradiation would facilitate better engraftment. Irradiation at 14-18 Gy is commonly used to clear the muscle niche of progenitor cells, increasing the engraftment potential of newly injected cells.⁹⁸⁻¹⁰⁰

In these preliminary experiments, we tested 4 different cell types: 1) iDRM, NCAM/CD56+ progenitor cells, LiCl differentiated iPSCs, and Wnt7a iPSCs. For initial experiments, a tamoxifen-inducible MyoD vector was used to differentiate the iDRM. We needed to troubleshoot the delivery and differentiation conditions *in vivo*. At the time, directed differentiation was the only option, given that the MyoD vector was not selectable and could not be used in iPSC, which are more difficult to transform. However, the Miceli lab subsequently created a tamoxifen-inducible MyoD vector with a puromycin selectable marker, which enabled the use of MyoD-overexpressing iPSC in future engraftment studies.

In the preliminary studies, we aimed to identify the ideal cell type that could best represent human DMD muscle *in vivo* in engraftment studies. The iPSCs used in these experiments are DMD-hiPSCs that are cultured in BMP4 (2 days) then cultured in either Wnt7a or LiCl. Treatment with Wnt7a and LiCl results in a higher percentage of cells expressing Pax7, a marker for muscle progenitor cells.

Mice were sacrificed 2 or 3 weeks following engraftment of cells. At sacrifice, half of each TA was flash frozen in liquid nitrogen for RNA analysis, while the other half was embedded in OCT for IHC analysis.

We sought to detect levels of engraftment by qPCR and IHC to look for human-specific mRNA transcript and protein. By qPCR, we looked for human-specific mRNA transcript for Dystrophin, MyoG, Desmin, and GAPDH. By IHC, we looked for human-specific spectrin, dystrophin, and general dystrophin and MHC (for muscle markers).

In order to identify the areas that would have the best chance of engraftment, we cut each TA into intervals of 90 10 micron sections. Within each interval, a section was stained with H&E and scored for centronucleation and inflammation as markers of cardiotoxin-induced damage and therefore regions where engraftment was most likely to occur. Intervals that had sections with increased centronucleation and inflammation were then stained for IHC markers mentioned previously.

Results and Discussion

In the xenografts based on iDRMs, we detected human desmin, MyoG, and GAPDH transcripts, confirming that human cells engrafted (**Figure 4-2**). Antibody to human spectrin was also used but has subsequently been reported to cross-react with regenerating mouse myofibers¹⁰¹ and therefore the data are not included. Both engrafted iPSC and iDRM cells expressed dystrophin transcript, suggesting that these cells had differentiated to muscle lineage within the muscle niche (**Figure 4-2**). We found that a range of 1 to 3 million cells was adequate for engraftment. Cells engrafted in both 2 and 3 week studies. Looking across all 74 engraftment

procedures analyzed 75% of SCID/Bge mice expressed hGAPDH and hMHC mRNA. When comparing cardiotoxin vs cardiotoxin + irradiation niche pre-treatment, combination treatment resulted in 22% higher frequency of hGAPDH mRNA expression in samples. We tested 1, 3, and 5M cell injections for engraftment. 100% of the 3M cell injections results in hGAPDH mRNA expression in the TA. A high proportion of 14 days experiments resulted in hGAPDH, hMHC and hDystrophin mRNA as compared to 21 days experiments. For example, 61% of 14 days experiments resulted in GAPDH+ mRNA compared to 33% of 21 days experiments. In conclusion, the techniques developed in these preliminary studies helped guide the engraftment experiments performed in the Appendix.

Materials and Methods

Engraftment into Immunodeficient Mice

Mdx, *rag2*^{-/-}*γc*^{-/-}, and SCID/Beige mice were acquired from Jackson Laboratory. Five- to seven-week-old NSG-*mdx* mice were pretreated with 50 ml of 10 mM cardiotoxin (Sigma-Aldrich) injected into the TA 24 hr prior to engraftment. We tested 4 different cell types: 1) iDRM, NCAM/CD56+ progenitor cells, LiCl differentiated iPSCs, and Wnt7a iPSCs. We wanted to identify the ideal cell type that could best represent human DMD muscle *in vivo* in engraftment studies. The iPSCs used in these experiments are DMD-hiPSCs that are cultured in BMP4 (2 days) then cultured in either Wnt7a or LiCl. Treatment with Wnt7a and LiCl results in a higher percentage of cells expressing Pax7, a marker for muscle progenitor cells. 1

to 5×10^6 cells in 50uL PBS were injected intramuscularly and the TA was harvested after 14 or 21 days.

Mice and Tissue Preparation

Procedures involving all mdx mice were approved by the Institutional Animal Care and Use Committee (IACUC) of the University of California, Los Angeles (UCLA). The TA were harvested and the right muscle was frozen in optimal cutting temperature compound (OCT) for sectioning and analysis by immunohistochemistry, whereas the left muscle was cut in half and snap-frozen for analysis by Western blot and ddPCR.

RNA isolation, RT-PCR, and qPCR

RNA was isolated with TRIzol (Invitrogen; mouse cells) and the Qiagen RNeasy Micro Kit (human cells and intervals from the TA muscle). RNA was isolated from frozen skeletal muscle with the Qiagen RNeasy Fibrous Tissue Kit. Total RNA from mice was reverse-transcribed with oligo(dT)20 (Invitrogen). A nested RT-PCR was performed between Dmd exons 20 and 26.36 Products were run on a 2% agarose gel and visualized with ethidium bromide. Densitometry quantitation of gels was performed in ImageJ. The quantitative TaqMan assay to assess specific full-length or skipped Dmd exon 23 mRNAs used primer-probe sets that have been previously described.⁶⁶ Briefly, primer-probe sets specific to the internal loading control, Rplp0, are complexed with primer-probe sets that amplify either the Dmd full-

length or exon 23 skip product. The skip-to-full-length mRNA ratio was calculated as:

in which CTRS and CTRFL are the Ct values for the ribosomal gene in either the skip (S) or the full-length (FL) reaction. CTS and CTFL are the Ct values corresponding to detection of Dmd exon 23-skipped or full-length mRNA product. In human cells, dystrophin complementary DNA (cDNA) was reverse-transcribed with 200 ng of RNA with a DMD exon 54-specific primer. A nested RT-PCR between DMD exons 43 to 52 was then performed with previously described primers.⁴¹ For detection of muscle markers, 100 to 400 ng of RNA were reverse-transcribed into cDNA with oligo(dT)₂₀ and RT-PCRs were performed for endogenous MyoD, desmin, myogenin, utrophin, myosin heavy chain, and glyceraldehyde-3-phosphate dehydrogenase (GAPDH) as input control.

Sequences of primers used for RT-PCR

The following primers were used for RT-PCR of various muscle markers. For identifying muscle markers in reprogrammed fusing myotubes, 100 to 400 ng of RNA were reverse-transcribed with oligo(dT)₂₀.

MyoD: forward, 5'-GCAGGTGTAACCGTAACC-3'; reverse,
5'-ACGTACAAATTCCTGTAGC-3' (53)

Myosin heavy chain: forward, 5'-CTGGCTCTCCTCTTTGTTGG-3';
reverse, 5'-AGTTTCATTGGGGATGATGC-3'

Desmin: forward, 5'-CCTACTCTGCCCTCAACTTC-3'; reverse,
5'-AGTATCCCAACACCCTGCTC-3' (53)

Myogenin: forward, 5'-GCCACAGATGCCACTACTTC-3'; reverse,
5'-CAACTTCAGCACAGGAGACC-3' (53)

GAPDH: forward, 5'-GAGCCACATCGCTCAGACAC-3'; reverse,
5'-CATGTAGTTGAGGTCAATGAAGG-3' (54)

RyR1 PCR1: forward, 5'-CATCAACTATGTCACCAGCATCCG-3';
reverse, 5'-GGCTGAACCTTAGAAGAGTC-3'

RyR1 PCR2: forward, 5'-GAGACCTTCTATGATGCAGC-3'; reverse,
5'-AGAGCTCGTGGATGTTCTC-3'

Utrophin: forward, 5'-TGTCGGTTCACCGCCAGAGT-3'; reverse,
5'-GTGGCCTGCTGGGAACATTT-3' (55).

The thermocycler conditions for MyoD, myosin heavy chain, desmin, myogenin, and GAPDH were 94°C for 2 min, followed by 33 cycles of 94°C for 30 s, 62°C for 30 s, and 72°C for 30 s, with a final extension of 72°C for 10 min. Amplification of the RyR1 required a nested PCR. Conditions for the first ryanodine receptor PCR were 95°C for 5 min, 20 cycles of 95°C for 30 s, 56°C for 2 min, 72°C for 90 s, and a final extension of 72°C for 10 min. The nested PCR conditions were 95°C for 5 min, 35 cycles of 95°C for 30 s, 59°C for 2 min, 72°C for 90 s, and a final extension of 72°C for 10 min. Thermocycler conditions for the amplification of utrophin required a single PCR. Conditions were 94°C for 5 min, 94°C for 1 min, 60°C for 1 min, 72°C for 1 min, repeat steps 2 to 4 for 35 cycles, and a final extension of 72°C for 10 min.

PMO and dantrolene in vivo administration

PMOE23 morpholino (5'-GGCCAAACCTCGGCTTACCTGAAAT-3'; Gene Tools) was injected intramuscularly into the TA muscle in 25 ml of saline. Intravenous administration was performed through the tail vein in 200 ml of saline or retro-orbitally in 50 ml. Dantrolene (Sigma) was resuspended in DMSO, heated to 50°C, and diluted in saline (final 20% DMSO) before twice-daily intraperitoneal injections.

Figure Legends

Figure 4-1. Overview of General Engraftment Experiment

Proposed protocol for engraftment of human DMD patient-derived cell lines into *mdx* mouse Tibialis anterior.

Figure 4-2. DMD patient–derived iDRM 5017 and iPSC 5017 engraft into *mdx* TA and express muscle markers

(a) Effect of dantrolene on PMOE23 induction of Dmd exon 23 skipping

Table 4-1. Engraft Conditions Explored for Preliminary Experiments

Table 4-2. DMD patient–derived iDRM 5017 temporally express muscle markers at the RNA and protein level during the fusion process.

(a) Expression of human desmin, human myogenin, and human GAPDH assessed by RTPCR of tibialis anterior following 2 and 3 weeks engraftment protocol. **(b)**

Expression of human dystrophin assessed by RTPCR of tibialis anterior following 3 week engraftment.

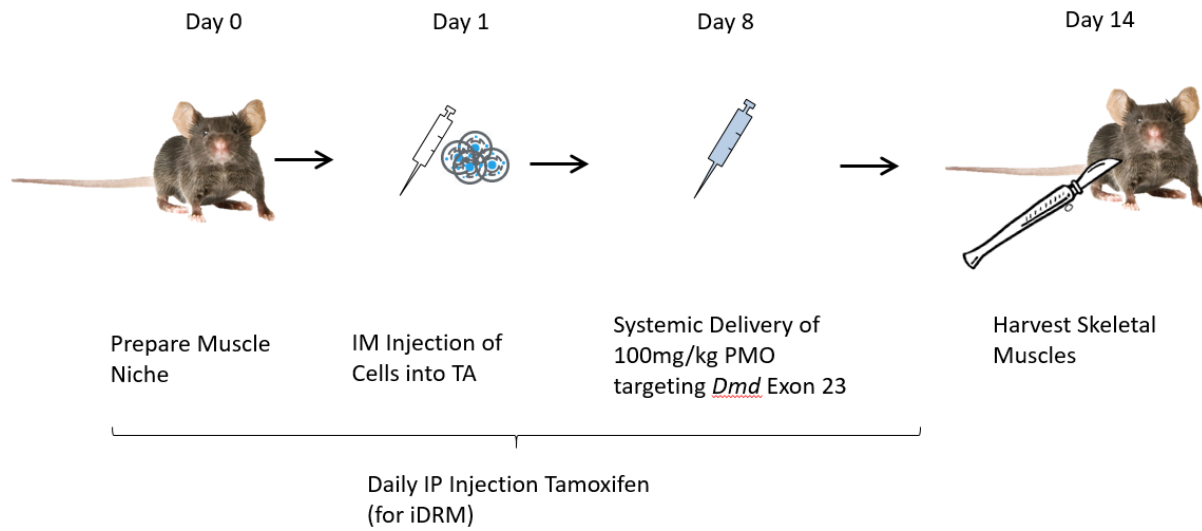


Figure 4-1. Overview of General Engraftment Experiment

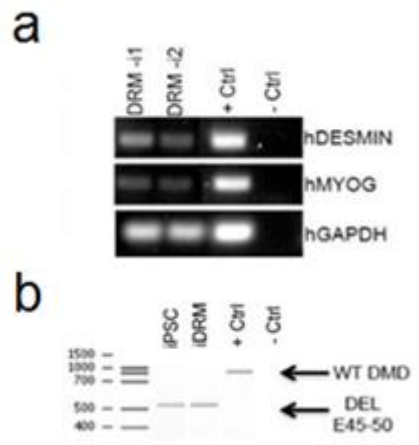


Figure 4-2. DMD patient–derived iDRM 5017 and iPSC 5017 engraft into *mdx* TA and express muscle markers

Mouse Background	Niche Pre-Treatment	Cell Type	Cell Number	Length of Study
SCID/Beige N=16	<u>Cardiotoxin</u> N=62	iDRM N=43	1x10 ⁶ N=38	14 Day N=56
<u>rag^{-/-}/γ_c^{-/-}</u> N=54	<u>Cardiotoxin</u> + <u>Irradiation</u> N=12	<u>NCAM/CD56+ iPSC</u> N=8	3x10 ⁶ N=10	21 Day N=18
mdx/nude N=4		<u>LiCl</u> Directed Differentiation iPSC N=6	5x10 ⁶ N=16	
		Wnt7a Directed Differentiation iPSC N=4		

Table 4-1. Engraftment Conditions Explored for Preliminary Experiments

Human GAPDH Positive Mice

Sample ID	Side Box	Strain	TA	Notes	TAM	Cell Line	# of cells (in 50ul PBS)	Systemic Administration	IP Dexamethasone (10 mg/kg in 200ul H2O)	Length of Experiment	DOB	Date of Sac.	hGAPDH mRNA (>2% hSkM1)	vs WT	hMyHC mRNA (>3% hSkM1)	vs WT	hSkipped Dys	vs WT
CRRM3.M1.TAL	5624	SCIDBge	L	Lost 15ul CTX		05017 NCAM+ (new) [LV-AON]	1*10 ⁶	--	--	14 days	9/19/2011	11/7/2011	+	6.41	+	5.26		
CRRM3.M1.TAR		SCIDBge	R	Lost 10ul CTX		05017 NCAM+ (new) [LV-AON]	1*10 ⁶	--	--	14 days	9/19/2011	11/7/2011	+	4.84	+	4.62		
CRRM3.M3.TAR	5621	SCIDBge	R	Lost 15ul of cell injection		05017 NCAM+ (new)	1*10 ⁶	Tail Vein	+	14 days	9/19/2011	11/7/2011	+	4.31	+	4.95		
CRRM3.M4.TAR	5625	SCIDBge	R	No Tamoxifen Day 0	+	GM05017 H10 M15 p. 31	1*10 ⁶	Tail Vein	+	14 days	9/19/2011	11/7/2011	+	52.15	+	47.98		
CRRM3.M5.TAL		SCIDBge	L		-	DMD WT 1001 H7 M15 p.30	1*10 ⁶	15ul Tail ven 85ul Intraocular	+	14 days	9/19/2011	11/7/2011	+	56.51	+	57.20		
CRRM3.M5.TAR	5622	SCIDBge	R		-	GM05017 H10 M15 p. 31	1*10 ⁶	15ul Tail ven 85ul Intraocular	+	14 days	9/19/2011	11/7/2011	+	17.20	-	16.38		
CRRM3.M6.TAL	5626	SCIDBge	L		+	DMD WT 1001 H7 M15 p.30	1*10 ⁶	10ul Tail ven 90ul Intraocular	+	14 days	9/19/2011	11/7/2011	+	53.74	+	50.93		
CRRM3.M6.TAR		SCIDBge	R		+	GM05017 H10 M15 p. 31	1*10 ⁶	10ul Tail ven 90ul Intraocular	+	14 days	9/19/2011	11/7/2011	+	6.05	+	4.51		
CRRM3.M7.TAL		SCIDBge	L		+	GM05017 H10 M15 p. 31	of 1*10 ⁶	Intraocular	+	14 days	9/19/2011	11/7/2011	+	9.75	+	8.36		
CRRM3.M7.TAR		SCIDBge	R		-	GM05017 H10 M15 p. 31	1*10 ⁶	Intraocular	+	14 days	9/19/2011	11/7/2011	+	29.84	+	27.69		
CRRM3.M8.TAL	5623	SCIDBge	L		-	GM05017 H10 M15 p. 31	2*10 ⁶	Intraocular	+	14 days	9/19/2011	11/7/2011	+	44.38	+	43.01		
CRRM3.M8.TAR		SCIDBge	R		-	GM05017 H10 M15 p. 31	1*10 ⁶	Intraocular	+	14 days	9/19/2011	11/7/2011	+	62.51	-	59.7 wrong size		
CRRM4.M14.TAR		Rag2 ^{-/-} -fyc ^{-/-}	R	lost 30*150ul cells	+	GM05017 H10 MP20	3*10 ⁶	Day 7 (100mg/kg)	Day 10, 12 (50ug)	14 Days	12/1/2011	12/16/2011	+	125.98	-	0		
CRRM4.M15.TAR	5628	Rag2 ^{-/-} -fyc ^{-/-}	R		+	GM05017 H10 MP20	3*10 ⁶	Day 7 (100mg/kg)	Day 10, 12 (50ug)	14 Days	12/1/2011	12/16/2011	+	134.26	-	0		
CRRM4.M17.TAR		Rag2 ^{-/-} -fyc ^{-/-}	R		+	GM05017 H10 M15	1*10 ⁶	Day 7 (100mg/kg)	--	14 Days	12/1/2011	12/16/2011	+	70.69	-	0		
CRRM4.M18.TAL		Rag2 ^{-/-} -fyc ^{-/-}	L		-	GM05017 H10 M15	1*10 ⁶	Day 7 (100mg/kg)	Day 10, 12 (50ug)	14 Days	12/1/2011	12/16/2011	+	102.32	-	0		
CRRM4.M18.TAR		Rag2 ^{-/-} -fyc ^{-/-}	R		-	GM05017 H10 M15	1*10 ⁶	Day 7 (100mg/kg)	Day 10, 12 (50ug)	14 Days	12/1/2011	12/16/2011	+	37.25	-	0		
CRRM4.M19.TAR		Rag2 ^{-/-} -fyc ^{-/-}	R	lost 20*150ul cells	-	GM05017 H10 MP20	3*10 ⁶	Day 7 (100mg/kg)	Day 10, 12 (50ug)	14 Days	12/1/2011	12/16/2011	+	122.60	-	0		
CRRM4.M2.TAL	5637	Rag2 ^{-/-} -fyc ^{-/-}	L	lost 10ul CTX		Directed differentiation NCAM	1*10 ⁶	Day 7, 14 (100mg/kg)	Day 17, 19 (50 ug)	21 Days	11/29/2011	12/21/2011	+	18.70	-	0.00		
CRRM4.M2.TAR	5638	Rag2 ^{-/-} -fyc ^{-/-}	R			Directed differentiation NCAM	2.0*10 ⁶	Day 7, 14 (100mg/kg)	Day 17, 19 (50 ug)	21 Days	11/29/2011	12/21/2011	+	79.90	-	0.00		
CRRM4.M20.TAL	5629	Rag2 ^{-/-} -fyc ^{-/-}	L		+	DMD WT 1001 H7 M15	1*10 ⁶	--	--	14 Days	12/1/2011	12/16/2011	+	23.12	-	0		

Table 4-2. DMD patient-derived iDRM 5017 temporally express muscle markers at the RNA and mRNA level during the fusion process.

Chapter 5

Concluding Remarks: Future Perspectives and Directions

This dissertation aims to establish the safety and efficacy profile of long term dosing of PMO and dantrolene in *mdx* mice to inform the improvement of current exon skipping therapies on the market and in the pipeline for DMD. This dissertation also aims to further develop scientific tools for the use of researchers studying DMD and other muscular dystrophies.

The current standard of care for DMD aims to target and ameliorate symptoms associated with the progressive wasting of muscles ¹⁰². Newer therapies aim to target the molecular basis of the disease by restoring or facilitating dystrophin protein expression. In addition to combating DMD, these therapies are setting the stage for personalized medicine. When treating such a genetically heterogeneous population like DMD, it is critical that each therapy be individualized to the subpopulation it aims to treat. These new personalized therapies for DMD include: stop codon read-through agents, dystrophin-expressing AAV vectors, and exon skipping therapies. Ataluren is an oral agent that suppresses nonsense mutations in genetic diseases and, in DMD, facilitates readthrough of stop codons to allow expression of dystrophin protein in the 10% of DMD patients who have nonsense mutations ¹⁰³⁻¹⁰⁵. The European Medicines Agency gave Ataluren conditional approval for DMD in 2014 and renewed that approval in 2016. On the other hand, the FDA filed a Refuse to File letter in 2016, claiming the the results of the phase IIb study and ACT DMD phase III trial did not demonstrate adequate evidence of effectiveness ¹⁰⁶. Ataluren is not the only new DMD therapeutic to face a tough regulatory landscape.

The initial exon skipping therapies to seek regulatory approval were Biomarin's drisapersen and Sarepta's Exondys51. Drisapersen was rejected by the

FDA in January of 2016 ¹⁰⁷ on the basis of toxicity and lack of strong data regarding efficacy, while Exondys51 received accelerated approval from the FDA based on dystrophin protein expression and a difference 6 minute walk test in treated subject group deemed that was deemed a reasonably likely to cause clinical benefit. The approval in 2016 by the FDA of Exondys51 is the first therapeutic for DMD, and a groundbreaking achievement by the DMD field ¹⁰⁸. Exondys51 was granted accelerated approval based for DMD patients amenable to exon 51 skip, 13% of the DMD population⁴³. This is an example of mutation specific precision therapy targeted at the fundamental defect of one of the most common genetic diseases and sets the stage for numerous additional therapies.

In the wake of these therapeutic achievements, it is the responsibility of researchers to continue moving the field closer and closer to a cure. While the approval is an exciting development, it is also clear that the effect is small and not adequate to arrest the disease progression. Thus, substantial work is needed to enhance the amount of dystrophin induced in muscles of Duchenne children. A common thread amongst the commercial-stage therapies discussed is the pursuit of and need for improved efficacy. This dissertation attempts to address this need and show that dantrolene can safely improve the efficacy of exon skipping therapies like Exondys51. The aim of this dissertation is in-line with other 'second generation' treatments in development for DMD: improving upon current treatment modalities. Near term, second generation treatments include peptide-conjugated PMO (PPMO) and mini-dystrophin-expressing AAV vectors, both of which are likely to be tested in human clinical trials in the coming year. PPMO provides the promise of increased cellular uptake of AON resulting in more dystrophin rescue compared to traditional

PMOs like Exondys51¹⁰⁹. Newer AAV vectors with codon optimized micro-dystrophin constructs aim to provide a more effective replacement for the missing dystrophin protein^{110, 111}. More distant strategies to remove exons from DNA using CRISPR/cas9 are a promising avenue of research as well^{112, 113}.

Looking forward, the data from this dissertation shows that dantrolene has the potential ability to improve current and new exon skipping therapies for Duchenne muscular dystrophy in the mdx mouse model. It is true that translation from mouse to human efficacy is not always observed, but these data support the rationale for a human clinical trial. Both agents are proven to be safe individually and well tolerated in longterm exposure^{31, 73, 114}, and from this thesis in combination. Further with an increasing group of patients being administered Exondys51, assessing the clinical utility of adding dantrolene is viable. A reasonable clinical trial strategy would be a comparison of dantrolene with Exondys51 versus those treated with Exondys51. Since the effect observed in mouse is convincing, but modest, a longerterm study of at least two years in mid-ambulant boys with Duchenne is the most promising strategy. This allows the assessment of preservation of 6MWT between double-blind placebo controlled groups. A concern in clinical trials in ambulatory boys is the possibility that dantrolene, through its effect on the RyR could induce transient muscle weakness and result in falls or functional limitations. However, the dosing tested in mouse is not associated with a dramatic decrease in muscle strength in humans. Further, it may also be worthwhile to determine whether or dantrolene can be used to boost exon skipping therapies used to treat other diseases as a large number of diseases may be amenable to a similar strategy. This dissertation highlights the evolving

relevance of personalized therapies in today's healthcare landscape with specific application to DMD.

Appendix

A Single CRISPR-Cas9 Deletion Strategy that Targets the Majority of DMD Patients Restores Dystrophin Function in hiPSC-Derived Muscle Cells

The Appendix includes a paper that was published in *Cell Stem Cell*¹¹² by Young et al, in the laboratories of Dr. April Pyle and Dr. Melissa Spencer titled, "A Single CRISPR-Cas9 Deletion Strategy that Targets the Majority of DMD Patients Restores Dystrophin Function in hiPSC-Derived Muscle Cells." While none of the data I generated was directly included in the paper, troubleshooting related to the engraftment and *in vitro/in vivo* induction of differentiation by a tamoxifen-inducible MyoD vector provided a starting point for components of this study. My contributions include performing preliminary experiments aimed at establishing conditions for: 1) MyoD expression and induction in culture and *in vivo* and 2) conditions for engrafting DMD patient-derived cells in the *mdx* mouse model of DMD, as outlined in Chapter 4. Conditions that I tested in Chapter 4 were not used in the following publication because techniques were modified and led to improved engraftment. Also, the studies in the following paper were performed in NSG/*mdx* mice, which I did not use in my preliminary studies.

Summary

Mutations in DMD disrupt the reading frame, prevent dystrophin translation, and cause Duchenne muscular dystrophy (DMD). Here we describe a CRISPR/Cas9 platform applicable to 60% of DMD patient mutations. We applied the platform to DMD-derived hiPSCs where successful deletion and non-homologous end joining of up to 725 kb reframed the DMD gene. This is the largest CRISPR/Cas9-mediated deletion shown to date in DMD. Use of hiPSCs allowed evaluation of dystrophin in

disease-relevant cell types. Cardiomyocytes and skeletal muscle myotubes derived from reframed hiPSC clonal lines had restored dystrophin protein. The internally deleted dystrophin was functional as demonstrated by improved membrane integrity and restoration of the dystrophin glycoprotein complex in vitro and in vivo. Furthermore, miR31 was reduced upon reframing, similar to observations in Becker muscular dystrophy. This work demonstrates the feasibility of using a single CRISPR pair to correct the reading frame for the majority of DMD patients.

Introduction

Duchenne muscular dystrophy (DMD) is the most common fatal genetic disease of childhood, affecting ~1 in 3,500–5,000 boys. In DMD, progressive muscle degeneration generally leads to death in the twenties, and there are currently no highly effective therapies. DMD is often caused by frameshifting exonic deletions in DMD, which encodes dystrophin. Dystrophin stabilizes the dystrophin glycoprotein complex (DGC) at the sarcolemma; loss of functional dystrophin leads to the degradation of DGC components, which results in muscle membrane fragility and leakage of creatine kinase (CK).¹¹⁵ Approximately 60% of mutations causing DMD occur between DMD exons 45–55.¹¹⁶ Multiple independent clinical reports in patients and dystrophic mice have revealed that in frame deletions of exons 45–55 produce an internally deleted dystrophin protein and are associated with a very mild Becker muscular dystrophy (BMD) disease course, with some patients still asymptomatic in their sixties.¹¹⁶⁻¹¹⁹ Thus, genetic manipulation to create a large

deletion of exons 45–55 is a therapeutic strategy to restore the reading frame for 60% of DMD patients with mutations in this region.

One promising approach to induce genetic correction of DMD is through the use of the bacterially acquired immune surveillance system known as clustered regularly interspaced short palindromic repeats (CRISPR) and CRISPR-associated nuclease (Cas) 9. In this system a short guide RNA (gRNA), which is complimentary to a specific site in the genome, is used to target the Cas9 nuclease and induce double-stranded breaks (DSBs). The DSBs can be repaired through non-homologous end joining (NHEJ) or homology-directed repair.

Previous work has shown that CRISPR/Cas9 components can modify the DMD gene.¹²⁰⁻¹²⁶ In this investigation, we describe a therapeutically relevant CRISPR/Cas9 platform that we designed to modify DMD. Our platform involves excision of exons 45–55 and NHEJ to reframe dystrophin through creation of an internally deleted protein that is stable and functional. The internally deleted protein mimics the naturally occurring exon 45–55 deletion observed in mild BMD patients and encompasses 60% of DMD patient mutations.

For the first time, we demonstrate CRISPR/Cas9-mediated deletion and NHEJ of up to 725 kb of the DMD gene in human induced pluripotent stem cell (hiPSC) lines. We show that CRISPR/Cas9 reframed, hiPSC-derived skeletal and cardiac muscle cells express stable dystrophin that improves membrane stability and restores a DGC member, b-dystroglycan. We also demonstrate reduced microRNA 31 (miR31) levels after the reading frame is restored, consistent with the observations made in BMD patients.¹²⁷ Furthermore, we show restoration of dystrophin and b-dystroglycan in vivo after engraftment of reframed hiPSC-derived

skeletal muscle cells into a mouse model of DMD. This work sets the stage for use of reframed DMD hiPSC-derived cells or in vivo correction strategies using CRISPR/Cas9 for direct translation to patients with DMD.

Results

DMD hiPSC Lines Are Pluripotent and Genetically Stable

We have developed several xenobiotic-free hiPSC lines derived from wild-type and DMD patient fibroblasts using current good manufacturing practice protocols. Each DMD hiPSC line harbors a unique frameshifting DMD mutation within the exon 45–55 hotspot region. All hiPSC lines (Center for Duchenne Muscular Dystrophy [CDMD] 1003, 1006, and 1008) express pluripotency markers (NANOG and SOX2) and are karyotypically normal (**Figures 1A and 1B**). CDMD hiPSCs maintain pluripotency, as they form teratomas in vivo that represent all three germ layers (**Figure 1C**), and each harbor unique mutations (**Figure 1D**).

CRISPR/Cas9-Mediated Deletion and NHEJ of up to 725 kb in the DMD Gene

In order to delete exons 45–55 of DMD, gRNAs were designed to target introns 44 and 55. gRNA sites were chosen to only retain ~500 bp of the intron next to each of the flanking exons (44 and 56). The rationale for this design is to

develop gRNAs applicable to as many patient mutations as possible and to ensure that a small functional chimeric intron is generated. During NHEJ, the 30 end of intron 44 and the 50 end of intron 55 join to create a ~1 kb chimeric intron (**Figure 2A**). We expect that introns generated in this manner are functional and splice correctly to create an in-frame transcript, with exon 44 joined with exon 56.

Since hiPSCs are challenging to genetically manipulate, human embryonic kidney (HEK) 293FT cells were used to screen five gRNAs at each intronic region. All gRNAs demonstrated individual cutting activity on Surveyor assay up to 34% (**Figures S1A and S1B**). Using multiplex PCR, gRNAs transfected in pairs were shown to effectively delete the entire 708 kb region encompassing exons 45–55 (**Figures S1C and S1D**).

In order to assess the feasibility of an exon 45–55 deletion across different patient mutations, we applied our gRNAs to three DMD hiPSC lines. The lines (CDMD 1003, 1006, and 1008) require ~530 kb, 670 kb, or 725 kb, respectively, for successful deletion and NHEJ of DMD. The gRNAs used were shown to be active in all three lines and effectively deleted exons 45–55 (**Figures S2 and S3**). Transient puromycin selection of cells nucleofected with the CRISPR plasmids improved the efficiency of deletion in CDMD 1003 and 1006 hiPSCs (**Figure S3D**).

Clonal Reframed DMD hiPSC Lines Contain No Off - Target Activity at Candidate Sites

Stably deleted DMD hiPSC lines were generated from CDMD 1003 and 1006 by clonal selection after nucleofection with the gRNA pair 44C4 and 55C3 (**Figures**

2B and 2C) and are pluripotent (**Figures 2C and S4B**). All reframed lines were karyotypically normal except for one clone (CDMD 1003-81), which was found to contain a 1q32 amplification confirmed via FISH analysis (**Figure S4A**), also observed in the original parental line and in all daughter clones after post hoc analysis. The 1q32 amplification is common in hPSCs after extended propagation in culture, and thus was not a result of CRISPR mediated off-target activity.¹²⁸ To determine off-target activity of our gRNAs, the top ten homologous sites per guide were determined by COSMID and sequenced in all clonal and parental lines.¹²⁹ No off-target mutations were observed at any site (**Table S2**). All variants, besides a heterozygous SNP in chromosome 11, were detected in less than 1% of reads, which is consistent with error in the sequencing method.

Dystrophin (DYS^{Δ45–55}) Expression Is Restored in Reframed DMD hiPSC-Derived Cardiomyocytes and Skeletal Myotubes

CRISPR/Cas9-mediated deletion of DMD should result in an internally deleted dystrophin protein lacking exons 45-55 (hereafter referred to as $DYS^{\Delta 45-55}$). As hiPSCs do not express dystrophin, we differentiated the reframed DMD hiPSC clonal lines to two disease-relevant cell types, cardiomyocytes and skeletal muscle myotubes, using directed differentiation or overexpression (OE) of MyoD to evaluate rescue of $DYS^{\Delta 45-55}$. PCR and sequencing of the exon 44/56 boundary in cDNA from the reframed cardiomyocyte clones demonstrated correct splicing of the dystrophin transcript (**Figures S4C and S4D**). Additionally, both the reframed cardiac and skeletal muscle cell lines restored dystrophin expression as assayed by

immunocytochemistry and western blot (**Figures 3A–3C**). Compared to wild-type CDMD 1002 or human skeletal muscle myotubes (HSMM), the band was truncated by ~66 kDa as expected.

DYSD45–55 Protein Restores Membrane Functionality to Cardiomyocytes and Skeletal Myotubes In Vitro

Cardiomyocytes or skeletal myotubes lacking dystrophin demonstrate membrane fragility in vitro and respond to osmotic stress by releasing elevated levels of CK, as is seen in human patients.^{115, 130, 131} To determine whether $DYS^{\Delta 45-55}$ could restore stability to dystrophic plasma membranes, we subjected differentiated cardiomyocytes and skeletal muscle myotubes derived from reframed and out-of-frame hiPSCs to hypo-osmotic conditions. Cells were stressed by incubation in hypo-osmolar solutions (66–240 mosmol) and CK release into the supernatant was measured to show functional improvement after dystrophin restoration. Both the reframed CDMD 1003-49 cardiomyocytes and skeletal muscle cells demonstrated reduced CK release, similar to wild-type (CDMD 1002), versus the out-of-frame CDMD 1003 cells, indicating that $DYS^{\Delta 45-55}$ was capable of reducing membrane fragility (**Figure 4A**). The same trend was also observed with CDMD 1006/1006-1 cardiomyocytes. (**Figure S4E**). After normalizing and pooling all experiments, we observed that significantly less CK was released at 93, 135, and 240 mosmol in the reframed and wild-type cells compared to out-of-frame (**Figure S4F**).

CRISPR/Cas9 Reframing Correlates with miR31 Levels in Skeletal Myotubes In Vitro

Elevated levels of miR31 have been observed in DMD patient biopsies compared to wild-type or BMD.¹²⁷ We measured levels of miR31 using droplet digital PCR (ddPCR) after differentiation of out-of-frame and reframed CDMD hiPSCs to skeletal myotubes. Reframing DMD reduced levels of miR31 (similar to wild-type cells) compared to out-of-frame DMD, as is observed in human dystrophinopathies (**Figure 4B**). Thus, reframing the DMD gene normalizes miR31 levels similar to BMD, demonstrating functional rescue of the dystrophic phenotype to a BMD phenotype.

DYS45–55 Protein Restores the DGC In Vitro and In Vivo

As a third assay of DYS^{A45–55} functionality, we evaluated its ability to restore the DGC in vitro and in vivo. The DGC member b-dystroglycan was restored and detected at the membrane of reframed hiPSCs, but not out-of-frame hiPSCs, after directed differentiation to skeletal muscle in vitro by immunostaining and western blot (**Figures 4C and 4D**). Additionally, skeletal muscle cells derived from a wild-type (CDMD 1002), out-of-frame (CDMD 1003), or reframed (CDMD 1003-49) hiPSC line were injected into the tibialis anterior (TA) of NOD scid IL2Rgamma (NSG)-mdx mice. Correctly localized dystrophin and b-dystroglycan was only observed in engrafted human cells (demarcated by human lamin A/C and spectrin) from the reframed or wildtype lines (**Figures 4E and 4F**). These studies taken

together with the hypo-osmotic stress assays demonstrate the ability of $DYS^{\Delta 45-55}$ to functionally reassemble the DGC and restore membrane stability in vitro and in vivo.

Discussion

Using CRISPR/Cas9 gene editing, we have induced the largest deletion accomplished to date in DMD hiPSCs and restored a functional dystrophin protein. Deletion of DMD exons 45–55 has the potential to be therapeutically relevant to 60% of DMD patients. Since this internal deletion has been associated with a very mild disease course in multiple independent patients, a therapy utilizing this approach should create a highly functional dystrophin. We showed successful deletion of exons 45–55 using a single gRNA pair and did not identify any off-target activity at the top ten homologous sites; however, a more comprehensive and unbiased approach should be undertaken such as whole-genome sequencing. Importantly, removal of exons 45–55 resulted in stable dystrophin protein ($DYS^{\Delta 45-55}$) in both cardiomyocytes and skeletal myotubes in vitro. Functionality of $DYS^{\Delta 45-55}$ was tested in cardiomyocytes and skeletal muscle derived from reframed DMD hiPSCs and demonstrated improved membrane stability by a physiologically relevant measure of CK release, similar to wild-type. The ability to evaluate cardiomyocyte functionality is an advantage of using hiPSCs, as some current preclinical and clinical studies for DMD therapies do not efficiently target the heart.¹³² Additionally, we demonstrated a normalization in miR31 levels, a

microRNA that inhibits dystrophin, after reading frame restoration, similar to what is observed in human BMD patients.¹²⁷ Finally, we show restored DGC localization in vitro and in vivo, which further validates the functionality of DYS^{Δ45-55}. Previous work by demonstrated that multiplexed gRNAs can restore the DMD reading frame in primary myoblasts.¹²³ However, myoblasts do not provide a renewable source of stem cells, which is a requirement for long-term therapeutic efficacy.¹³³ In contrast, we used hiPSCs, which offer the opportunity to evaluate the internally deleted dystrophin protein in multiple cell types that are affected in DMD, and in future studies, they may provide a renewal source of corrected progenitor cells.

Our work is further distinguished from previous studies as we are the only group to show restoration of dystrophin function on membrane integrity, miR31 expression, and the DGC in cardiac and skeletal muscle cells following CRISPR-mediated gene editing.

An advantage of our CRISPR platform is the therapeutic potential of a single pair of gRNAs to treat the majority of DMD patients. By designing gRNAs that accomplish a deletion that encompasses the majority of DMD mutations, this approach is optimized for future clinical studies. It would be unreasonable to design, validate, and evaluate off targets for every new CRISPR pair tailored for each individual patient.

Additionally, CRISPR/Cas9 is advantageous over exon skipping, as it results in permanent restoration of the reading frame as opposed to transient effects on RNA splicing. Previously, Li et al. (2015) used CRISPR/Cas9 to induce exon skipping, frameshifting, or exon knock in to restore dystrophin in a DMD hiPSC line with an exon 44 deletion; however, their platform is only applicable to 3%–9% of DMD

patients, and two of their strategies relied on the creation of indels, which would be difficult to apply consistently to each patient.¹³⁴ While Ousterout et al. deleted exons 45–55, they removed significantly less of the intervening region (336 kb) and thus their approach would cover fewer patient mutations within the hotspot region. This is because many mutations extend into the intronic region; thus, by designing gRNAs that encompass more of the intron, our platform is applicable to more patients.

Another benefit of using this platform to delete a large portion of DMD, as opposed to single exons, is the known correlation of $DYS^{\Delta 45-55}$ with a mild BMD phenotype. Large deletions in the rod domain of dystrophin often produce a more functional (more like wild-type) protein, than even very small deletions.¹³⁵ Larger deletions, which remove hinge III (exons 50–51), are believed to lead to a milder BMD phenotype than smaller deletions, or those that retain hinge III.¹³⁶ Thus, in many cases larger deletions are more therapeutically beneficial than smaller ones, due to the way they affect the secondary structure of the protein.

In summary, we have developed a potentially therapeutic gene editing platform for DMD to permanently restore the dystrophin reading frame in multiple patient-derived hiPSCs. Our approach using CRISPR/Cas9 and NHEJ deletes up to 725 kb of DMD encompassing exons 45–55 and restores dystrophin protein function in both cardiomyocytes and skeletal muscle cells derived from reframed hiPSCs. A current limitation of this platform is that clinical protocols still need to be developed that allow rapid clonal line derivation and the utilization of hiPSC-derived cardiac and skeletal muscle progenitors combined with gene correction.¹²⁰ Alternatively, CRISPR/Cas9 to restore the reading frame in DMD mouse models has been

delivered directly in vivo.^{122, 124, 137} Thus, applications of this platform in the future will allow for the development of an in situ gene strategy or ex vivo gene correction followed by autologous cell transplantation, either of which offers tremendous potential for DMD.

EXPERIMENTAL PROCEDURES

Differentiation of hiPSCs to Skeletal Muscle Cells and Cardiomyocytes

Skeletal muscle differentiation from hiPSCs was induced using OE of a tamoxifen inducible MyoD-ERT lentivirus or an adapted 50 day directed differentiation protocol where NCAM+ HNK1 cells underwent fluorescence-activated cell sorting at day 50. Cardiomyocytes were derived through aggregates over 30 days. See Supplemental Experimental Procedures.

Engraftment into Immunodeficient Mice

NSG immunodeficient mice (Jackson Laboratory) were crossed to mdx scid mice (Jackson Laboratory) to generate NSG-mdx mice (see Supplemental Experimental Procedures). Five- to seven-week-old NSG-mdx mice were pretreated with 50 ml of 10 mM cardiotoxin (Sigma-Aldrich) injected into the right TA 24 hr prior to engraftment. For MyoD OE cells, 100 ml of 5 mg/ml tamoxifen (Sigma-Aldrich) was i.p. injected for 5 days beginning on the day prior to engraftment. 1.3×10^6 cells in HBSS were injected intramuscularly and the TA was harvested after 30 days. See Supplemental Experimental Procedures.

Hypo-osmotic Stress CK Release Assay

Terminally differentiated skeletal muscle cells and cardiomyocytes plated in duplicate were stressed by incubation in hypo-osmolar solutions ranging from 66 to 240 mosmol (see Supplemental Experimental Procedures) for 20 min at 37°C. CK was measured in triplicate from the supernatant and cell lysate with the Creatine Kinase-SL kit (Sekisui Diagnostics) according to the manufacturer's instructions.

SUPPLEMENTAL EXPERIMENTAL PROCEDURES

Cloning of gRNAs

Five guide RNAs were designed to target DMD introns 44 and 55 using the Zhang lab CRISPR design tool (crispr.mit.edu) and cloned into the spCas9 plasmids pX330 or pX459 from Feng Zhang (Addgene #42230, #48139 respectively) adapted from Ran et al. (2013). In brief, oligos complementary to each other containing the gRNA sequence and BbsI restriction enzyme site were obtained from Integrated DNA Technologies and annealed. The annealed oligos and plasmid were simultaneously digested with BbsI (New England Biotechnologies) and ligated with T4 DNA ligase (Life Technologies).

gRNA sequences and oligos used for cloning

Name	Sequence	Sense oligo	Antisense oligo
44C1	GTGGTGCCTTTGAATATGCAGG	CACCGTGGTGCCTTTGAATATGC	AAACGCATATTCAAAGGACACCAC
44C2	AGATTGTCCAGGATATAAATTGG	CACCGAGATTGTCCAGGATATAAATT	AAACAATTATATCCTGGACAATCTC
44C3	TTAGCAACCAAATTATATCCTGG	CACCGTTAGCAACCAAATTATATCC	AAACGGATATAAATTGGTTGCTAAC
44C4	GTTGAAATTAACACTACACACTGG	CACCGTTGAAATTAACACTACACAC	AAACGTGTGTAGTTTAATTTCAAC
44C5	ATCTTTACCTGCATATTCAAAGG	CACCGATCTTTACCTGCATATTCAA	AAACTTGAATATGCAGGTAAGATC
55C1	TACACATTTTTAGGCTTGACAGG	CACCGTACACATTTTTAGGCTTGAC	AAACGTCAAGCCTAAAAATGTGTAC
55C2	CATTCTGGGAGTCTGTCATGGG	CACCGATTCTGGGAGTCTGTCAT	AAACATGACAGACTCCCAGGAATGC
55C3	TGTATGATGCTATAATACCAAGG	CACCGTGTATGATGCTATAATACCA	AAACTGGTATTATAGCATCATACAC
55C4	GTGAAAAGTACATAGGACCTTGG	CACCGTGGAAAAGTACATAGGACCT	AAACAGGTCTTATGTACTTTCCAC
55C5	TCTTATCATAACTCTTACCAAGG	CACCGTCTTATCATAACTCTTACCA	AAACTGGTAAGAGTTATGATAAGAC

Red text is NGG PAM sequence

Mice

All animal work was conducted under protocols approved by the UCLA Animal Research Committee in the Office of Animal Research Oversight. Mice used for engraftment experiments were generated by crossing mdx scid (Jackson Laboratory) with NOD scid IL2Rgamma (Jackson Laboratory) mice. Briefly, female B10ScSn.Cg-PrkdcscidDmdmdx/J were crossed with male NOD.Cg-PrkdcscidIL2rgtm1Wjl /SzJ. Then the F1 females from that cross were crossed with male mdx-scid. The F3 males were screened for dystrophin and gamma mutations and the mutants were then backcrossed again with mdx-scid females. F4 females were crossed with F3 mutant males which generated homozygous NSG-mdx mice. Genotyping was performed through TransnetYX.

Cell culture

Human embryonic kidney (HEK) 293FT cells (Life Technologies) were grown in standard conditions with growth medium consisting of DMEM (high glucose) with

10% fetal bovine serum (FBS, Life Technologies), 0.1mM non-essential amino acids (NEAA, Life Technologies), 6mM L-glutamine (Life Technologies). Human skeletal muscle myoblasts (HSMM, Lonza) were maintained according to the manufacturer's instructions with SkGM-2 medium (Lonza). For terminal differentiation, they were cultured on Matrigel (Corning) until at least 80% confluent and then switched to N2 differentiation medium (DMEM/F12 with 1% N2 supplement (Life Technologies) and 1% insulin-transferrin-selenium (ITS, Life Technologies)) for 7 days. Human induced pluripotent stem cells (hiPSCs) were reprogrammed from skin fibroblasts with the STEMCCA cassette as previously described (Karumbayaram et al., 2012). They were grown on hESC qualified Matrigel (Corning), fed daily with mTeSR1 medium (Stem Cell Technologies) and passaged with 0.5mM EDTA every 5-7 days. Karyotype and FISH analyses were performed by Cell Line Genetics®.

Teratoma injections

To prepare hiPSCs for injection, 1-2 confluent wells were collected using 1mg/ml of collagenase type IV or 0.5mM EDTA. Colonies were dissociated using a 5ml pipette and centrifuged at 1000rpm. Cell pellets were resuspended in 40µl of Hank's Balanced Salt Solution (HBSS) and injected into the testes of 6-8 week-old SCID BEIGE mice (Charles River) as described previously (Alva et al., 2011). After 4-8 weeks, teratomas were isolated and fixed in 4% paraformaldehyde (PFA) for 24 hours, then 70% ethanol. Fixed teratomas were embedded and processed by the Tissue Procurement Core Laboratory, Department of Pathology and Laboratory Medicine, David Geffen School of Medicine at UCLA. If teratomas were large, four to

six quadrants were isolated and fixed in PFA as described above. Tumors were stained with hematoxylin and eosin and imaged with an Olympus BX51 microscope.

Transfection and nucleofection of gRNAs

3x10⁵ HEK293FT cells were seeded per 12 well and transfected in duplicate the following day with 1µg DNA using 3µl TransIT293 (Mirus Bio) according to the manufacturer's instructions. Amaxa 4D (Lonza) nucleofection of hiPSCs was performed according to the manufacturer's instructions. In brief, hiPSCs were pre-treated with 10µM ROCK inhibitor Y-27632 (ROCKi, Tocris Bioscience) for 1hr and trypsinized into a single cell suspension with TrypLE (Life Technologies). 8x10⁵ hiPSCs were nucleofected per 100µl cuvette using solution P3, 2µg or 3.5µg total DNA, and program CA-137 (Lonza). pMAX GFP (Lonza) was used as a transfection control. After nucleofection, cells were immediately plated in mTeSR1 with ROCKi. For selection, 0.35µg/ml of puromycin in mTeSR1 was added to the cells for 24hrs the day after nucleofection.

Generation of clonal hiPSC lines

For generation of clonal lines, the day following nucleofection of gRNAs 44C4 and 55C3 (in pX459) cells were selected with 0.35µg/ml of puromycin in mTeSR1 for one day. The cells were expanded for 7-9 days in mTeSR1 and then either single cell sorted in ROCKi using a FACS Aria sorter (BD) into individual 96 wells or plated at low densities of 3x10⁵-5x10⁵ cells per 10cm dish in mTeSR1 plus ROCKi. After 2

weeks, individual colonies were scrapped into a corresponding 48 well and a subset of the colony was manually dissected and screened using the deletion genotyping PCR below.

Deletion genotyping PCR

For determining if the exon 45-55 deletion occurred, either individual PCR reactions or a multiplex PCR containing both sets of primers was performed with AccuPrime Taq High Fidelity (Life Technologies). One primer pair flanked the deleted region (del) and one pair was within the deleted region (undel). PCR products were run on a 1.2% agarose gel and visualized with ethidium bromide staining.

Primer sequences for PCR

Primer name, <i>purpose</i>	Sequence
44_F, <i>forward primer for del genotyping</i>	CTGGACGGAGCTGGTTTATCT
55surv2_R, <i>reverse primer for del genotyping</i>	CCCTTTTCTTGCGTATTGCC
55undel1_F, <i>forward primer for undel genotyping</i>	GCCTGGGTCTCTGCTATCAA
55undel1_R, <i>reverse primer for undel genotyping</i>	GCCACTTTGTACTCCGCACT

Analysis of the rejoining sequence after an exon 45-55 deletion was performed by blunt cloning the deleted PCR products into the Zero Blunt TOPO backbone (Life Technologies), according to the manufacturer's instructions, and sequencing of the insert by Laragen Inc.

Differentiation of hiPSC-derived skeletal muscle

hiPSCs were differentiated into skeletal muscle cells by overexpression of MyoD, adapted from Abujarour et al. (2014). Cells were trypsinized with TrypLE and plated as single cells on Matrigel in SMC4 (basal medium: DMEM/F-12 with 20% knock-out serum replacement (KOSR, Life Technologies), 1% NEAA, 1% Glutamax (Life Technologies), 100µM beta-mercaptoethanol, 10ng/mL basic fibroblast growth factor (bFGF, Life Technologies); SMC4: basal media with daily addition of 5µM ROCKi, 0.4µM PD0325901 (Sigma-Aldrich), 2µM SB431542 (Tocris Bioscience), 1µM CHIR99021 (Tocris Bioscience)) at 3.5×10^5 cells/ 6 well. When they reached approximately 60-80% confluent they were infected with 0.06µg/mL of a tamoxifen inducible MyoD-ERT lentivirus (adapted from Kimura et al., 2008) with 4µg/mL protamine sulfate per well and spun inoculated at 1250rpm for 90mins at 32°C. After a day of recovery they were selected with 2µg/ml puromycin in SMC4 for 2 days. The cells were then split and plated on Matrigel in basal medium without bFGF plus 10µM ROCKi at approximately 1×10^5 cells/cm² and induced in DMEM with 15% FBS and 5µM tamoxifen for 4 days. Following induction, the cells were differentiated in low glucose DMEM with 5% horse serum and 1µM tamoxifen for 5-7 days. Medium was changed daily. An alternative protocol for MyoD overexpression was used for engraftment. Cells were single cell plated at 2.5×10^4 cells/cm² on Matrigel in mTeSR1 with ROCKi. Beginning the following day, they were treated with 3µM CHIR99021 in DMEM/F12 with 1% ITS for 2 days. The cells were split to approximately 6×10^4 cells/cm² in DMEM with 10% FBS and 1% NEAA and infected with the MyoD-ERT lentivirus as above. After a day of recovery, the cells were selected with 1µg/ml puromycin for 4 days followed by induction in IMDM containing 15% FBS, 10% horse serum (HS), 1% chick

embryo extract, 50µg/ml ascorbic acid, 4.5mM monothioglycerol, 5ng/ml bFGF with 5µM tamoxifen for 2 days and used for engraftment as described below. A directed differentiation protocol for hiPSCs adapted from Shelton et al. (2014) was also used to obtain SMPCs. Cells were single cell plated in mTeSR1 with 10µM ROCKi at 3.75x10⁵ cells/6 well. The following day, 10µM of CHIR99021 was added in Essential 6 medium (E6, Stem Cell Technologies) for 2 days and the cells were allowed to differentiate until day 12 in E6. StemPro (Gibco) containing 20ng/ml bFGF was added between days 12 to 20. E6 was then added until day 35 when the cells were switched to N2 medium in order to terminally differentiate. At day 50, cells were fluorescently activated cell sorted to remove neural crest cells with HNK1- (1:300, Sigma-Aldrich) and enrich for SMPCs with BV650-NCAM+ (1:25, BD Bioscience). The SMPCs were cultured in expansion media (20% FBS, 5% HS, 1% chick embryo extract, 0.5% penicillin/streptomycin) until confluent when they were changed to N2 medium for 7 days to induce terminal differentiation.

Differentiation of hiPSC-derived cardiomyocytes

Confluent hiPSCs were enzymatically dissociated to form aggregates and differentiated into the cardiomyocyte lineage as previously described (Arshi et al. 2013; Minami et al. 2012). The medium was changed every 2 days up to day 15, and every 5 days up to day 30. At day 30, cardiomyocytes were harvested for analysis or subjected to the hypoosmotic stress assay.

Surveyor assay

For testing the activity of different gRNAs, genomic DNA (gDNA) was extracted on day 3 or 4 after transfection/nucleofection using the Quick gDNA mini prep kit (Zymo Research) or Quick Extract DNA Extraction Solution 1.0 (Epicenter) according to the manufacturer's instructions. PCR for use in Surveyor assay was performed with AccuPrime Taq High Fidelity with primers flanking the target region. The Surveyor assay (Integrated DNA Technologies) was performed according to the manufacturer's instructions. In brief, approximately 300ng of PCR product in 1x AccuPrime buffer up to 20µl was denatured and reannealed by heating at 95°C for 10min and slowly step-wise cooling to 4°C. Then 2µl MgCl₂, 1µl Surveyor enhancer, and 1.2µl Surveyor enzyme were added and incubated at 42°C for 1hr. The G/C plasmids provided in the Surveyor kit were used as a positive control for every gel. The products were run on a 6% or 4-20% TBE polyacrylamide gel (Bio-Rad) and visualized with ethidium bromide staining. The percent of cutting was determined using ImageJ (Rasband, 1997).

Primer sequences for PCR

Primer name, purpose	Sequence
<i>44surv_F forward primer for intron 44 surveyor</i>	GAGAGTTTGCCTGGACGGA
<i>44surv_R, reverse primer for intron 44 surveyor</i>	CCTCTCTATACAAATGCCAACGC
<i>55surv2_F, forward primer for intron 55 surveyor</i>	TCCAGGCCTCCTCTCTTTGA
<i>55surv2_R, reverse primer for intron 55 surveyor</i>	CCCTTTTCTTGCGTATTGCC

Hypoosmotic stress CK release assay

Hypoosmolar salt solutions ranging from 66-240mosmol were made by adding varying amounts of sucrose (~25-175mM) to a basic salt solution consisting of

5mM HEPES, 5mM KCl, 1mM MgCl₂, 5mM NaCl, 1.2mM CaCl₂, 1mM glucose. Osmolarities were measured with a Wescor Vapro 5520 osmometer. Differentiated MyoD OE skeletal myotubes and cardiomyocytes were plated in a 384 or 96 well plate in duplicate per condition tested. 100µl (or 30µl for 384 well plates) of the hypoosmolar solution was added to each well and the cells were incubated at 37°C for 20mins. The solution (supernatant) was then removed and stored at - 80°C until CK analysis. The cells were trypsinized and lysed in 100µl dI water by repeated freeze/thawing three times. The lysate was stored at -80°C until CK analysis. CK was measured in triplicate with 2µl or 8µl of undiluted sample using the Creatine Kinase-SL kit (Sekisui Diagnostics) according to the manufacturer's instructions. Any negative readings were forced to be 0 and outliers were discounted from the analysis. The percent of CK release into the supernatant was determined and the standard error was propagated throughout all calculations.

RNA extraction, cDNA, and PCR

RNA was extracted from differentiated cardiomyocytes using the RNeasy Micro Kit (Qiagen) according to the manufacturer's instructions. cDNA synthesis was performed on 50-250ng of RNA using the iScript Reverse Transfection Supermix for RT-qPCR (Bio-Rad). Two PCR reactions were done on all samples, one with primers internal to the deletion and one with primers flanking the deletion for 40 cycles using AccuPrime Taq. PCR products were cloned using the TOPO-TA cloning kit (Life Technologies) according to the manufacturer's instructions and sequenced at the UCLA GenoSeq Core.

Primer sequences for PCR

Primer name, <i>purpose</i>	Sequence
DMD_E43-44_F, <i>forward primer for cDNA, deleted</i>	CCGACAAGGGCGATTTGACA
DMD_E57_R, <i>reverse primer for cDNA, deleted</i>	AAGTCGCCTCCAATAGGTGC
DMD_E52_F, <i>forward primer for cDNA, undeleted</i>	ACTCATTACCGCTGCCCAAA
DMD_E55_R, <i>reverse primer for cDNA, undeleted</i>	TCTTCCAAAGCAGCCTCTCG

miRNA extraction, cDNA, and ddPCR

miRNA was isolated from fused myotubes obtained by MyoD OE using a microRNA purification kit (Norgen Biotek Corp) according to the manufacturer's instructions. cDNA synthesis was performed on 5µl of miRNA with TaqMan microRNA reverse transcription kit (Applied Biosystems) using a TaqMan MicroRNA Assay (Applied Biosystems) for hsa-miR-31 (assay ID 002279) and U6 snRNA (assay ID 001973) with specific RT primers. PCR reactions were prepared in a premix of 22µl with 1.46µl of cDNA (either diluted 1:30 for U6 or undiluted for miR31) in ddPCR supermix for probes (without UTP) (Bio-Rad) and 1.1µl 20x TaqMan assay probes for each sample in duplicate. 20µl of the PCR reaction premix was used to generate droplets according to the manufacturer's protocol. Briefly, PCR premix was added to a droplet generator cartridge with 70µl of oil and droplets were generated with the QX200 droplet generator (Bio-Rad). 40µl of this reaction mix was transferred to a PCR plate and run on at T100 thermal cycler (Bio-Rad) at 95°C for 10mins, 40 cycles of 95°C 15sec, 60°C for 60sec, followed by 98°C for 10mins. A no template control was included for each PCR reaction. FAM fluorescence was evaluated using the QX200 droplet reader and QuantaSoft software (Bio-Rad). The percent of positive droplets for miR31 was normalized to the percent of positive droplets for

U6. Standard deviation error was propagated through all calculations. All lines were normalized to CDMD 1002 wild type.

Engraftment into immunodeficient mice

NOD scid IL2Rgamma (NSG) immunodeficient mice (Jackson Laboratory) were crossed to mdx scid mice (Jackson Laboratory) to generate NSG-mdx mice, see above. 24hrs prior to engraftment, the right tibialis anterior (TA) of 5-7 week-old NSG-mdx mice was pretreated with 50 μ l of 10 μ M cardiotoxin (Sigma-Aldrich). For MyoD OE cells, 100 μ L of 5mg/ml tamoxifen (Sigma-Aldrich) was also IP injected for 5 days with tamoxifen pretreatment starting the day before engraftment (Muir et al., 2014). 1x10⁶ cells obtained from MyoD OE after induction were pelleted and resuspended in 5 μ L HBSS and injected intramuscularly into the TA. Tissue was harvested after 30 days and analyzed as described below. Engraftment was considered successful when we identified human cells that were both lamin A/C and spectrin positive. Successful engraftment was seen in the following: CDMD 1002 N=4/4 engrafted successfully; CDMD 1003 N=1/1 engrafted successfully; and CDMD 1003-49 N=1/2 engrafted successfully.

Immunostaining

hiPSCs were fixed in 4% PFA for 20mins, permeabilized with 0.3% Triton X for 10mins and blocked in 10% goat serum for 1hr. Primary antibodies to SOX2 (1:200, Cell Signaling) and NANOG (1:800, Cell Signaling) were added in 1% goat

serum and 0.1% Triton X overnight at 4°C followed by secondary antibodies for 2hrs the following day. Differentiated skeletal myotubes obtained from MyoD overexpression were fixed in 80% acetone for 7mins at -20°C, blocked with 10% goat serum for 1hr and stained with dystrophin (1:300, Abcam) and myosin heavy chain (1.9µg/ml, MF20, DHSB) as above. Differentiated cardiomyocytes and skeletal myotubes obtained from the 50 day directed differentiation protocol were fixed in 4% PFA for 20mins, permeabilized with 0.3% Triton X for 10mins, blocked in 10% goat serum for 1hr and stained with dystrophin (1:5, MANDYS106, MDA Monoclonal Antibody Resource, (Man and Morris, 1993)) or beta-dystroglycan (1:100, Leica Biosystems) and myosin heavy chain (1.9µg/ml, MF20, DHSB). Images were obtained with the Axio Observer Z1 microscope (Zeiss). Harvested TA muscles were flash frozen in isopentane. 10µm cryosections were obtained at intervals throughout the entire muscle and stored at -20°C. For staining, they were blocked in 0.25% gelatin, 0.1% Tween, 3% bovine serum albumin for 1hr. The M.O.M. blocking kit (Vector Laboratories) was applied according to the manufacturer's instructions. Primary antibodies consisting of human lamin A/C (1:125, Vector Laboratories), human spectrin (1:75, Leica Biosystems), human dystrophin (1:5, MANDYS106), laminin (1:200, Sigma-Aldrich), dystrophin (1:75, Abcam), and beta-dystroglycan (1:50, Leica Biosystems) were applied overnight at 4°C. The following day secondary antibodies were incubated for 1hr and the slides were mounted with VECTASHIELD containing DAPI (Vector Laboratories) and imaged on the Axio Observer Z1 microscope.

Western blot analysis

Terminally differentiated skeletal muscle cells and cardiomyocytes were trypsinized, pelleted, and flash frozen in liquid nitrogen. Cell pellets were stored in liquid nitrogen until lysis. For Western blotting, samples were prepared as described in Woo et al. (2010) with slight modifications. In brief, cells were solubilized in 500 μ l of lysis buffer (10mM Tris-HCl (pH 7.4), 1% Triton X-100, 10% glycerol, 150mM NaCl, 5mM EDTA, and HALT protease and phosphatase inhibitor cocktail (ThermoScientific)) per a 10cm culture dish, followed by incubation at 4°C for 30 min with gentle rotation. Then lysates were mixed with 100 μ l of 6 \times RSB and passed several times through a syringe needle to reduce viscosity. Afterwards samples were boiled for 3 min, cooled on ice, passed through a syringe needle again and centrifuged for 5 min at 13,000g. Clarified lysates were transferred to new tubes, aliquoted and stored at -80°C till use. To evaluate dystrophin and MyHC content, cell lysates were subjected to 6% polyacrylamide gel electrophoresis (PAGE) for 3 hours at constant current (10mA per gel); followed by blotting to nitrocellulose membrane at constant voltage (100V) for 2.5 hours on ice. 0.1% sodium dodecyl sulfate (SDS) and 10mM dithiothreitol was added to the transfer buffer to facilitate blotting of high molecular proteins. Immunoblot assay was carried out with mouse anti-MyHC (1:1,000; MF20, DHSB), and mouse anti-dystrophin (1:500; Mandys8, Sigma-Aldrich) antibodies. Secondary antibodies used were anti-mouse peroxidase conjugates from Sigma-Aldrich (1:10,000). Blots were developed using ChemiGlow West chemiluminescent detection kit (ProteinSimple). Signals were registered by the FluorChem FC2 digital imaging system (Alpha Innotech). For β -dystroglycan, a 7.5% PAGE gel was run for 1.5hrs at 100V. Transfer was performed in Tris/Glycine with 20% MetOH for 1hr 15min at 100V.

Immunoblotting was performed with mouse anti- β -dystroglycan (1:200, MANDAG2(7D11), DHSB) and MyHC antibody as above.

Off target analysis

The top 10 unique off target sites for each gRNA used (44C4 and 55C3) were determined with COSMID (Cradick et al., 2014) using the following criteria: NRG PAM, 3 mismatches with no indels, and 2 mismatches with 1-base deletions or insertions. Access Array primers corresponding to the potential off target locations were designed, manufactured and validated by Fluidigm. gDNA extracted from the parental and deleted clonal lines was run on an Access Array (Fluidigm) and sequenced with MiSeq in the UCLA GenoSeq Core. Reads were trimmed with Trimmomatic and aligned to the genome using BWA. A base quality score recalibration and indel realignment was performed using GATK and SNP calling was done using two separate programs, GATK and LoFreq on the 20bp gRNA homologous region. A true induced mutation was considered possible if the fraction of reads with a given variant was substantially higher than error rate of base calling.

Top potential off target sites as determined by COSMID

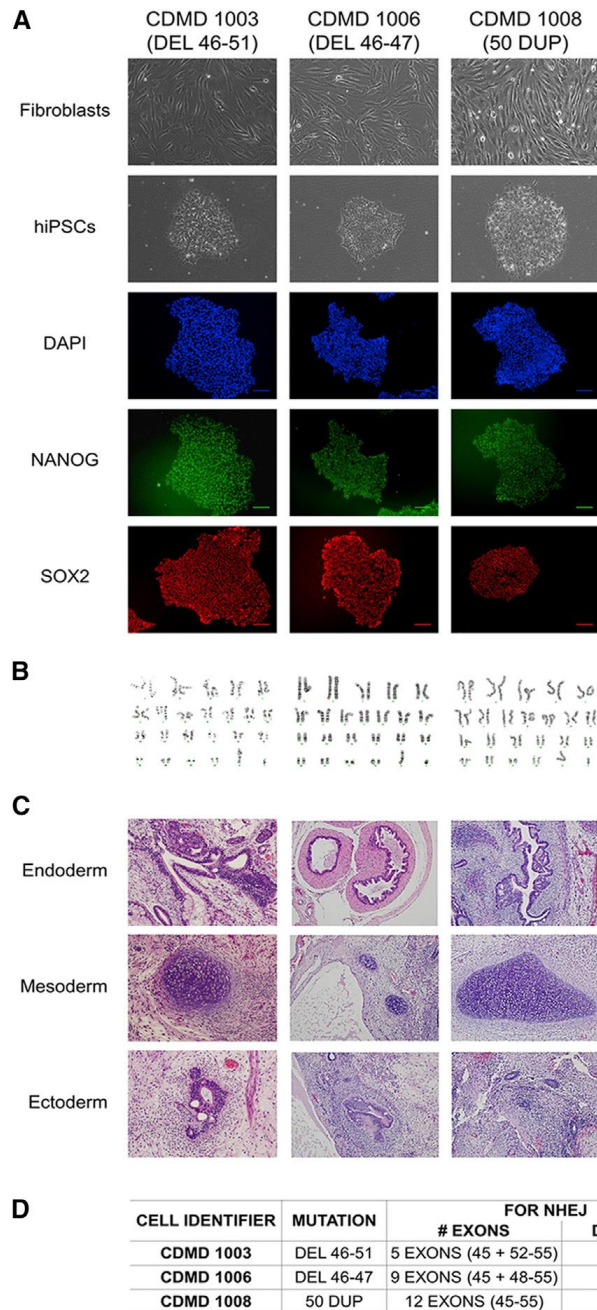
Name	Genomic location (hg19)
44C4_OT1	Chr11:87808333-87808355
44C4_OT2	Chr3:160301263-160301285
44C4_OT3	Chr4:168882168-168882190
44C4_OT4	Chr11:12974242-12974264
44C4_OT5	Chr11:28401278-28401300
44C4_OT6	Chr11:96681660-96681682
44C4_OT7	ChrX:44266358-44266380
44C4_OT8	Chr6:75606852-75606874
44C4_OT9	Chr1:91110525-91110547
44C4_OT10	Chr3:145258890-145258912
55C3_OT1	Chr18:31956684-31956706
55C3_OT2	Chr2:28730131-28730153
55C3_OT3	Chr10:4923833-4923855
55C3_OT4	Chr13:68797419-68797440
55C3_OT5	Chr13:70672235-70672256
55C3_OT6	Chr4:101494350-101494372
55C3_OT7	Chr3:81046407-81046428
55C3_OT8	Chr11:45856883-45856904
55C3_OT9	Chr1:171162826-171162847
55C3_OT10	Chr3:108717117-108717140

Statistical analysis

Statistical analyses were performed using a two-tailed t-test on two groups of data. First an F-test was used to determine if the variances were equal or unequal, then the corresponding t-test was used. Significance was determined by a p-value less than 0.05.

Figure Legends

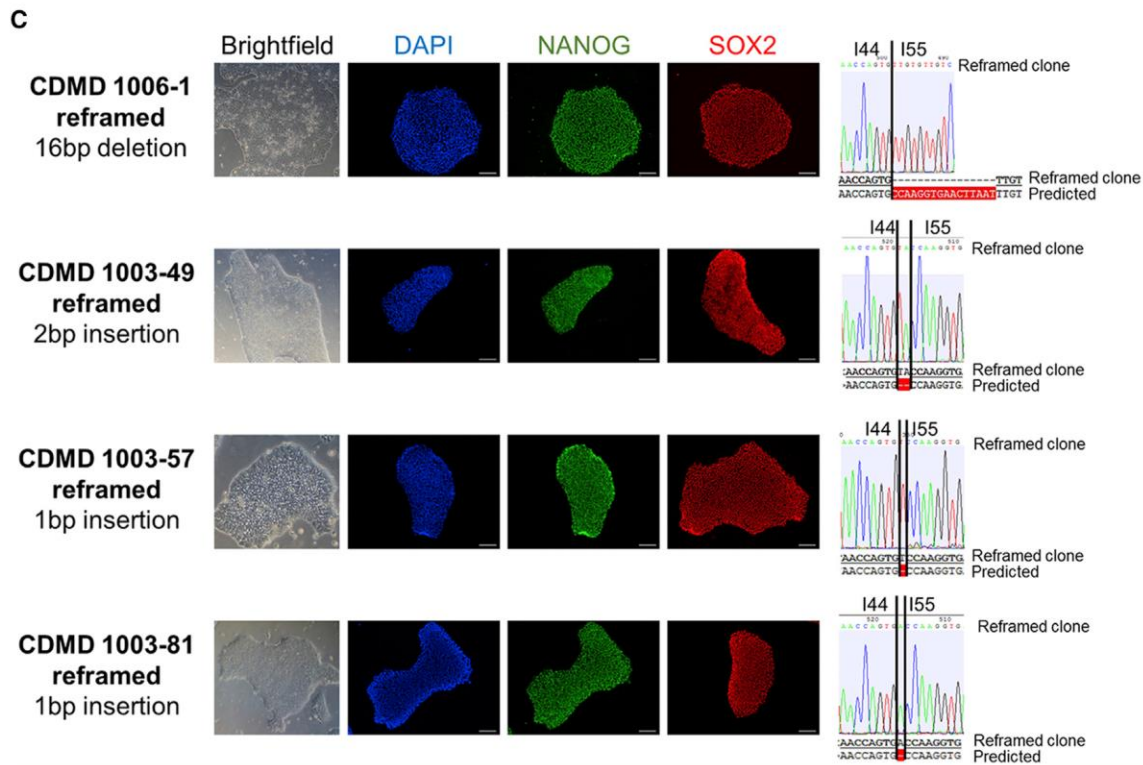
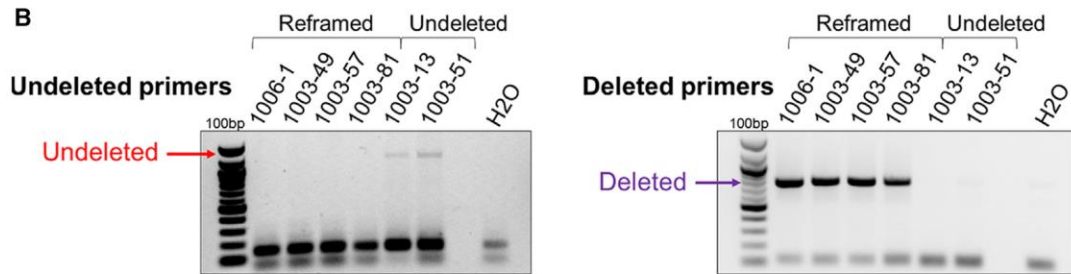
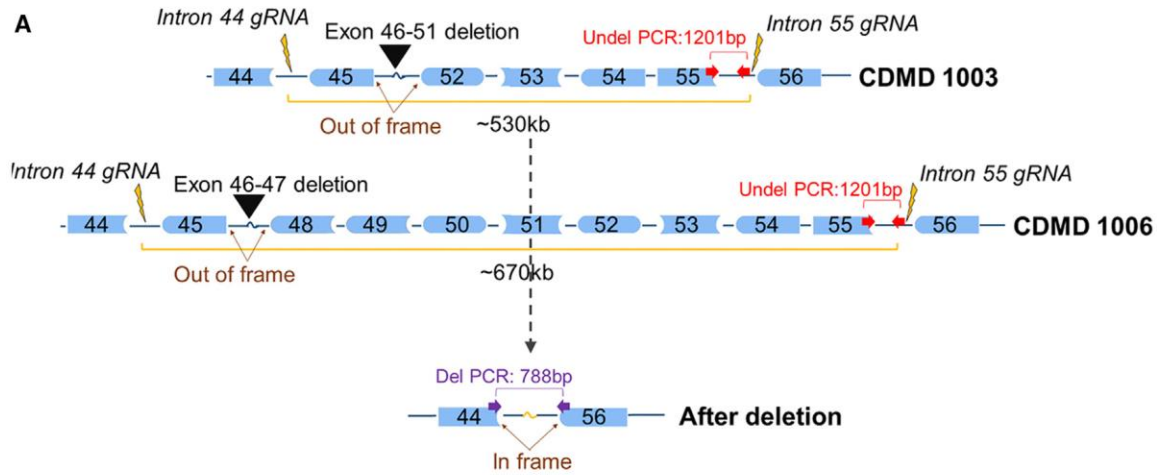
Figure A-1. CDMD hiPSCs Are Pluripotent and Genetically Stable



(A) CDMD hiPSCs were generated from DMD fibroblasts. Brightfield images depict fibroblasts before and after reprogramming to hiPSCs. Immunocytochemical

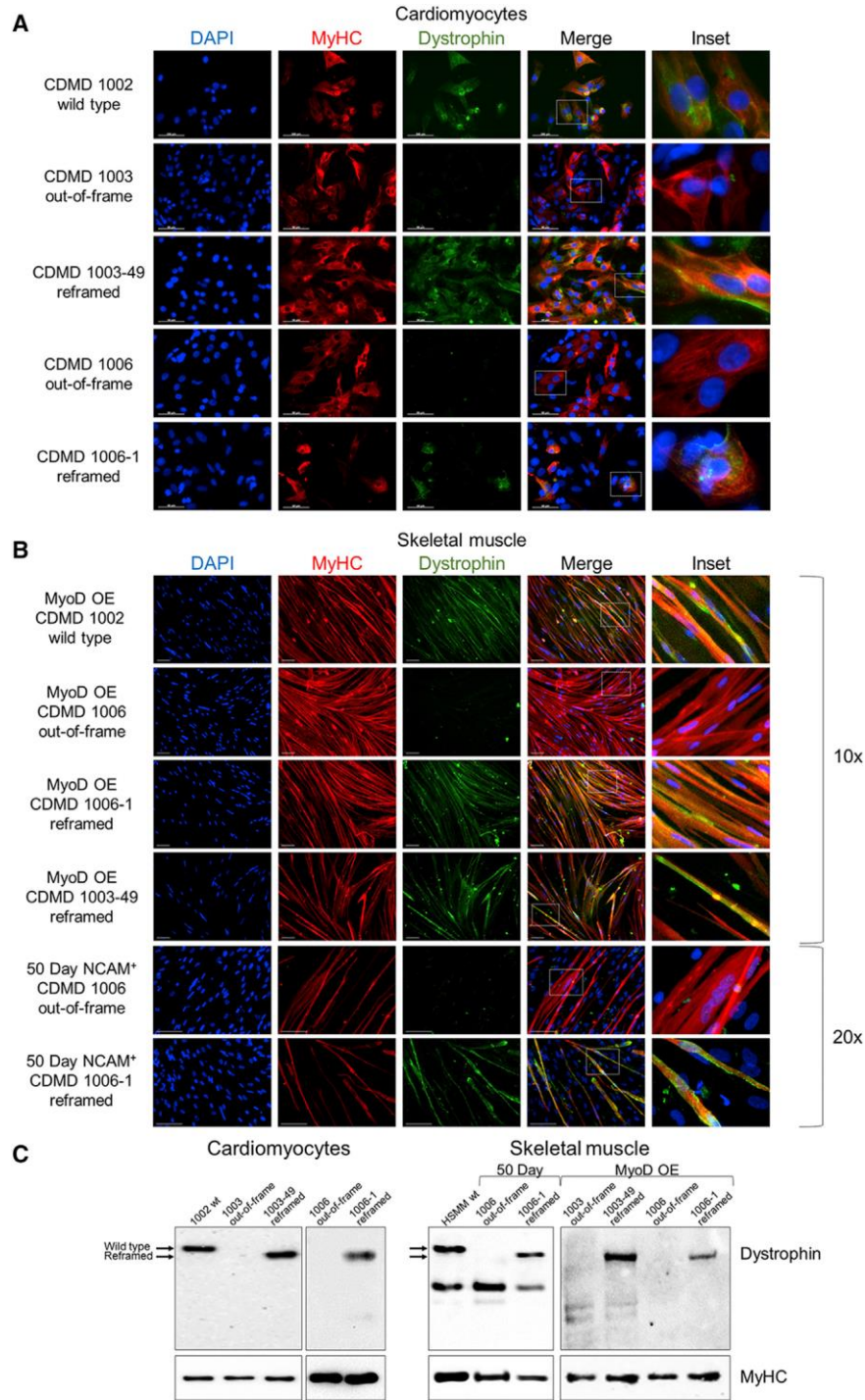
staining reveals that cells express pluripotency markers NANOG (green) and SOX2 (red). Scale bar, 100 μ m. (B) Karyotyping of all lines is shown. (C) CDMD hiPSCs were injected into mice to test teratoma formation *in vivo*. Representative H&E stainings of the three germ layers (endoderm, mesoderm, and ectoderm) are shown. (D) Patient mutations for each CDMD hiPSC line are shown. In addition, the number of exons and the approximate distance necessary for successful NHEJ is indicated, based on comparative genomic hybridization data for the patient's underlying mutation size.

Figure A-2. Generation of Stable, Pluripotent CDMD hiPSC Lines with an Exon 45–55 Deletion



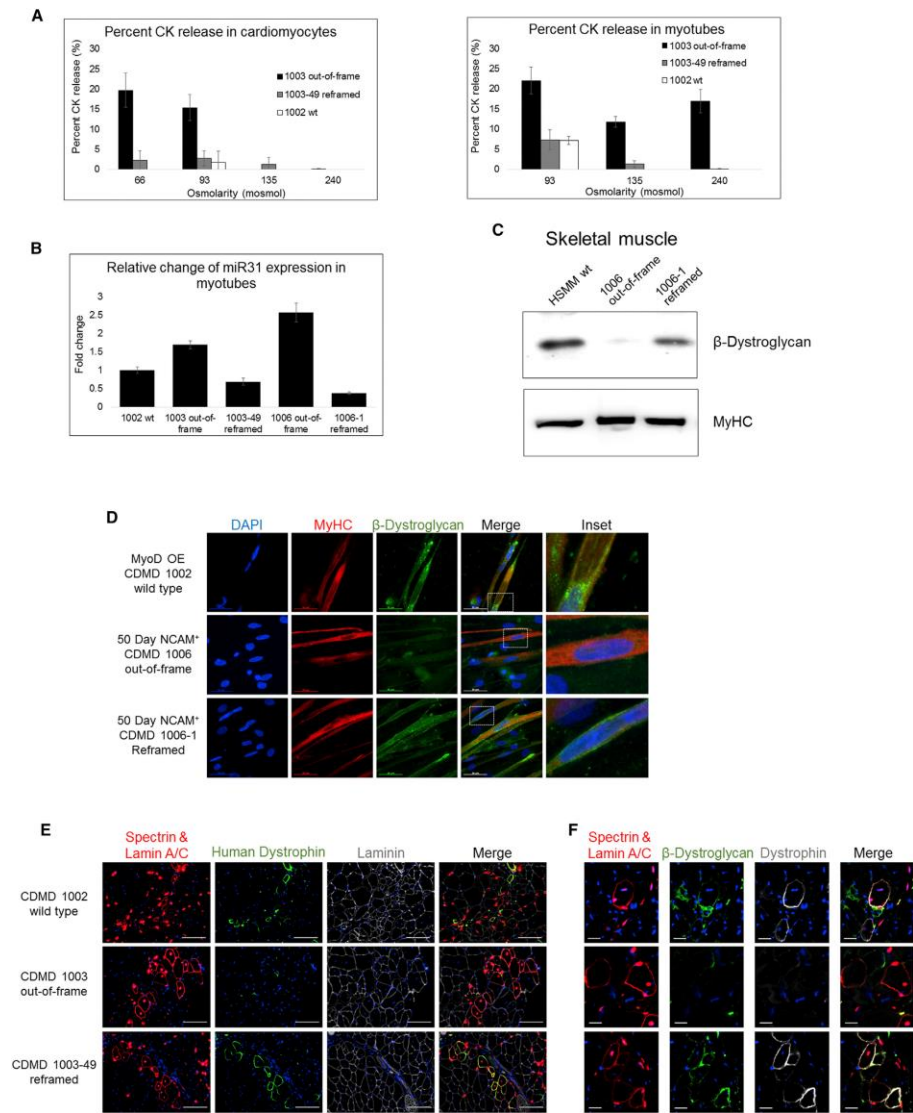
(A) Shown is a cartoon (not to scale) of the region of DMD targeted for CRISPR/Cas9-mediated deletion using gRNAs specific to introns 44 and 55 (lightning bolts). Successful NHEJ deletes exons 45–55 and restores the reading frame for mutations within this region. Different deletion sizes are required depending on the patient's underlying mutation (black arrow heads). (B) PCR genotyping of 117 and 109 single-cell clones from parental lines CDMD 1006 and 1003, respectively, was carried out on cells nucleofected with gRNAs 44C4 and 55C3. One clone from CDMD 1006 (CDMD 1006-1) and three from CDMD 1003 (CDMD 1003-49, 1003-57, and 1003-81) were identified as stably deleted. Deletion PCR genotyping results for six hiPSC clonal lines is shown. One pair of primers (red arrows in A) was located internal to the deletion and only produced a 1,201 bp band in the undeleted clones CDMD 1003-13 and 1003-51. Another primer set (purple arrows in A) flanked the deletion region and produced a 788 bp band only when the deletion and NHEJ occurred successfully, as in the reframed clones CDMD 1006-1, 1003-49, 1003-57, and 1003-81. (C) Each clonal line maintained normal morphology (brightfield) and expressed NANOG (green) and SOX2 (red) by immunocytochemistry. Scale bar, 100 μ m. Shown to the right is the sequence of the gDNA at the rejoining site between introns 44 (I44) and 55 (I55). Sequencing revealed a 16 bp deletion in CDMD 1006-1, a 2 bp insertion in CDMD 1003-49, and 1 bp insertions in CDMD 1003-57 and CDMD 1003-81.

Figure A-3. Reframed CDMD hiPSC-Derived Skeletal Muscle and Cardiomyocytes Restore Dystrophin Expression



(A) Immunocytochemical staining of human myosin heavy chain (MyHC, red) and dystrophin (green) of wild-type (CDMD 1002), out-of-frame (CDMD 1003 or 1006) or reframed (CDMD 1003-49 or 1006-1) cardiomyocytes derived from hiPSCs by directed differentiation. Inset depicts zoomed in region defined by the white box. Scale bar, 50 mm. (B) Immunocytochemical staining of MyHC (red) and dystrophin (green) of wild-type (CDMD 1002), out-of-frame (CDMD 1006) or reframed (CDMD 1006-1 or 1003-49) skeletal muscle myotubes derived from hiPSCs. Myotubes were fused after MyoD OE or from sorted NCAM+ cells after an adapted directed differentiation 50-day protocol was used. Inset depicts zoomed-in region defined by the white box. Scale bar, 100 mm. (C) Western blots of cell extracts probed with antidystrophin. Extracts were from out-of-frame and reframed cardiomyocytes (left) and skeletal muscle myotubes (right), derived from CDMD hiPSCs. Wild-type (wt) hiPSCs (CDMD 1002) or human skeletal muscle myotubes (HSMM) were used as a control for dystrophin. The molecular weight shift caused by the exon 45–55 deletion (1779 bp, ~66 kDa) is evident in reframed versus wild-type dystrophin (arrows). A non-specific band around 220 kDa was seen in some samples. Samples were also probed with anti-MyHC as a loading control (bottom panels).

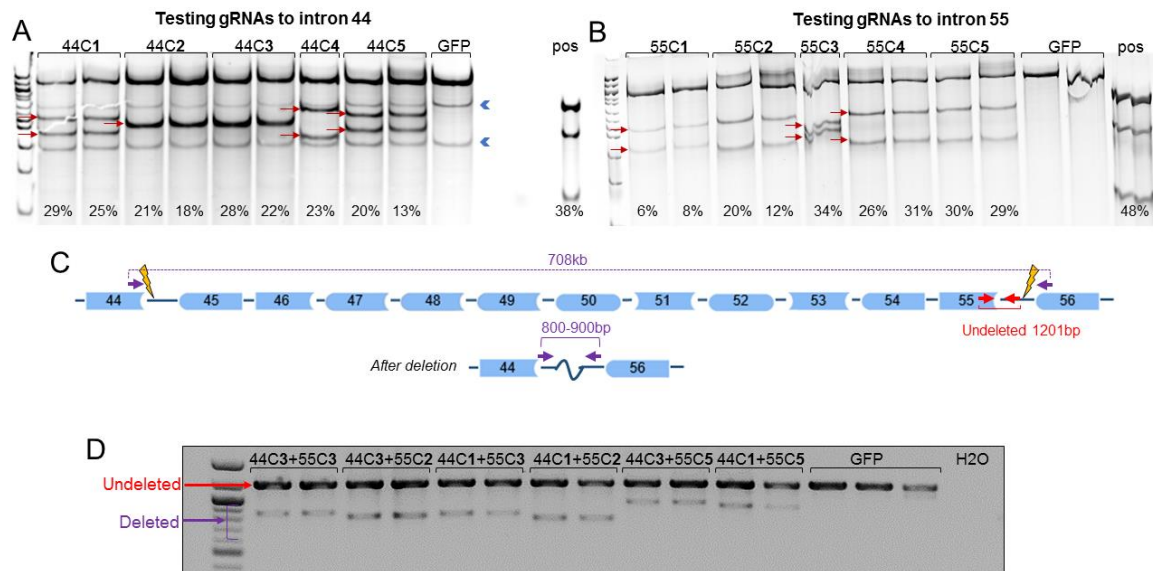
Figure A-4. Reframed hiPSC-Derived Cardiomyocytes and Skeletal Muscle Cells Demonstrate Restored Function In Vitro and In Vivo



(A) Representative graphs of CK release assays from cells exposed to hypo-osmotic conditions. Cardiomyocytes and skeletal muscle myotubes derived from hiPSCs were subjected to a range of osmolarities below 240 mosmol, and CK release to the supernatant was measured as an indication of membrane fragility. Data are

presented as average \pm SE. (B) Fold change in expression of miR31 measured by ddPCR in myotubes derived from out-of-frame or reframed hiPSCs by MyoD OE, normalized to wild-type (CDMD 1002). Data are presented as average \pm SD. (C) Western blots of cell extracts probed with anti-b-dystroglycan. Extracts were from out-of-frame and reframed skeletal muscle myotubes derived by MyoD OE. HSMM was used as a positive control. Samples were also probed with anti-MyHC as a loading control (bottom panel). (D) Immunocytochemical staining of MyHC (red) and b-dystroglycan (green), a component of the DGC, in wild-type (CDMD 1002), out-of-frame (CDMD 1006), or reframed (CDMD 1006-1) skeletal muscle myotubes. Inset depicts zoomed-in region defined by the white box. Scale bar, 50 μ m. (E) Assessment of human dystrophin restoration in wild-type (CDMD 1002), out-of-frame (CDMD 1003), and reframed (CDMD 1003-49) MyoD OE cells engrafted into the TA of NSG-mdx mice. Engrafted human cells were identified by co-immunostaining for human spectrin and lamin A/C (shown in red). Positive staining for human dystrophin is shown in green and all fibers are shown using laminin (gray). All sections were stained with DAPI (blue) to identify nuclei. Scale bar, 100 μ m. (F) Assessment of b-dystroglycan restoration in human fibers from wild-type (CDMD 1002), out-of-frame (CDMD 1003), and reframed (CDMD 1003-49) MyoD OE cells engrafted into the TA of NSG-mdx mice. Engrafted human cells were identified by co-immunostaining for human spectrin and lamin A/C (shown in red). Positive staining for dystrophin is shown in gray and b-dystroglycan is shown in green. All sections were stained with DAPI (blue) to identify nuclei. Cell order is the same as noted in (E). Scale bar, 20 μ m.

Figure A-S1: gRNA activity and exon 45-55 deletion in 293FT cells

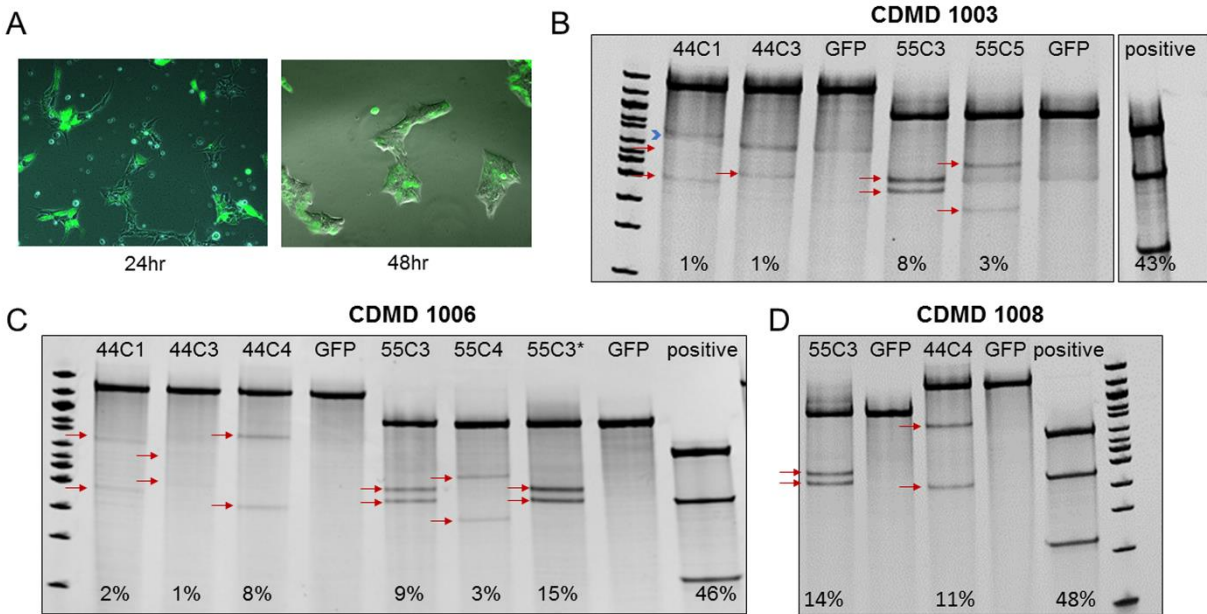


A-B. Five gRNAs targeted to introns 44 and 55 respectively, show activity on Surveyor assay in HEK293FT cells. Red arrows denote expected cleavage product bands (Table S1). Note in A, the bands highlighted by the blue arrowheads are likely non-specific PCR products and were discounted from the analysis. The estimated percent of cutting is shown below each lane. The positive control (pos) is provided with the Surveyor kit. A 100bp ladder was used.

C. Cartoon highlighting the region of DNA targeted by CRISPR pairs and indicating primers used for PCR. CRISPR gRNA sites are shown by lightning bolts. When pairs of gRNAs targeted to introns 44 and 55 are co-transfected, an exon 45-55 deletion (~708kb) results after NHEJ. This deletion is measured using multiplex PCR where the primer pair shown in red will amplify the undeleted product while the purple primer pair flanking the deleted region only gives a product when successful rejoining has occurred. D. Example of a multiplex PCR, using the primers indicated

in C, in which effective deletion of exons 45-55 was achieved with all gRNA pairs tested in 293FT cells. A 100bp ladder was used.

Figure A-S2: gRNAs show cutting by Surveyor assay in CDMD hiPSCs.

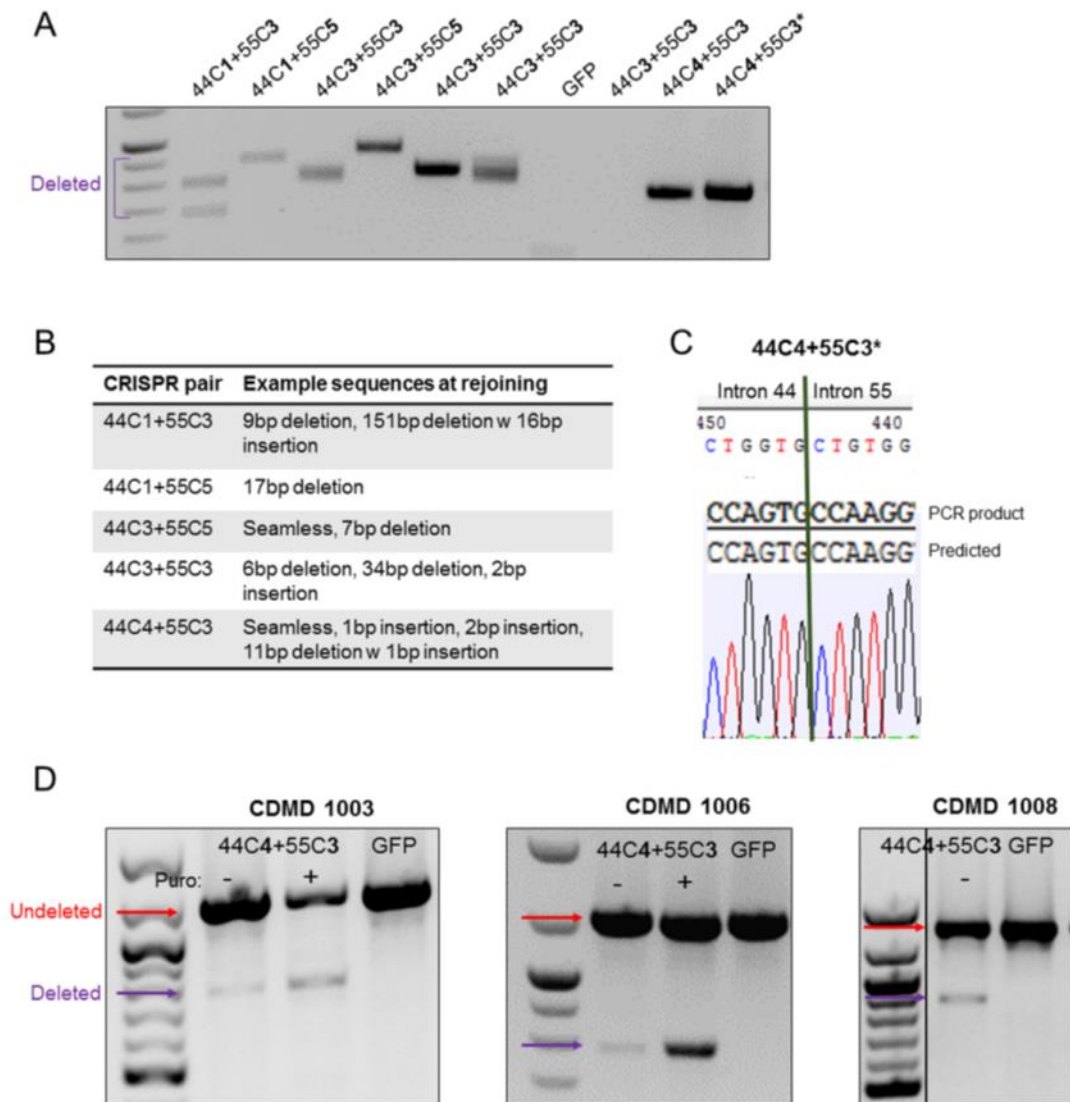


A. CDMD 1006 hiPSCs nucleofected with GFP serve as an untreated control and demonstrate ~40% transfection efficiency.

B-D. gRNAs demonstrate activity on Surveyor assay in CDMD 1003, 1006 and 1008 lines respectively. *3x the amount of 55C3 DNA was added during nucleofection.

Red arrows denote expected cleavage product bands (Table S1). Note the band in B highlighted by the blue arrow head is likely a non-specific PCR product and was discounted from analysis. The estimated percent of cutting is shown below each lane. A 100bp ladder was used.

Figure A-S3: Nucleofection of paired gRNAs results in an exon 45-55 deletion in CDMD hiPSCs.



A. PCR using primers flanking the deleted region show bands for successful deletion and rejoining after nucleofection of a variety of CRISPR pairs in hiPSC CDMD 1006.

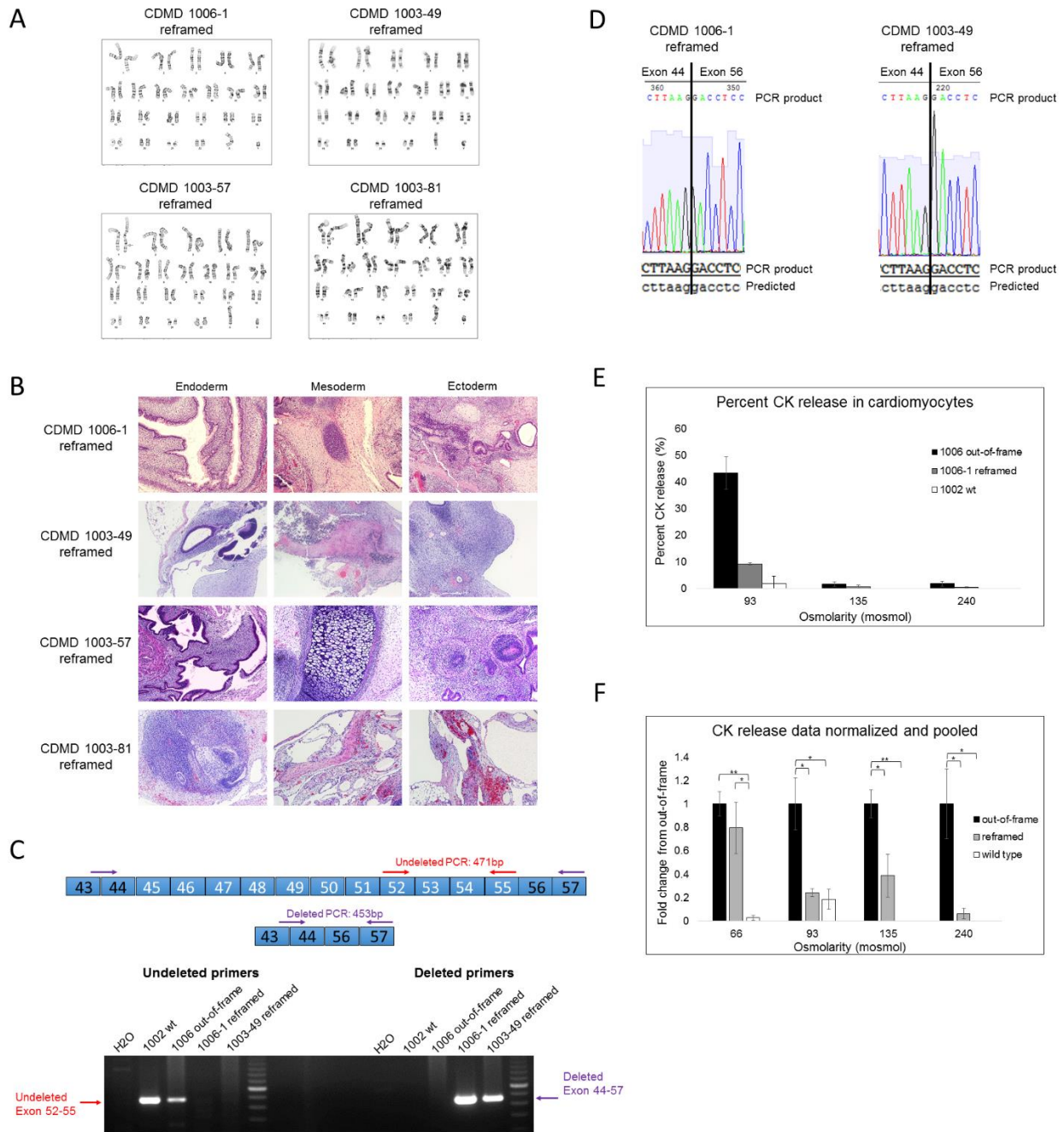
A 100bp ladder was used.

B. Examples of the types of different rejoined products identified after sequencing.

C. The sequencing for 44C4 + 55C3* seamless rejoining is shown.

D. Multiplex PCR shows an exon 45-55 deletion product in all lines nucleofected with 44C4 and 55C3 gRNAs. A significant increase in the efficiency of deletion in CDMD 1006 and 1003 after selection with 0.35µg/ml puromycin for one day is shown. *3x the amount of 55C3 DNA was added during nucleofection. A 100bp ladder was used.

Figure A-S4: Additional characterization of reframed lines.



A. All reframed lines were determined to be karyotypically normal except for CDMD 1003-81, which was found to contain a 1q32 amplification via FISH analysis. Upon retrospective analysis, the 1q32 amplification was determined to have existed in

the parent line (CDMD 1003 line at 22%) and was found in all daughter lines (CDMD 1003-57 and 1003-49 at 82.5%) and was not a result of CRISPR activity.

B. Reframed lines CDMD 1006-1, 1003-49, 1003-57, and 1003-81 formed teratomas consisting of the three germ layers in vivo.

C. Analysis of the mRNA from reframed lines. PCR using primers within the deleted region (red arrows) or flanking the deleted region (purple arrows) on dystrophin cDNA from hiPSC-derived cardiomyocytes shows undeleted bands in both CDMD 1002 and 1006 and deleted bands in both CDMD 1006-1 and 1003-49. A 100bp ladder was used.

D. Sequencing confirms exon 44 and 56 rejoining in reframed CDMD 1006-1 and 1003-49.

E. Graph of data from CK release assay of hiPSC-derived cardiomyocytes exposed to hypoosmotic conditions below 240mosmol. The same CDMD 1002 control data as in Figure 4A are shown. Data are presented as average \pm standard error.

F. CK release assay data normalized to out-of-frame cells and pooled from all experiments shown (n=6 for out-offrame and reframed (n=5 for reframed 135mosmol), n=4 for wild type). Data are presented as average \pm standard error.

Table A-S1: Expected cleavage product sizes from Surveyor assay.

gRNA	Expected sizes (bp)
44C1	423, 480
44C2	445, 458
44C3	449, 454
44C4	387, 516
44C5	419, 484
55C1	379, 490
55C2	364, 505
55C3	411, 458
55C4	357, 512
55C5	351, 518

References

- [1] Henricson EK, Abresch RT, Cnaan A, Hu F, Duong T, Arrieta A, Han J, Escolar DM, Florence JM, Clemens PR, Hoffman EP, McDonald CM, Investigators C: The cooperative international neuromuscular research group Duchenne natural history study: glucocorticoid treatment preserves clinically meaningful functional milestones and reduces rate of disease progression as measured by manual muscle testing and other commonly used clinical trial outcome measures. *Muscle Nerve* 2013, 48:55-67.
- [2] Matthews PM, Karpati G: Pattern of X-chromosome inactivation as a key determinant of the clinicopathologic phenotype of Duchenne muscular dystrophy carriers. *Neurology* 1996, 46:1189-91.
- [3] Bushby K, Finkel R, Birnkrant DJ, Case LE, Clemens PR, Cripe L, Kaul A, Kinnett K, McDonald C, Pandya S, Poysky J, Shapiro F, Tomezsko J, Constantin C, Group DMDCCW: Diagnosis and management of Duchenne muscular dystrophy, part 2: implementation of multidisciplinary care. *Lancet Neurol* 2010, 9:177-89.
- [4] Mendell JR, Shilling C, Leslie ND, Flanigan KM, al-Dahhak R, Gastier-Foster J, Kneile K, Dunn DM, Duval B, Aoyagi A, Hamil C, Mahmoud M, Roush K, Bird L, Rankin C, Lilly H, Street N, Chandrasekar R, Weiss RB: Evidence-based path to newborn screening for Duchenne muscular dystrophy. *Ann Neurol* 2012, 71:304-13.
- [5] Morikawa Y, Heallen T, Leach J, Xiao Y, Martin JF: Dystrophin glycoprotein complex sequesters Yap to inhibit cardiomyocyte proliferation. *Nature* 2017.
- [6] Bhat HF, Mir SS, Dar KB, Bhat ZF, Shah RA, Ganai NA: ABC of multifaceted Dystrophin glycoprotein complex (DGC). *J Cell Physiol* 2017.
- [7] Robinson-Hamm JN, Gersbach CA: Gene therapies that restore dystrophin expression for the treatment of Duchenne muscular dystrophy. *Hum Genet* 2016, 135:1029-40.

- [8] Wilton SD, Veedu RN, Fletcher S: The emperor's new dystrophin: finding sense in the noise. *Trends Mol Med* 2015, 21:417-26.
- [9] Navarro C: [Dystrophin and dystrophin-associated proteins. Their evaluation at the neuromuscular pathology laboratory]. *Rev Neurol* 1999, 28:154-8.
- [10] Ervasti JM, Campbell KP: Dystrophin-associated glycoproteins: their possible roles in the pathogenesis of Duchenne muscular dystrophy. *Mol Cell Biol Hum Dis Ser* 1993, 3:139-66.
- [11] van Westering TL, Betts CA, Wood MJ: Current understanding of molecular pathology and treatment of cardiomyopathy in duchenne muscular dystrophy. *Molecules* 2015, 20:8823-55.
- [12] Legardinier S, Legrand B, Raguenes-Nicol C, Bondon A, Hardy S, Tascon C, Le Rumeur E, Hubert JF: A Two-amino Acid Mutation Encountered in Duchenne Muscular Dystrophy Decreases Stability of the Rod Domain 23 (R23) Spectrin-like Repeat of Dystrophin. *J Biol Chem* 2009, 284:8822-32.
- [13] Abdul-Razak H, Malerba A, Dickson G: Advances in gene therapy for muscular dystrophies. *F1000Res* 2016, 5.
- [14] Whitehead NP, Kim MJ, Bible KL, Adams ME, Froehner SC: Simvastatin offers new prospects for the treatment of Duchenne muscular dystrophy. *Rare Dis* 2016, 4:e1156286.
- [15] Nakamura A: Moving towards successful exon-skipping therapy for Duchenne muscular dystrophy. *J Hum Genet* 2017.
- [16] Le Rumeur E: Dystrophin and the two related genetic diseases, Duchenne and Becker muscular dystrophies. *Bosn J Basic Med Sci* 2015, 15:14-20.
- [17] Bello L, Campadello P, Barp A, Fanin M, Semplicini C, Soraru G, Caumo L, Calore C, Angelini C, Pegoraro E: Functional changes in Becker muscular dystrophy: implications for clinical trials in dystrophinopathies. *Sci Rep* 2016, 6:32439.

- [18] Sander HW, Menkes DL, Hood DC, Williams DA: A 60-year-old woman with weakness, fatigue, and acute respiratory failure: case report and discussion of the differential diagnosis. *Mil Med* 1998, 163:715-8.
- [19] Laing NG, Davis MR, Bayley K, Fletcher S, Wilton SD: Molecular diagnosis of duchenne muscular dystrophy: past, present and future in relation to implementing therapies. *Clin Biochem Rev* 2011, 32:129-34.
- [20] Nakamura A, Takeda S: Exon-skipping therapy for Duchenne muscular dystrophy. *Neuropathology* 2009, 29:494-501.
- [21] Echigoya Y, Mouly V, Garcia L, Yokota T, Duddy W: In silico screening based on predictive algorithms as a design tool for exon skipping oligonucleotides in Duchenne muscular dystrophy. *PLoS One* 2015, 10:e0120058.
- [22] Tanabe Y, Esaki K, Nomura T: Skeletal muscle pathology in X chromosome-linked muscular dystrophy (mdx) mouse. *Acta Neuropathol* 1986, 69:91-5.
- [23] Dunckley MG, Manoharan M, Villiet P, Eperon IC, Dickson G: Modification of splicing in the dystrophin gene in cultured Mdx muscle cells by antisense oligoribonucleotides. *Hum Mol Genet* 1998, 7:1083-90.
- [24] Shimatsu Y, Katagiri K, Furuta T, Nakura M, Tanioka Y, Yuasa K, Tomohiro M, Kornegay JN, Nonaka I, Takeda S: Canine X-linked muscular dystrophy in Japan (CXMDJ). *Exp Anim* 2003, 52:93-7.
- [25] Sharp NJ, Kornegay JN, Van Camp SD, Herbstreith MH, Secore SL, Kettle S, Hung WY, Constantinou CD, Dykstra MJ, Roses AD, et al.: An error in dystrophin mRNA processing in golden retriever muscular dystrophy, an animal homologue of Duchenne muscular dystrophy. *Genomics* 1992, 13:115-21.
- [26] Partridge TA: The mdx mouse model as a surrogate for Duchenne muscular dystrophy. *FEBS J* 2013, 280:4177-86.

[27] Tanganyika-de Winter CL, Heemskerk H, Karnaoukh TG, van Putten M, de Kimpe SJ, van Deutekom J, Aartsma-Rus A: Long-term Exon Skipping Studies With 2'-O-Methyl Phosphorothioate Antisense Oligonucleotides in Dystrophic Mouse Models. *Mol Ther Nucleic Acids* 2012, 1:e44.

[28] Malerba A, Boldrin L, Dickson G: Long-term systemic administration of unconjugated morpholino oligomers for therapeutic expression of dystrophin by exon skipping in skeletal muscle: implications for cardiac muscle integrity. *Nucleic Acid Ther* 2011, 21:293-8.

[29] Lim KR, Maruyama R, Yokota T: Eteplirsen in the treatment of Duchenne muscular dystrophy. *Drug Des Devel Ther* 2017, 11:533-45.

[30] McDonald CM, Henricson EK, Abresch RT, Florence J, Eagle M, Gappmaier E, Glanzman AM, Group PG-DS, Spiegel R, Barth J, Elfring G, Reha A, Peltz SW: The 6-minute walk test and other clinical endpoints in duchenne muscular dystrophy: reliability, concurrent validity, and minimal clinically important differences from a multicenter study. *Muscle Nerve* 2013, 48:357-68.

[31] Mendell JR, Goemans N, Lowes LP, Alfano LN, Berry K, Shao J, Kaye EM, Mercuri E, Eteplirsen Study G, Telethon Foundation DMDIN: Longitudinal effect of eteplirsen versus historical control on ambulation in Duchenne muscular dystrophy. *Ann Neurol* 2016, 79:257-71.

[32] Kendall GC, Mokhonova EI, Moran M, Sejbuk NE, Wang DW, Silva O, Wang RT, Martinez L, Lu QL, Damoiseaux R, Spencer MJ, Nelson SF, Miceli MC: Dantrolene enhances antisense-mediated exon skipping in human and mouse models of Duchenne muscular dystrophy. *Sci Transl Med* 2012, 4:164ra0.

[33] Mah JK, Korngut L, Dykeman J, Day L, Pringsheim T, Jette N: A systematic review and meta-analysis on the epidemiology of Duchenne and Becker muscular dystrophy. *Neuromuscul Disord* 2014, 24:482-91.

[34] Emery AE: The muscular dystrophies. *Lancet* 2002, 359:687-95.

[35] Biressi S, Miyabara EH, Gopinath SD, Carlignani PM, Rando TA: A Wnt-TGFbeta2 axis induces a fibrogenic program in muscle stem cells from dystrophic mice. *Sci Transl Med* 2014, 6:267ra176.

- [36] Tanihata J, Takeda S: [Changes in cytosolic Ca²⁺dynamics associated with muscular dystrophy.]. Clin Calcium 2016, 26:1677-83.
- [37] Bellinger AM, Reiken S, Carlson C, Mongillo M, Liu X, Rothman L, Matecki S, Lacampagne A, Marks AR: Hypernitrosylated ryanodine receptor calcium release channels are leaky in dystrophic muscle. Nat Med 2009, 15:325-30.
- [38] Samaha FJ, Quinlan JG: Dystrophinopathies: clarification and complication. J Child Neurol 1996, 11:13-20.
- [39] Emery AE, Skinner R: Clinical studies in benign (Becker type) X-linked muscular dystrophy. Clin Genet 1976, 10:189-201.
- [40] Nicolas A, Lucchetti-Miganeh C, Yaou RB, Kaplan JC, Chelly J, Leturcq F, Barloy-Hubler F, Le Rumeur E: Assessment of the structural and functional impact of in-frame mutations of the DMD gene, using the tools included in the eDystrophin online database. Orphanet J Rare Dis 2012, 7:45.
- [41] Mann CJ, Honeyman K, Cheng AJ, Ly T, Lloyd F, Fletcher S, Morgan JE, Partridge TA, Wilton SD: Antisense-induced exon skipping and synthesis of dystrophin in the mdx mouse. Proc Natl Acad Sci U S A 2001, 98:42-7.
- [42] Foster H, Popplewell L, Dickson G: Genetic therapeutic approaches for Duchenne muscular dystrophy. Hum Gene Ther 2012, 23:676-87.
- [43] Kole R, Krieg AM: Exon skipping therapy for Duchenne muscular dystrophy. Adv Drug Deliv Rev 2015, 87:104-7.
- [44] Alter J, Lou F, Rabinowitz A, Yin H, Rosenfeld J, Wilton SD, Partridge TA, Lu QL: Systemic delivery of morpholino oligonucleotide restores dystrophin expression bodywide and improves dystrophic pathology. Nat Med 2006, 12:175-7.
- [45] Goemans NM, Tulinius M, van den Akker JT, Burm BE, Ekhart PF, Heuvelmans N, Holling T, Janson AA, Platenburg GJ, Sipkens JA, Sitsen JM, Aartsma-Rus A, van Ommen GJ, Buyse G, Darin N, Verschuuren

JJ, Campion GV, de Kimpe SJ, van Deutekom JC: Systemic administration of PRO051 in Duchenne's muscular dystrophy. *N Engl J Med* 2011, 364:1513-22.

[46] Kinali M, Arechavala-Gomez V, Feng L, Cirak S, Hunt D, Adkin C, Guglieri M, Ashton E, Abbs S, Nihoyannopoulos P, Garralda ME, Rutherford M, McCulley C, Popplewell L, Graham IR, Dickson G, Wood MJ, Wells DJ, Wilton SD, Kole R, Straub V, Bushby K, Sewry C, Morgan JE, Muntoni F: Local restoration of dystrophin expression with the morpholino oligomer AVI-4658 in Duchenne muscular dystrophy: a single-blind, placebo-controlled, dose-escalation, proof-of-concept study. *Lancet Neurol* 2009, 8:918-28.

[47] van Deutekom JC, Janson AA, Ginjaar IB, Frankhuizen WS, Aartsma-Rus A, Bremmer-Bout M, den Dunnen JT, Koop K, van der Kooi AJ, Goemans NM, de Kimpe SJ, Ekhardt PF, Venneker EH, Platenburg GJ, Verschuuren JJ, van Ommen GJ: Local dystrophin restoration with antisense oligonucleotide PRO051. *N Engl J Med* 2007, 357:2677-86.

[48] Yokota T, Lu QL, Partridge T, Kobayashi M, Nakamura A, Takeda S, Hoffman E: Efficacy of systemic morpholino exon-skipping in Duchenne dystrophy dogs. *Ann Neurol* 2009, 65:667-76.

[49] Lu QL, Mann CJ, Lou F, Bou-Gharios G, Morris GE, Xue SA, Fletcher S, Partridge TA, Wilton SD: Functional amounts of dystrophin produced by skipping the mutated exon in the mdx dystrophic mouse. *Nat Med* 2003, 9:1009-14.

[50] Voit T, Topaloglu H, Straub V, Muntoni F, Deconinck N, Campion G, De Kimpe SJ, Eagle M, Guglieri M, Hood S, Liefwaard L, Loubakos A, Morgan A, Nakielny J, Quarcoo N, Ricotti V, Rolfe K, Servais L, Wardell C, Wilson R, Wright P, Kraus JE: Safety and efficacy of drisapersen for the treatment of Duchenne muscular dystrophy (DEMAND II): an exploratory, randomised, placebo-controlled phase 2 study. *Lancet Neurol* 2014, 13:987-96.

[51] Flanigan KM, Voit T, Rosales XQ, Servais L, Kraus JE, Wardell C, Morgan A, Dorricott S, Nakielny J, Quarcoo N, Liefwaard L, Drury T, Campion G, Wright P: Pharmacokinetics and safety of single doses of

drisapersen in non-ambulant subjects with Duchenne muscular dystrophy: results of a double-blind randomized clinical trial. *Neuromuscul Disord* 2014, 24:16-24.

[52] FDA: FDA Briefing Document - NDA 206488 Eteplirsen - Peripheral and Central Nervous System Drugs Advisory Committee Meeting;

<https://www.fda.gov/downloads/advisorycommittees/committeesmeetingmaterials/drugs/peripheralandcentralnervoussystemdrugsadvisorycommittee/ucm497063.pdf>. April 25, 2016.

[53] Beggs AH, Hoffman EP, Snyder JR, Arahata K, Specht L, Shapiro F, Angelini C, Sugita H, Kunkel LM: Exploring the molecular basis for variability among patients with Becker muscular dystrophy: dystrophin gene and protein studies. *Am J Hum Genet* 1991, 49:54-67.

[54] van Putten M, Hulsker M, Nadarajah VD, van Heiningen SH, van Huizen E, van Iterson M, Admiraal P, Messemaker T, den Dunnen JT, t Hoen PA, Aartsma-Rus A: The effects of low levels of dystrophin on mouse muscle function and pathology. *PLoS One* 2012, 7:e31937.

[55] van Putten M, Hulsker M, Young C, Nadarajah VD, Heemskerk H, van der Weerd L, t Hoen PA, van Ommen GJ, Aartsma-Rus AM: Low dystrophin levels increase survival and improve muscle pathology and function in dystrophin/utrophin double-knockout mice. *FASEB J* 2013, 27:2484-95.

[56] Sharp PS, Bye-a-Jee H, Wells DJ: Physiological characterization of muscle strength with variable levels of dystrophin restoration in mdx mice following local antisense therapy. *Mol Ther* 2011, 19:165-71.

[57] van den Bergen JC, Wokke BH, Janson AA, van Duinen SG, Hulsker MA, Ginjaar HB, van Deutekom JC, Aartsma-Rus A, Kan HE, Verschuuren JJ: Dystrophin levels and clinical severity in Becker muscular dystrophy patients. *J Neurol Neurosurg Psychiatry* 2014, 85:747-53.

[58] Phelps SF, Hauser MA, Cole NM, Rafael JA, Hinkle RT, Faulkner JA, Chamberlain JS: Expression of full-length and truncated dystrophin mini-genes in transgenic mdx mice. *Hum Mol Genet* 1995, 4:1251-8.

- [59] Wells DJ, Wells KE, Asante EA, Turner G, Sunada Y, Campbell KP, Walsh FS, Dickson G: Expression of human full-length and minidystrophin in transgenic mdx mice: implications for gene therapy of Duchenne muscular dystrophy. *Hum Mol Genet* 1995, 4:1245-50.
- [60] van Putten M, van der Pijl EM, Hulsker M, Verhaart IE, Nadarajah VD, van der Weerd L, Aartsma-Rus A: Low dystrophin levels in heart can delay heart failure in mdx mice. *J Mol Cell Cardiol* 2014, 69:17-23.
- [61] Wilton SD, Lloyd F, Carville K, Fletcher S, Honeyman K, Agrawal S, Kole R: Specific removal of the nonsense mutation from the mdx dystrophin mRNA using antisense oligonucleotides. *Neuromuscul Disord* 1999, 9:330-8.
- [62] Kimura E, Han JJ, Li S, Fall B, Ra J, Haraguchi M, Tapscott SJ, Chamberlain JS: Cell-lineage regulated myogenesis for dystrophin replacement: a novel therapeutic approach for treatment of muscular dystrophy. *Hum Mol Genet* 2008, 17:2507-17.
- [63] Kilkenny C, Parsons N, Kadyszewski E, Festing MF, Cuthill IC, Fry D, Hutton J, Altman DG: Survey of the quality of experimental design, statistical analysis and reporting of research using animals. *PLoS One* 2009, 4:e7824.
- [64] Quinn JL, Huynh T, Uaesoontrachoon K, Tatem K, Phadke A, Van der Meulen JH, Yu Q, Nagaraju K: Effects of Dantrolene Therapy on Disease Phenotype in Dystrophin Deficient mdx Mice. *PLoS Curr* 2013, 5.
- [65] Quinlan JG, Johnson SR, Samaha FJ: Dantrolene normalizes serum creatine kinase in MDX mice. *Muscle Nerve* 1990, 13:268-9.
- [66] Enwere EK, Boudreault L, Holbrook J, Timusk K, Earl N, LaCasse E, Renaud JM, Korneluk RG: Loss of cIAP1 attenuates soleus muscle pathology and improves diaphragm function in mdx mice. *Hum Mol Genet* 2013, 22:867-78.
- [67] Karpati G, Carpenter S, Prescott S: Small-caliber skeletal muscle fibers do not suffer necrosis in mdx mouse dystrophy. *Muscle Nerve* 1988, 11:795-803.

- [68] Malerba A, Thorogood FC, Dickson G, Graham IR: Dosing regimen has a significant impact on the efficiency of morpholino oligomer-induced exon skipping in mdx mice. *Hum Gene Ther* 2009, 20:955-65.
- [69] Janssen PM, Murray JD, Schill KE, Rastogi N, Schultz EJ, Tran T, Raman SV, Rafael-Fortney JA: Prednisolone attenuates improvement of cardiac and skeletal contractile function and histopathology by lisinopril and spironolactone in the mdx mouse model of Duchenne muscular dystrophy. *PLoS One* 2014, 9:e88360.
- [70] Kobayashi YM, Rader EP, Crawford RW, Campbell KP: Endpoint measures in the mdx mouse relevant for muscular dystrophy pre-clinical studies. *Neuromuscul Disord* 2012, 22:34-42.
- [71] Banks GB, Combs AC, Odom GL, Bloch RJ, Chamberlain JS: Muscle structure influences utrophin expression in mdx mice. *PLoS Genet* 2014, 10:e1004431.
- [72] Dantrolene, FDA label.
- [73] Bertorini TE, Palmieri GM, Griffin J, Igarashi M, Hinton A, Karas JG: Effect of dantrolene in Duchenne muscular dystrophy. *Muscle Nerve* 1991, 14:503-7.
- [74] Moulton HM, Moulton JD: Morpholinos and their peptide conjugates: therapeutic promise and challenge for Duchenne muscular dystrophy. *Biochim Biophys Acta* 2010, 1798:2296-303.
- [75] Han G, Gu B, Cao L, Gao X, Wang Q, Seow Y, Zhang N, Wood MJ, Yin H: Hexose enhances oligonucleotide delivery and exon skipping in dystrophin-deficient mdx mice. *Nat Commun* 2016, 7:10981.
- [76] Martone J, Briganti F, Legnini I, Morlando M, Picillo E, Sthandier O, Politano L, Bozzoni I: The lack of the Celf2a splicing factor converts a Duchenne genotype into a Becker phenotype. *Nat Commun* 2016, 7:10488.
- [77] Hu Y, Wu B, Zillmer A, Lu P, Benrashid E, Wang M, Doran T, Shaban M, Wu X, Long Lu Q: Guanine Analogues Enhance Antisense Oligonucleotide-induced Exon Skipping in Dystrophin Gene In Vitro and In Vivo. *Mol Ther* 2010, 18:812-8.

- [78] O'Leary DA, Sharif O, Anderson P, Tu B, Welch G, Zhou Y, Caldwell JS, Engels IH, Brinker A: Identification of small molecule and genetic modulators of AON-induced dystrophin exon skipping by high-throughput screening. *PLoS One* 2009, 4:e8348.
- [79] Meyler WJ, Mols-Thurkow HW, Wesseling H: Relationship between plasma concentration and effect of dantrolene sodium in man. *Eur J Clin Pharmacol* 1979, 16:203-9.
- [80] Wuis EW, Vree TB, Van Der Kleijn E: Pharmacokinetics of intravenously administered dantrolene and its 5-hydroxy metabolite in dogs. *Int J Clin Pharmacol Res* 1990, 10:203-10.
- [81] Flewellen EH, Nelson TE: Dantrolene dose response in malignant hyperthermia-susceptible (MHS) swine: method to obtain prophylaxis and therapeutics. *Anesthesiology* 1980, 52:303-8.
- [82] Flewellen EH, Nelson TE, Bee DE: Effect of dantrolene on neuromuscular block by d-tubocurarine and subsequent antagonism by neostigmine in the rabbit. *Anesthesiology* 1980, 52:126-30.
- [83] Meyler WJ, Mols-Thurkow I, Scaf AH, Sargo S, Wesseling H: The effect of dantrolene sodium on rat skeletal muscle in relation to the plasma concentration. *Eur J Pharmacol* 1979, 53:335-42.
- [84] Flewellen EH, Nelson TE, Jones WP, Arens JF, Wagner DL: Dantrolene dose response in awake man: implications for management of malignant hyperthermia. *Anesthesiology* 1983, 59:275-80.
- [85] Meyler WJ, Bakker H, Kok JJ, Agoston S, Wesseling H: The effect of dantrolene sodium in relation to blood levels in spastic patients after prolonged administration. *J Neurol Neurosurg Psychiatry* 1981, 44:334-9.
- [86] Kobayashi S, Yano M, Suetomi T, Ono M, Tateishi H, Mochizuki M, Xu X, Uchinoumi H, Okuda S, Yamamoto T, Koseki N, Kyushiki H, Ikemoto N, Matsuzaki M: Dantrolene, a therapeutic agent for malignant hyperthermia, markedly improves the function of failing cardiomyocytes by stabilizing interdomain interactions within the ryanodine receptor. *J Am Coll Cardiol* 2009, 53:1993-2005.
- [87] Kobayashi S, Bannister ML, Gangopadhyay JP, Hamada T, Parness J, Ikemoto N: Dantrolene stabilizes domain interactions within the ryanodine receptor. *J Biol Chem* 2005, 280:6580-7.

- [88] Oo YW, Gomez-Hurtado N, Walweel K, van Helden DF, Imtiaz MS, Knollmann BC, Laver DR: Essential Role of Calmodulin in RyR Inhibition by Dantrolene. *Mol Pharmacol* 2015, 88:57-63.
- [89] Mannino JL, Kim W, Wernick M, Nguyen SV, Braquet R, Adamson AW, Den Z, Batzer MA, Collins CC, Brown KD: Evidence for alternate splicing within the mRNA transcript encoding the DNA damage response kinase ATR. *Gene* 2001, 272:35-43.
- [90] Xie J, Black DL: A CaMK IV responsive RNA element mediates depolarization-induced alternative splicing of ion channels. *Nature* 2001, 410:936-9.
- [91] An P, Grabowski PJ: Exon silencing by UAGG motifs in response to neuronal excitation. *PLoS Biol* 2007, 5:e36.
- [92] Gebiski BL, Mann CJ, Fletcher S, Wilton SD: Morpholino antisense oligonucleotide induced dystrophin exon 23 skipping in mdx mouse muscle. *Hum Mol Genet* 2003, 12:1801-11.
- [93] Hindson CM, Chevillet JR, Briggs HA, Gallichotte EN, Ruf IK, Hindson BJ, Vessella RL, Tewari M: Absolute quantification by droplet digital PCR versus analog real-time PCR. *Nat Methods* 2013, 10:1003-5.
- [94] Bodnar AG, Ouellette M, Frolkis M, Holt SE, Chiu CP, Morin GB, Harley CB, Shay JW, Lichtsteiner S, Wright WE: Extension of life-span by introduction of telomerase into normal human cells. *Science* 1998, 279:349-52.
- [95] Price FD, von Maltzahn J, Bentzinger CF, Dumont NA, Yin H, Chang NC, Wilson DH, Frenette J, Rudnicki MA: Inhibition of JAK-STAT signaling stimulates adult satellite cell function. *Nat Med* 2014, 20:1174-81.
- [96] Wernig G, Janzen V, Schafer R, Zweyer M, Knauf U, Hoegemeier O, Mundegar RR, Garbe S, Stier S, Franz T, Wernig M, Wernig A: The vast majority of bone-marrow-derived cells integrated into mdx muscle fibers are silent despite long-term engraftment. *Proc Natl Acad Sci U S A* 2005, 102:11852-7.

- [97] Darabi R, Pan W, Bosnakovski D, Baik J, Kyba M, Perlingeiro RC: Functional myogenic engraftment from mouse iPS cells. *Stem Cell Rev* 2011, 7:948-57.
- [98] Montanaro F, Liadaki K, Volinski J, Flint A, Kunkel LM: Skeletal muscle engraftment potential of adult mouse skin side population cells. *Proc Natl Acad Sci U S A* 2003, 100:9336-41.
- [99] Dell'Agnola C, Wang Z, Storb R, Tapscott SJ, Kuhr CS, Hauschka SD, Lee RS, Sale GE, Zellmer E, Gisburne S, Bogan J, Kornegay JN, Cooper BJ, Gooley TA, Little MT: Hematopoietic stem cell transplantation does not restore dystrophin expression in Duchenne muscular dystrophy dogs. *Blood* 2004, 104:4311-8.
- [100] Camirand G, Rousseau J, Ducharme ME, Rothstein DM, Tremblay JP: Novel Duchenne muscular dystrophy treatment through myoblast transplantation tolerance with anti-CD45RB, anti-CD154 and mixed chimerism. *Am J Transplant* 2004, 4:1255-65.
- [101] Rozkalne A, Adkin C, Meng J, Lapan A, Morgan JE, Gussoni E: Mouse regenerating myofibers detected as false-positive donor myofibers with anti-human spectrin. *Hum Gene Ther* 2014, 25:73-81.
- [102] Reinig AM, Mirzaei S, Berlau DJ: Advances in the Treatment of Duchenne Muscular Dystrophy: New and Emerging Pharmacotherapies. *Pharmacotherapy* 2017, 37:492-9.
- [103] Bladen CL, Rafferty K, Straub V, Monges S, Moresco A, Dawkins H, Roy A, Chamova T, Guergueltcheva V, Korngut L, Campbell C, Dai Y, Barisic N, Kos T, Brabec P, Rahbek J, Lahdetie J, Tuffery-Giraud S, Claustres M, Leturcq F, Ben Yaou R, Walter MC, Schreiber O, Karcagi V, Herczegfalvi A, Viswanathan V, Bayat F, de la Caridad Guerrero Sarmiento I, Ambrosini A, Ceradini F, Kimura E, van den Bergen JC, Rodrigues M, Roxburgh R, Lusakowska A, Oliveira J, Santos R, Neagu E, Butoianu N, Artemieva S, Rasic VM, Posada M, Palau F, Lindvall B, Bloetzer C, Karaduman A, Topaloglu H, Inal S, Oflazer P, Stringer A, Shatillo AV, Martin AS, Peay H, Flanigan KM, Salgado D, von Rekowski B, Lynn S, Heslop E, Gainotti S, Taruscio D, Kirschner J, Verschuuren J, Bushby K, Beroud C, Lochmuller H: The TREAT-NMD

Duchenne muscular dystrophy registries: conception, design, and utilization by industry and academia. Hum Mutat 2013, 34:1449-57.

[104] Finkel RS: Read-through strategies for suppression of nonsense mutations in Duchenne/ Becker muscular dystrophy: aminoglycosides and ataluren (PTC124). J Child Neurol 2010, 25:1158-64.

[105] Finkel RS, Flanigan KM, Wong B, Bonnemann C, Sampson J, Sweeney HL, Reha A, Northcutt VJ, Elfring G, Barth J, Peltz SW: Phase 2a study of ataluren-mediated dystrophin production in patients with nonsense mutation Duchenne muscular dystrophy. PLoS One 2013, 8:e81302.

[106] PRNewswire. PTC Therapeutics reports fourth quarter and fullyear 2015 financial results and provides corporate update. Available from <http://www.prnewswire.com/news-releases>. Accessed October 22, 2016.

[107] Yahoo Finance FrBsmwdSdifJ.

[108] FDA, Exondys51 Label for Duchenne Muscular Dystrophy.

[109] Sarepta TP-P, <https://www.sarepta.com/technology/technology-platform>.

[110] Fairclough RJ, Wood MJ, Davies KE: Therapy for Duchenne muscular dystrophy: renewed optimism from genetic approaches. Nat Rev Genet 2013, 14:373-8.

[111] Mendell JR, Rodino-Klapac L, Sahenk Z, Malik V, Kaspar BK, Walker CM, Clark KR: Gene therapy for muscular dystrophy: lessons learned and path forward. Neurosci Lett 2012, 527:90-9.

[112] Young CS, Hicks MR, Ermolova NV, Nakano H, Jan M, Younesi S, Karumbayaram S, Kumagai-Cresse C, Wang D, Zack JA, Kohn DB, Nakano A, Nelson SF, Miceli MC, Spencer MJ, Pyle AD: A Single CRISPR-Cas9 Deletion Strategy that Targets the Majority of DMD Patients Restores Dystrophin Function in hiPSC-Derived Muscle Cells. Cell Stem Cell 2016, 18:533-40.

[113] Mendell JR, Rodino-Klapac LR: CRISPR/Cas9 treatment for Duchenne muscular dystrophy. Cell Res 2016.

[114] Mendell JR, Rodino-Klapac LR, Sahenk Z, Roush K, Bird L, Lowes LP, Alfano L, Gomez AM, Lewis S, Kota J, Malik V, Shontz K, Walker CM, Flanigan KM, Corridore M, Kean JR, Allen HD, Shilling C, Melia KR, Sazani P, Saoud JB, Kaye EM, Eteplirsen Study G: Eteplirsen for the treatment of Duchenne muscular dystrophy. *Ann Neurol* 2013, 74:637-47.

[115] Pearce JM, Pennington RJ, Walton JN: Serum Enzyme Studies in Muscle Disease. Iii. Serum Creatine Kinase Activity in Relatives of Patients with the Duchenne Type of Muscular Dystrophy. *J Neurol Neurosurg Psychiatry* 1964, 27:181-5.

[116] Beroud C, Tuffery-Giraud S, Matsuo M, Hamroun D, Humbertclaude V, Monnier N, Moizard MP, Voelckel MA, Calemard LM, Boisseau P, Blayau M, Philippe C, Cossee M, Pages M, Rivier F, Danos O, Garcia L, Claustres M: Multiexon skipping leading to an artificial DMD protein lacking amino acids from exons 45 through 55 could rescue up to 63% of patients with Duchenne muscular dystrophy. *Hum Mutat* 2007, 28:196-202.

[117] Echigoya Y, Aoki Y, Miskew B, Panesar D, Touznik A, Nagata T, Tanihata J, Nakamura A, Nagaraju K, Yokota T: Long-term efficacy of systemic multiexon skipping targeting dystrophin exons 45-55 with a cocktail of vivo-morpholinos in mdx52 mice. *Mol Ther Nucleic Acids* 2015, 4:e225.

[118] Nakamura A, Yoshida K, Fukushima K, Ueda H, Urasawa N, Koyama J, Yazaki Y, Yazaki M, Sakai T, Haruta S, Takeda S, Ikeda S: Follow-up of three patients with a large in-frame deletion of exons 45-55 in the Duchenne muscular dystrophy (DMD) gene. *J Clin Neurosci* 2008, 15:757-63.

[119] Taglia A, Petillo R, D'Ambrosio P, Picillo E, Torella A, Orsini C, Ergoli M, Scutifero M, Passamano L, Palladino A, Nigro G, Politano L: Clinical features of patients with dystrophinopathy sharing the 45-55 exon deletion of DMD gene. *Acta Myol* 2015, 34:9-13.

[120] Li HL, Fujimoto N, Sasakawa N, Shirai S, Ohkame T, Sakuma T, Tanaka M, Amano N, Watanabe A, Sakurai H, Yamamoto T, Yamanaka S, Hotta A: Precise correction of the dystrophin gene in duchenne

muscular dystrophy patient induced pluripotent stem cells by TALEN and CRISPR-Cas9. *Stem Cell Reports* 2015, 4:143-54.

[121] Long C, McAnally JR, Shelton JM, Mireault AA, Bassel-Duby R, Olson EN: Prevention of muscular dystrophy in mice by CRISPR/Cas9-mediated editing of germline DNA. *Science* 2014, 345:1184-8.

[122] Nelson CE, Hakim CH, Ousterout DG, Thakore PI, Moreb EA, Castellanos Rivera RM, Madhavan S, Pan X, Ran FA, Yan WX, Asokan A, Zhang F, Duan D, Gersbach CA: In vivo genome editing improves muscle function in a mouse model of Duchenne muscular dystrophy. *Science* 2016, 351:403-7.

[123] Ousterout DG, Kabadi AM, Thakore PI, Majoros WH, Reddy TE, Gersbach CA: Multiplex CRISPR/Cas9-based genome editing for correction of dystrophin mutations that cause Duchenne muscular dystrophy. *Nat Commun* 2015, 6:6244.

[124] Tabebordbar M, Zhu K, Cheng JK, Chew WL, Widrick JJ, Yan WX, Maesner C, Wu EY, Xiao R, Ran FA, Cong L, Zhang F, Vandenberghe LH, Church GM, Wagers AJ: In vivo gene editing in dystrophic mouse muscle and muscle stem cells. *Science* 2016, 351:407-11.

[125] Wojtal D, Kemaladewi DU, Malam Z, Abdullah S, Wong TW, Hyatt E, Baghestani Z, Pereira S, Stavropoulos J, Mouly V, Mamchaoui K, Muntoni F, Voit T, Gonorazky HD, Dowling JJ, Wilson MD, Mendoza-Londono R, Ivakine EA, Cohn RD: Spell Checking Nature: Versatility of CRISPR/Cas9 for Developing Treatments for Inherited Disorders. *Am J Hum Genet* 2016, 98:90-101.

[126] Xu L, Park KH, Zhao L, Xu J, El Refaey M, Gao Y, Zhu H, Ma J, Han R: CRISPR-mediated Genome Editing Restores Dystrophin Expression and Function in mdx Mice. *Mol Ther* 2016, 24:564-9.

[127] Cacchiarelli D, Incitti T, Martone J, Cesana M, Cazzella V, Santini T, Sthandier O, Bozzoni I: miR-31 modulates dystrophin expression: new implications for Duchenne muscular dystrophy therapy. *EMBO Rep* 2011, 12:136-41.

[128] Dekel-Naftali M, Aviram-Goldring A, Litmanovitch T, Shamash J, Reznik-Wolf H, Laevsky I, Amit M, Itskovitz-Eldor J, Yung Y, Hourvitz A, Schiff E, Rienstein S: Screening of human pluripotent stem cells

using CGH and FISH reveals low-grade mosaic aneuploidy and a recurrent amplification of chromosome 1q. *Eur J Hum Genet* 2012, 20:1248-55.

[129] Cradick TJ, Qiu P, Lee CM, Fine EJ, Bao G: COSMID: A Web-based Tool for Identifying and Validating CRISPR/Cas Off-target Sites. *Mol Ther Nucleic Acids* 2014, 3:e214.

[130] Guan X, Mack DL, Moreno CM, Strande JL, Mathieu J, Shi Y, Markert CD, Wang Z, Liu G, Lawlor MW, Moorefield EC, Jones TN, Fugate JA, Furth ME, Murry CE, Ruohola-Baker H, Zhang Y, Santana LF, Childers MK: Dystrophin-deficient cardiomyocytes derived from human urine: new biologic reagents for drug discovery. *Stem Cell Res* 2014, 12:467-80.

[131] Menke A, Jockusch H: Extent of shock-induced membrane leakage in human and mouse myotubes depends on dystrophin. *J Cell Sci* 1995, 108 (Pt 2):727-33.

[132] Arechavala-Gomeza V, Anthony K, Morgan J, Muntoni F: Antisense oligonucleotide-mediated exon skipping for Duchenne muscular dystrophy: progress and challenges. *Curr Gene Ther* 2012, 12:152-60.

[133] Partridge T: Myoblast transplantation. *Neuromuscul Disord* 2002, 12 Suppl 1:S3-6.

[134] Bladen CL, Salgado D, Monges S, Foncuberta ME, Kekou K, Kosma K, Dawkins H, Lamont L, Roy AJ, Chamova T, Guergueltcheva V, Chan S, Korngut L, Campbell C, Dai Y, Wang J, Barisic N, Brabec P, Lahdetie J, Walter MC, Schreiber-Katz O, Karcagi V, Garami M, Viswanathan V, Bayat F, Buccella F, Kimura E, Koeks Z, van den Bergen JC, Rodrigues M, Roxburgh R, Lusakowska A, Kostera-Pruszczyk A, Zimowski J, Santos R, Neagu E, Artemieva S, Rasic VM, Vojinovic D, Posada M, Bloetzer C, Jeannet PY, Joncourt F, Diaz-Manera J, Gallardo E, Karaduman AA, Topaloglu H, El Sherif R, Stringer A, Shatillo AV, Martin AS, Peay HL, Bellgard MI, Kirschner J, Flanigan KM, Straub V, Bushby K, Verschuuren J, Aartsma-Rus A, Beroud C, Lochmuller H: The TREAT-NMD DMD Global Database: analysis of more than 7,000 Duchenne muscular dystrophy mutations. *Hum Mutat* 2015, 36:395-402.

[135] Harper SQ, Crawford RW, DelloRusso C, Chamberlain JS: Spectrin-like repeats from dystrophin and alpha-actinin-2 are not functionally interchangeable. *Hum Mol Genet* 2002, 11:1807-15.

[136] Carsana A, Frisso G, Tremolaterra MR, Lanzillo R, Vitale DF, Santoro L, Salvatore F: Analysis of dystrophin gene deletions indicates that the hinge III region of the protein correlates with disease severity. *Ann Hum Genet* 2005, 69:253-9.

[137] Long C, Amoasii L, Mireault AA, McAnally JR, Li H, Sanchez-Ortiz E, Bhattacharyya S, Shelton JM, Bassel-Duby R, Olson EN: Postnatal genome editing partially restores dystrophin expression in a mouse model of muscular dystrophy. *Science* 2016, 351:400-3.